Pharmacological tools for the NPY receptors: [^{35}S]GTPγS binding assays, luciferase gene reporter assays and labeled peptides

Dissertation

zur Erlangung des Doktorgrades der Naturwissenschaften (Dr. rer. nat.)

an der Fakultät für Chemie und Pharmazie

der Universität Regensburg

vorgelegt von

Stefanie Dukorn

aus Straubing

2017

Die vorliegende Arbeit entstand in der Zeit von Januar 2013 bis März 2017 unter der Leitung von Herrn Prof. Dr. Armin Buschauer am Institut für Pharmazie der Naturwissenschaftlichen Fakultät IV - Chemie und Pharmazie - der Universität Regensburg.

Das Promotionsgesuch wurde eingereicht im März 2017.

Tag der mündlichen Prüfung: 21. April 2017

Prüfungsausschuss:

Prof. Dr. S. Elz	(Vorsitzender)
Prof. Dr. A. Buschauer	(Erstgutachter)
Prof. Dr. G. Bernhardt	(Zweitgutachter)
Prof. Dr. J. Wegener	(Drittprüfer)

Danksagungen

An dieser Stelle möchte ich mich herzlich bedanken bei:

Herrn Prof. Dr. Armin Buschauer, dass ich die Möglichkeit für dieses vielseitige Projekt erhalten habe, seine wissenschaftlichen Anregungen sowie Förderungen und seine konstruktive Kritik bei der Durchsicht der Arbeit,

Herrn Prof. Dr. Günther Bernhardt für seine Hilfsbereitschaft und sein Interesse am Fortschritt der Arbeit, sein Fachwissen und die Durchsicht der Arbeit,

Herrn Prof. Dr. Oliver Zerbe und Dr. Jacopo Marino für die Kooperation zu Beginn meiner Arbeit, mit Unterstützung von Dr. Oliver Biehlmaier der Imaging Core Facility in Basel,

Herrn Dr. Paul Baumeister, der zu Beginn und im weiteren Verlauf meiner Doktorarbeit immer ein offenes Ohr für jegliche Angelegenheiten hatte und entsprechend seinen fachlichen Ratschlägen,

Herrn Dr. Max Keller für die wertvollen fachlichen Tipps, die hervorragende Zusammenarbeit, das Bereitstellen von verschiedenen Substanzen, sowie für die fachlichen Diskussionen und Ratschläge,

Herrn Dr. Kilian Kuhn für die sehr gute Zusammenarbeit, NPY hat uns beide während dieser Zeit begleitet und entsprechend beschäftigt,

Herrn Timo Littmann für die Durchführung der Arrestin Assays,

Frau Prof. Dr. Chiara Cabrele für die Bereitstellung der Peptide,

Frau Dr. Birgit Kraus für die Unterstützung bei der Fluoreszenzmikroskopie,

Frau Dr. Andrea Bleckmann für die Bereitstellung des Konfokalmikroskops,

Frau Elvira Schreiber für die Durchführung der zahlreichen pharmakologischen Bestimmungen am FACS und Durchführung von Calcium Assays,

Frau Brigitte Wenzl für die Unterstützung v.a. zu Beginn meiner praktischen Laborarbeit und für die gute Zusammenarbeit während der Praktikumsbetreuung,

Frau Susanne Bollwein und Frau Dita Fritsch für die Durchführung von HPLC-Läufen und Experimenten,

Frau Maria Beer- Krön für ihre Unterstützung und der Durchführung von [^{35}S]GTPγS Assays und Radioligand-Bindungsexperimenten,

meiner Praktikantin Lisa Schindler für die Durchführung von Calcium Assays,

Herrn Josef Kiermaier und Herrn Wolfgang Söllner für die Anfertigung der MS-Untersuchungen,

the office 14.2.08 for the great collegiality, especially Timo Littmann, Dr. Nicole Plank, Andrea Pegoli and Frauke Antoni,

meinem ehemaligen Kollegen Herrn Dr. Uwe Nordemann für die Betreuung während meines Forschungspraktikums,

Frau Karin Reindl, Frau Uta Hasselmann, Frau Silvia Heinrich und Herrn Peter Richthammer für die Unterstützung bei technischen und organisatorischen Angelegenheiten,

allen Mitgliedern des Lehrstuhls für ihre Kollegialität, Hilfsbereitschaft und ein gutes Arbeitsklima,

meinen Freunden für die gemeinsame Zeit und das Interesse am Fortgang meiner Arbeit, „*Freundschaft fließt aus vielen Quellen, am reinsten aus Vertrauen und Respekt.*“

Zuletzt all denjenigen, die mehr als nur Dank verdienen:
Meiner Familie. Ihnen ist die vorliegende Arbeit gewidmet.

Publications and Poster Presentations

Publications (published results prior to the submission of the thesis):

Kuhn K., Ertl T., Dukorn S., Keller M., Bernhardt G., Reiser O., Buschauer A., High Affinity Agonists of the Neuropeptide Y (NPY) Y_4 Receptor Derived from the C-terminal Pentapeptide of Human Pancreatic Polypeptide (hPP): Synthesis, Stereochemical Discrimination and Radiolabeling, *Journal of Medicinal Chemistry* **2016**, 59 (13), S. 6045-6058

Keller M., Weiss S., Hutzler C., Kuhn K., Mollereau C., Dukorn S., Schindler L., Bernhardt G., König B., Buschauer A., N(omega)-carbamoylation of the argininamide moiety: an avenue to insurmountable NPY Y_1 receptor antagonists and a radiolabeled selective high affinity molecular tool ([^{3}H]UR-MK299) with extended residence time, *Journal of Medicinal Chemistry* **2015**, 58 (22), S. 8834-8849

Poster Presentations:

Dukorn, S., Keller, M., Bernhardt, G., Buschauer, A., *Investigations on the effect of sodium on hY_4R binding using fluorescent and radiolabelled [Lys^4,Nle^{17,30}]hPP as new molecular tools*, 8th Summer School Medicinal Chemistry, Regensburg, **September 2016**.

Dukorn S., Keller M., Kuhn K., Cabrele C., Bernhardt G., Buschauer A., *Molecular tools for the NPY Y_4 receptor: Fluorescence- and radiolabelled [Lys^4,Nle^{17,30}]hPP*, 11th International NPY-PYY-PP Meeting, Leipzig, **August 2015**.

Dukorn S., Marino J., Zerbe O., Bernhardt G. and Buschauer A., *[^{3}H]Propionyl-K^{4}hPP: A novel radioligand for the neuropeptide Y (NPY) Y_4 receptor,* 7th Summer School Medicinal Chemistry, Regensburg, **September 2014**.

Dukorn, S., Marino, J., Zerbe, O., Bernhardt, G., Buschauer, A., *A valuable tool for the NPY Y_4 receptor: [^{3}H]Propionyl - K^{4}hPP*, Annual Meeting “Frontiers in Medicinal Chemistry”, Tübingen, **March 2014**.

Contents

Abbreviations

α	intrinsic activity or selectivity factor
AC	adenylyl cyclase
Ala	alanine
AMP	adenosine monophosphate
aq.	aqueous
Arg	arginine
Asp	aspartate (-acid)
a_s	specific activity
atm	atmosphere
ATP	adenosine 5'-triphosphate
a_v	activity concentration
B_{max}	maximum number of binding sites
Bq	becquerel
BSA	bovine serum albumin
c	concentration
cAMP	cyclic 3',5'-adenosine monophosphate
calcd.	calculated
$[Ca^{2+}]_i$	intracellular calcium ion concentration
cDNA	complementary DNA
CHO	chinese hamster ovary
Ci	curie
CLSM	confocal laser scanning microscopy
CNS	central nervous system
cpm	counts per minute
CRE	cAMP response element
CREB	cAMP response element binding protein
Cys	cysteine
DCC	N,N´-dicyclohexylcarbodiimide
DCM	dichloromethane
DIPEA	N,N´-diisopropyl-ethylamine
DMEM	Dulbecco's modified eagle medium
DMF	dimethylformamide
DMSO	dimethylsulfoxide
DNA	deoxyribonucleic acid
dpm	disintegrations per minute

DSMZ	Deutsche Sammlung von Mikroorganismen und Zellkulturen
DTT	dithiothreitole
EC_{50}	agonist concentration which induces 50 % of maximum response
ECL	extracellular loop
EDTA	ethylenediaminetetraacetic acid
EGF	epidermal growth factor
EGTA	ethyleneglycol-O,O'-bis(2-aminoethyl)-N,N,N',N'-tetraacetic acid
eq	equivalent(s)
E_{max}	maximal response relative to the endogenous ligand (1.00)
EtOH	ethanol
EMEM	Eagle's minimum essential medium
FACS	fluorescence activated cell sorter
FCS	fetal calf serum
Fl-4	fluorescence channel of the flow cytometer
FLIPR	fluorescence imaging plate reader
FRET	fluorescence-resonance energy transfer
FSK	forskolin
G418	geneticin
$G\alpha_{i2}$	α-subunit of the G-protein that inhibit adenylyl cyclase
Gβγ	βγ-subunits of a heterotrimeric G-protein
GF/C	glass microfiber, grade c (fine)
GDP	guanosine diphosphate
Gln	glutamine
Glu	glutamate
Gly	glycine
Gly-Gly	glycyl-glycine
GPCR	G-protein coupled receptor
GRK	G-protein coupled receptor kinase
GTP	guanosine triphosphate
GTPγS	guanosine 5'-thiotriphosphate
h	hour(s)/human (in context with receptor subtypes)
HEC-1B	human endometrial carcinoma
HEL	human erythroleukemia
HEPES	2-(4-(2-hydroxyethyl)-1-piperazinyl)ethansulfonic acid
HEK293 cells	human embryonic kidney cells
HPLC	high-pressure liquid chromatography
HR-MS	high resolution mass spectrometry

HTS	high throughput screening
Hz	hertz
IC_{50}	antagonist concentration which suppresses 50 % of an agonist induced effect or displaces 50 % of a labeled ligand from the binding site
ICER	induceable cAMP early repressor
ICL	intracellular loop
Ile	isoleucine
IP_3	inositol-1,4,5-trisphosphate
IR	infrared
k	retention (capacity) factor
K_b	dissociation constant derived from a functional assay
K_d	dissociation constant derived from a saturation experiment or kinetics
K_i	dissociation constant derived from a competition binding assay
k_{obs}	observed/macroscopic association rate constant
k_{off}	dissociation rate constant
k_{on}	association rate constant
L	liter
Leu	leucine
Lys	lysine
m	milli or mouse (in context with a receptor name)
M	molar (mol/L) or mega
mAU	milli absorbance units
MCF-7 cells	human breast adenocarcinoma cells
MeCN	acetonitrile
MeOH	methanol
Met	methionine
min	minute(s)
µ	micro
MS	mass spectrometry
mtAEQ	mitochondrially targeted apoaequorin
MW	molecular weight
n	nano or amount of substance
NaOH	sodium hydroxide
n.d.	not determined
N^G	guanidino-nitrogen
NHS	N-hydroxysuccinimide
Nle	norleucine

nm	nanometer
NMR	nuclear magnetic resonance
NPY	neuropeptide Y
p	porcine
PBS	phosphate buffered saline
pEC_{50}	negative decade logarithm of EC_{50}
PEI	polyethyleneimine
Phe	phenylalanine
PKA, PKC	protein kinase A or C, respectively
pK_i	negative decade logarithm of K_i
PP	Pancreatic polypeptide
ppm	parts per million
Pro	proline
PYY	peptide YY
QY	quantum yield
ref	reference
RGS	regulators of G-protein signaling
RLU	relative luminescence units
RP	reversed phase
rpm	revolutions per minute
rt	room temperature
s	second(s)
SEM	standard error of the mean
Ser	serine
Sf9	Spodoptera frugiperda (an insect cell line)
t_0	hold-up time
t_R	retention time
TFA	trifluoroacetic acid
THF	tetrahydrofurane
TM	transmembrane domain
Tris	tris(hydroxymethyl)aminomethane
UV	ultraviolet
Vis	visible
w/v	weight per volume
v/v	volume per volume
Y_n	NPY receptor subtypes, n = 1, 2, 4, 5, 6

Chapter 1

Introduction

1.1 Neuropeptide Y

Neuropeptide Y (NPY), a highly conserved 36-amino acid peptide neurotransmitter, was first isolated by Tatemoto et al. from porcine brain in 1982 (Tatemoto et al., 1982). It is one of the most abundant neuropeptides in the mammalian brain and structurally and functionally related to pancreatic peptide (PYY) and pancreatic polypeptide (PP) (Figure 1.1) (Michel et al., 1998). For all these peptides, C-terminal amidation is essential for biological activity (Wahlestedt et al., 1986). Between mammals, 22 positions are identical in all NPY sequences known (for reviews cf. (Merten and Beck-Sickinger, 2006; Mörl and Beck-Sickinger, 2015)).

YPSKPDNPGEDAPAEDMARYYSALRHYINLITRQRY-NH_2 hNPY (**1**)
YPSKPDNPGEDAPAEDLARYYSALRHYINLITRQRY-NH_2 pNPY (**2**)
YPIKPEAPGEDASPEELNRYYASLRHYLNLVTRQRY-NH_2 hPYY
APLEPVYPGDNATPEQMAQYAADLRRYINMLTRPRY-NH_2 hPP (**3**)

Figure 1.1. Amino acid sequences of hNPY, pNPY hPYY and hPP. Constant positions in all species for the peptides are underlined. The seven constant residues within the NPY-family are indicated (boxed) (Larhammar, 1996).

In the periphery NPY is abundant in sympathetic neurons, where it is co-stored and co-released with noradrenaline, and it was also found in the parasympathetic nervous system (Sundler et al., 1993; von Hörsten et al., 2004). In the central nervous system (CNS) NPY was found in numerous brain regions including basal ganglia, hypothalamus, amygdala, hippocampus, locus coeruleus, nucleus accumbens, and the cerebral cortex (Chronwall, 1985; Fetissov et al., 2004; Heilig and Widerlov, 1995). The NPY receptors are involved in the regulation of numerous physiological processes such as blood pressure, food intake, pain sensitivity, anxiety/anxiolysis, depression and hormone release (Brothers and Wahlestedt, 2010; Yulyaningsih et al., 2011). Recent reviews give an overview of the role of NPY (Gotzsche and Woldbye, 2016; Reichmann and Holzer, 2016; Tasan et al., 2016).

1.2 NPY receptors and their ligands

The physiological functions of NPY family of peptides are mediated by Y receptors which belong to the rhodopsin-like G_i coupled G protein-coupled receptor (GPCR) family. Four functional NPY receptor subtypes, designated Y_1R, Y_2R, Y_4R, and Y_5R, have been identified in humans (Blomqvist and Herzog, 1997; Bromee et al., 2006; Salaneck et al., 2008). Among the NPY receptors, the Y_4R is unique, as it prefers PP over NPY and PYY as the endogenous ligand. The y_6R is functional expressed in rabbit and mouse, while no y_6 gene was detected in rat (Burkhoff et al., 1998). In humans and other primates, the receptor is non-functional because of a frameshift mutation (single base deletion) in the third intracellular

loop leading to a truncated receptor protein after the 6th transmembrane region (Rose et al., 1997). The main signal transduction pathway of NPY receptors results in an inhibition of adenylyl cyclase mediated cAMP formation (Holliday et al., 2004; Michel et al., 1998). Additionally, elevation of the intracellular calcium concentration after NPY receptor stimulation has been shown in cells natively expressing (Michel et al., 1998; Müller et al., 1997) as well as in cells heterologously expressing NPY receptors (Bard et al., 1995; Gerald et al., 1995; Grouzmann et al., 2001; Selbie et al., 1995). Nevertheless, the Ca^{2+} response upon NPY receptor activation depends on the cell type (Wahlestedt et al., 1986). An overview of the most important characteristics of NPY receptors is given in Table 1.1 (for NPY receptor ligands see sections 1.2.1 and 1.2.2).

Table 1.1. Characteristics of the mammalian NPY receptor subtypes (adapted from (Merten and Beck-Sickinger, 2006)).

Y_1R	
Receptor properties	384 amino acids (AA), highly conserved, 90–96% overall identity across mammals
Expression pattern	Cerebral cortex, vascular smooth muscle cells, colon, human adipocytes
Physiological functions	Analgesia, anxiolysis, circadian rhythm regulation, endocrine regulation, increase in feeding, sedative, vasoconstriction
Ligand binding profile	NPY ≈ PYY ≈ [Leu^{31},Pro^{34}]NPY > NPY2-36 ≈ NPY3-36 ≥ PP ≈ NPY13-36
Y_2R	
Receptor properties	381 AA, highly conserved across species (sequence homology > 90%; ~ 80% identity mammalian compared to chicken Y_2R)
Expression pattern	Nerve fibers, hippocampus, intestine, blood vessels
Physiological functions	Angiogenesis, anxiogenesis, enhanced memory, decreased neurotransmitter secretion, decrease feeding, anticonvulsant
Ligand binding profile	PYY > PYY3-36 ≈ NPY3-36 ≈ NPY2-36 ≈ NPY13-36 >>[Leu^{31},Pro^{34}]NPY
Y_4R	
Receptor properties	375 AA, 74–86% sequence homology across species
Expression pattern	Hypothalamus, skeletal muscle, thyroid gland, stomach, small intestine, colon
Physiological functions	Pancreatic secretion, gall bladder contraction, LH secretion, decrease feeding
Ligand binding profile	PP ≥ GW1229 > PYY ≥ NPY > NPY2-36

Y_5R	
Receptor properties	445 AA, 82–95% overall identity between different mammals
Expression pattern	Hypothalamus, cerebral cortex, intestine, ovary, spleen, pancreas, skeletal muscle
Physiological functions	Circadian rhythm regulation, increase in feeding, anticonvulsant, reproduction
Ligand binding profile	NPY ≈ PYY ≈ NPY2-36 ≈ [Leu^{31},Pro^{34}]NPY > hPP >[D-Trp^{32}]NPY > NPY13-36 > rPP

1.2.1 The NPY Y_1, Y_2 and Y_5 receptors and their ligands

The Y_1 receptor was the first “PP-fold peptide” binding receptor to be cloned. Across all species, the Y_1 receptor displays more than 95% amino acid sequence identity in the transmembrane regions (Larhammar et al., 2001). High affinity for NPY and PYY and a low affinity for PP are characteristic of the Y_1 receptor (Cabrele and Beck-Sickinger, 2000). In the last years, a library of selective and highly potent non-peptidic Y_1R antagonists with affinities in the nanomolar and subnanomolar range have been developed, including the argininamides BIBP3226 and BIBO3304 (Rudolf et al., 1994; Wieland et al., 1998) (for a recent review on Y_1 antagonists cf. (Moreno-Herrera et al., 2014). Bioisosteric replacement of the guanidine group in BIBP3226 by an acyl- or carbamoylguanidine moiety afforded ligands with increased Y_1R affinity, including the radiolabeled Y_1R antagonists [^{3}H]UR-MK114 (Keller et al., 2008) and [^{3}H]UR-MK136 (Keller et al., 2011). Both compounds turned out to be high-affinity selective radioligands for the Y_1R. Recently, focussing on N^{ω}-carbamoylated argininamides, [^{3}H]UR-MK299 (Keller et al., 2015b) proved to be by far superior to the homolog [^{3}H]UR-MK136 regarding affinity and target residence time. Structural modifications of the argininamide-type Y_1R antagonist BIBO3304 were tolerated as well and led to highly selective antagonists with affinities in the single-digit nanomolar range, suggesting the preparation of radiolabeled analogs (Keller et al., 2015a). A selection of non-peptidic Y_1R antagonists is shown in Figure 1.2.

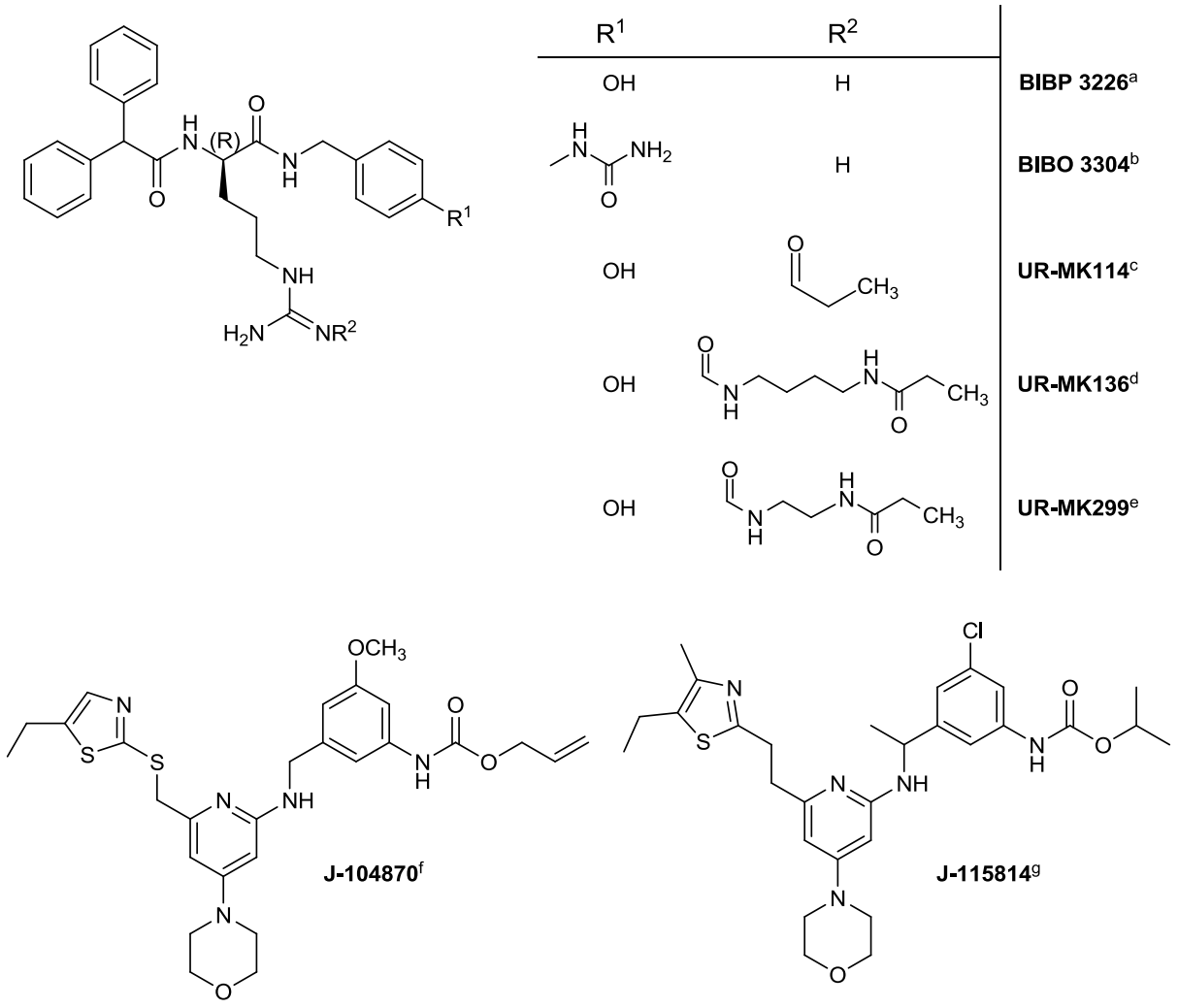

Figure 1.2. Examples of non-peptidic selective Y_1R ligands. [a](Rudolf et al., 1994), [b](Wieland et al., 1998), [c](Keller et al., 2008), [d](Keller et al., 2011), [e](Keller et al., 2015b), [f](Kanatani et al., 1999), [g](Kanatani et al., 2001)

Originally, the Y_2 receptor was postulated based on pharmacological studies with amino terminally truncated fragments of NPY and PYY, such as NPY3-36 and NPY13-36, using vascular preparations (Wahlestedt et al., 1986). In contrast to the Y_1 receptor, the truncated peptides were full agonists with similar potency as the native peptides at the postulated Y_2 receptor. A detailed structural model of NPY bound to the Y_2R suggested that larger peptide ligands also share the proposed common ligand binding cradle of rhodopsin-like GPCRs (Venkatakrishnan et al., 2013), even if they are not expected to bind deep in the transmembrane bundle. It was concluded from NMR studies that changes in the C-terminal amino acids can easily disturb receptor binding or switch receptor selectivity (Kaiser et al., 2015; Pedragosa Badia et al., 2013). Human cells endogenously expressing the Y_2R, for example SMS-KAN (Shigeri and Fujimoto, 1994), LN319 (Beck-Sickinger et al., 1992), CHP-234 (Lynch et al., 1994) and MHH-NB-11 cells (Hofliger et al., 2003), have a broad application for investigations on Y_2R mediated cellular reponses. Very recently, a molecular

basis was established to elucidate the actions of chicken Y_2, Y_5 and Y_7 receptors and their ligands in birds which may be helpful to uncover the conserved roles of these ligand-receptor pairs in vertebrates (He et al., 2016).

In 1999 the argininamide BIIE0246 was described as the first potent and selective Y_2R antagonist (Doods et al., 1999; Dumont et al., 2000). In the last decade, the Y_2R was put into focus as a potential therapeutic target, not least by brain penetrant, orally available Y_2R antagonists such as JNJ-31020028 (Shoblock et al., 2010), JNJ-5207787 (Bonaventure et al., 2004), SF-11 (Brothers et al., 2010) and analogs (cf. review (Mittapalli and Roberts, 2014). In our workgroup, a library of derivatives of the argininamide BIIE0246, including radiolabeled and fluorescence-labeled ligands, was synthesized and characterized at CHO cells stably expressing the hY_2R (Pluym et al., 2011). Most compounds showed Y_2R antagonistic activities and binding affinities similar to those of BIIE0246, confirming that the guanidine–acylguanidine replacement is an effective non-conventional bioisosteric approach (Pluym et al., 2011). Acylation with succinimidyl [^{3}H]propionate resulted in selective non-peptide radioligands [^{3}H]UR-PLN196 and [^{3}H]UR-PLN208 as pharmacological tools (Baumeister, 2014; Pluym et al., 2013). Very recently, docking studies showed that binding sites of BIIE0246 and SF-11 derivatives overlap with that of the endogenous agonist NPY. It is suggested that these antagonists share the same deep, hydrophobic binding pocket ($L^{4.60}$, $L^{5.46}$, $L^{6.51}$) and interact with TM2 and TM7 ($Y^{2.64}$, $F^{7.35}$). The interaction with $D^{6.59}$ is only observed in case of BIIE0246 (Burkert et al., 2016). A selection of Y_2R ligands is depicted in Figure 1.3.

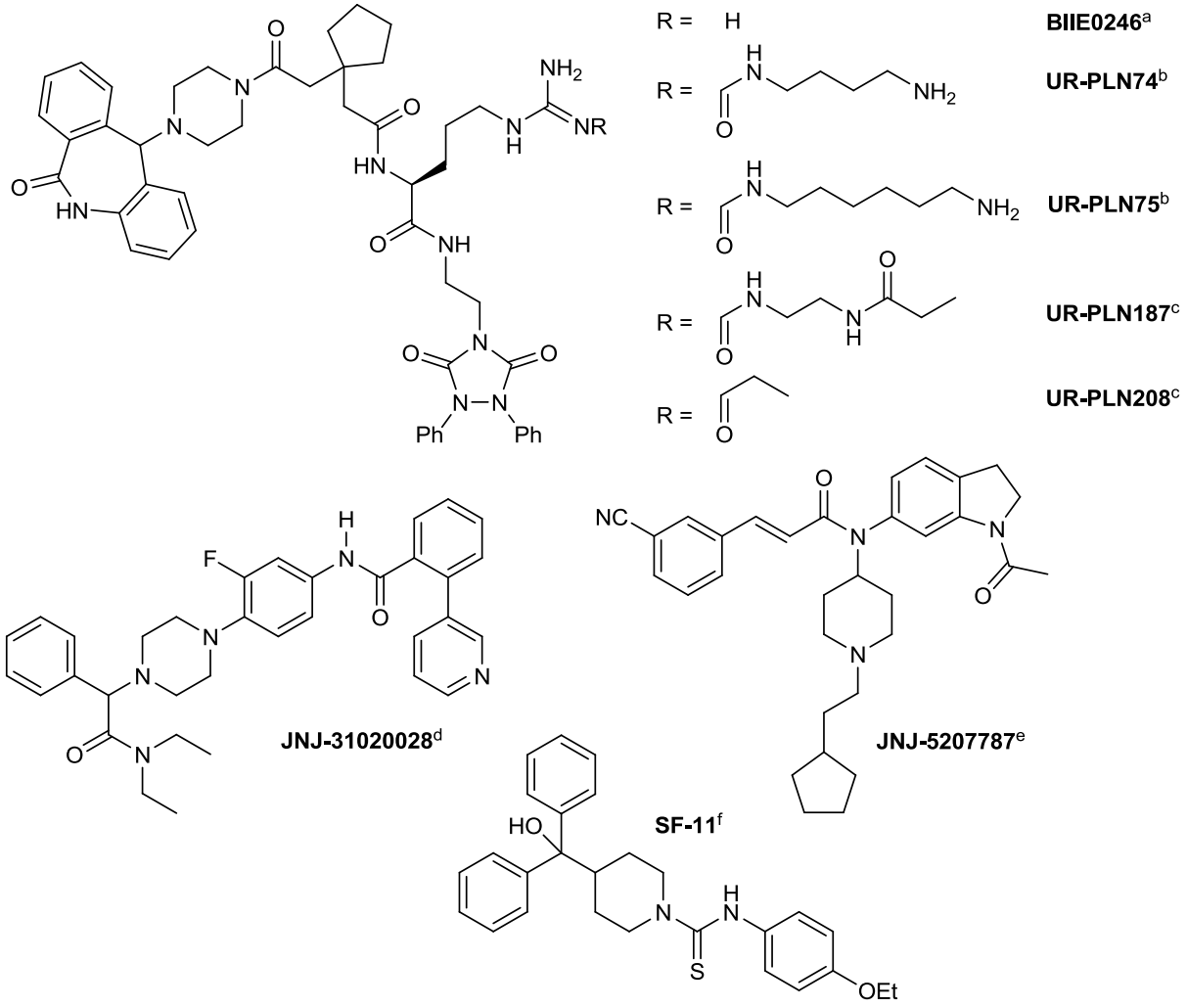

Figure 1.3. Structures of selected Y_2R antagonists. [a](Doods et al., 1999), [b](Pluym et al., 2013), [c](Baumeister, 2014), [d](Shoblock et al., 2010), [e](Bonaventure et al., 2004), [f](Brothers and Wahlestedt, 2010)

In 1992, the Y_5 receptor was first proposed as a variant of the Y_1R based on the observation that NPY and NPY2-36 produced a strong increase in food intake after intracerebroventricular administration in rats (Stanley et al., 1992). The first Y_5 selective agonist [Ala^{31},Aib^{32}]NPY (Aib = aminoisobutyric acid) was active in a cAMP assay and was also able to induce feeding in rats (Cabrele et al., 2000). In 1997, the first selective Y_5R antagonist was reported (Criscione L, 1997). CGP 71683A showed more than 1000-fold affinity to the Y_5R compared to the Y_1, Y_2 and Y_4 subtypes (Criscione et al., 1998). Due to off-target effects CGP 71683A is not an ideal tool to investigate the role of the Y_5 receptor in the regulation of food consumption *in vivo* (Della Zuana et al., 2001). However, the discovery of this compound stimulated the search for Y_5R antagonists as potential drugs for the treatment of obesity (Moreno-Herrera et al., 2014). Meanwhile, this approach is no longer considered promising. Very recently, a correlation between high serum NPY and metastases was reported. Increased Y_5R expression in angioinvasive neuroblastoma implicates that the

NPY/Y_5R axis as a metastatic pathway and patients with disseminated disease could be identified as a candidate for anti-NPY therapy. Due to high systemic NPY levels with disease relapse, the clinical utility as a minimally invasive biomarker for monitoring neuroblastoma progression could be important in future therapy (Galli et al., 2016). A selection of Y_5R antagonists with K_i values in the low nanomolar range is given in Figure 1.4.

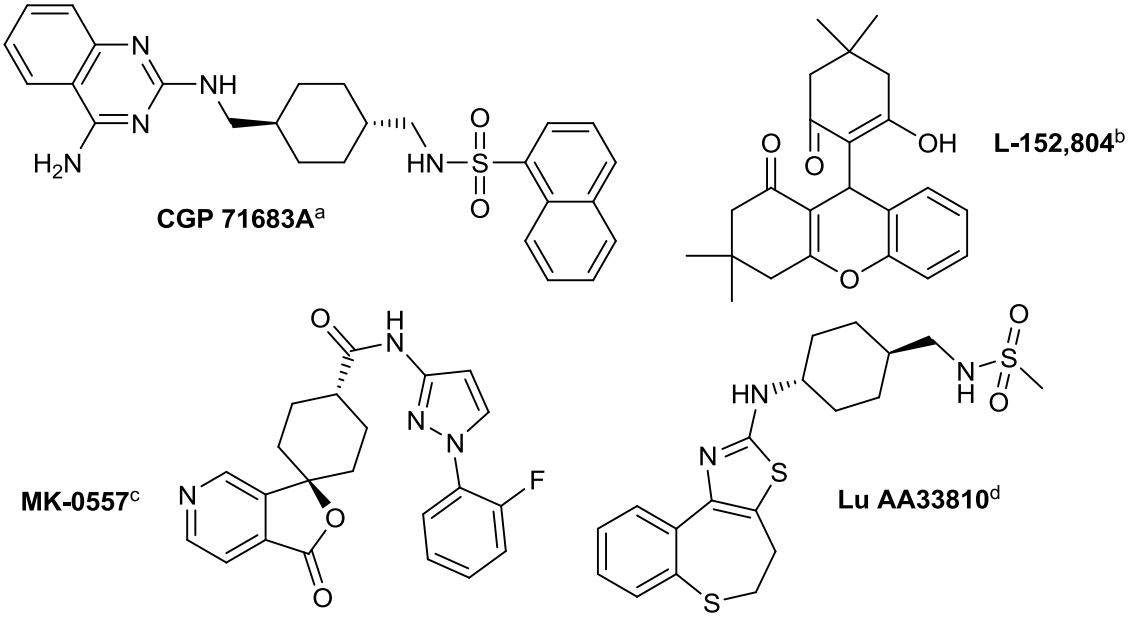

Figure 1.4. Selection of Y_5R antagonists. [a](Criscione et al., 1998), [b](Kanatani et al., 2000), [c](Erondu et al., 2006), [d](Walker et al., 2009)

1.2.2 The NPY Y_4 receptor and its ligands

The Y_4R shares only low sequence identity with the other NPY receptor subtypes and is an exception as it prefers PP as endogenous ligand (Lundell et al., 1995). First insights into the complex binding pocket of the hY_4R system, derived from a combination of modelling and mutagenesis, were recently described. According to this study the top of trans-membrane helix 2 (TM2) and the top of transmembrane helices 6 and 7 (TM6-TM7) form the core of the peptide binding pocket (Pedragosa-Badia et al., 2014).

The Y_4R shares the highest sequence identity (42%) with the Y_1R. A similarity between both receptors is also reflected by the Y_4R affinity of several ligands, which were initially designed as Y_1R antagonists, for example, the 'dimeric ligands' GW1229 (**4**) (Parker et al., 1998), a Y_1 antagonist/Y_4 agonist, and the non-peptidic Y_1 antagonist/Y_4 antagonist UR-MK188 (Keller et al., 2013). This suggests that Y_4R antagonists may be identified among or developed from known Y_1R ligands. Another example of a highly potent Y_4 receptor agonist is *D/L*-2,7-diaminooctanedioyl-bis(YRLRY-NH_2) (BVD-74D), a diastereomeric mixture of *D/L*-(2,7)-BVD-

74D (Balasubramaniam et al., 2006). Derived from the C-terminal pentapeptide of hPP, the respective pure diastereomers and a series of homo- and heterodimeric analogs were synthesized in our working group. In binding and functional cellular assays, (*2R,7R*)-BVD-74D was superior to (*2S,7S*)-BVD-74D, and two analogs gave access to the corresponding tritiated high affinity Y_4R radioligands [^{3}H]UR-KK193 (**5**) and [^{3}H]UR-KK200 (Kuhn et al., 2016). Recently, a fluorescently labeled analog of BVD-74D, (sulfo-Cy5) labeled (*R,R*)-analog (mono-sCy5-(*2R,7R*)-sub(YRLRY-NH_2)$_2$) was reported as a novel Y_4R agonist with nanomolar affinity (Liu et al., 2016).

With regard to the potential therapeutic use of Y_4R agonists, peptides with increased stability in plasma were developed. Lipidation and PEGylation of PP not only prolonged plasma half-life but also inhibited arrestin recruitment and receptor internalization (Mäde et al., 2014). Behavioural experiments with mice upon peripheral injection of a novel PEGylated derivative of PP, the selective Y_4R agonist [K^{30}(PEG2)]hPP2-36, suggest that these derivatives penetrate across the blood-brain barrier (Verma et al., 2016).

Truncated hPP analogs such as [Nle^{30}]hPP25−36 and [Leu^{34}]pNPY25−36 were found to be Y_4R selective partial agonists (Berlicki et al., 2013). [Ala^{27}]hPP and [Leu^{27}]hPP were used to localize specific interactions between hPP and the hY_4R (Pedragosa-Badia et al., 2014). Full-length PP/NPY chimeras were designed and characterized by Cabrele et al. (Cabrele et al., 2001). Aiming at labeled hPP derivatives using amino-reactive reagents the amino acid in position 4 was replaced by lysine ([Lys^4]hPP, **7**). This gave access to the fluorescent peptides S0586- and cy5-[Lys^4]hPP, which turned out to be valuable pharmacological tools for the investigation of Y_4R ligands, e. g. by flow cytometry or confocal microscopy (Ziemek, 2006; Ziemek et al., 2007). A selection of Y_4R ligands is given in Figure 1.5.

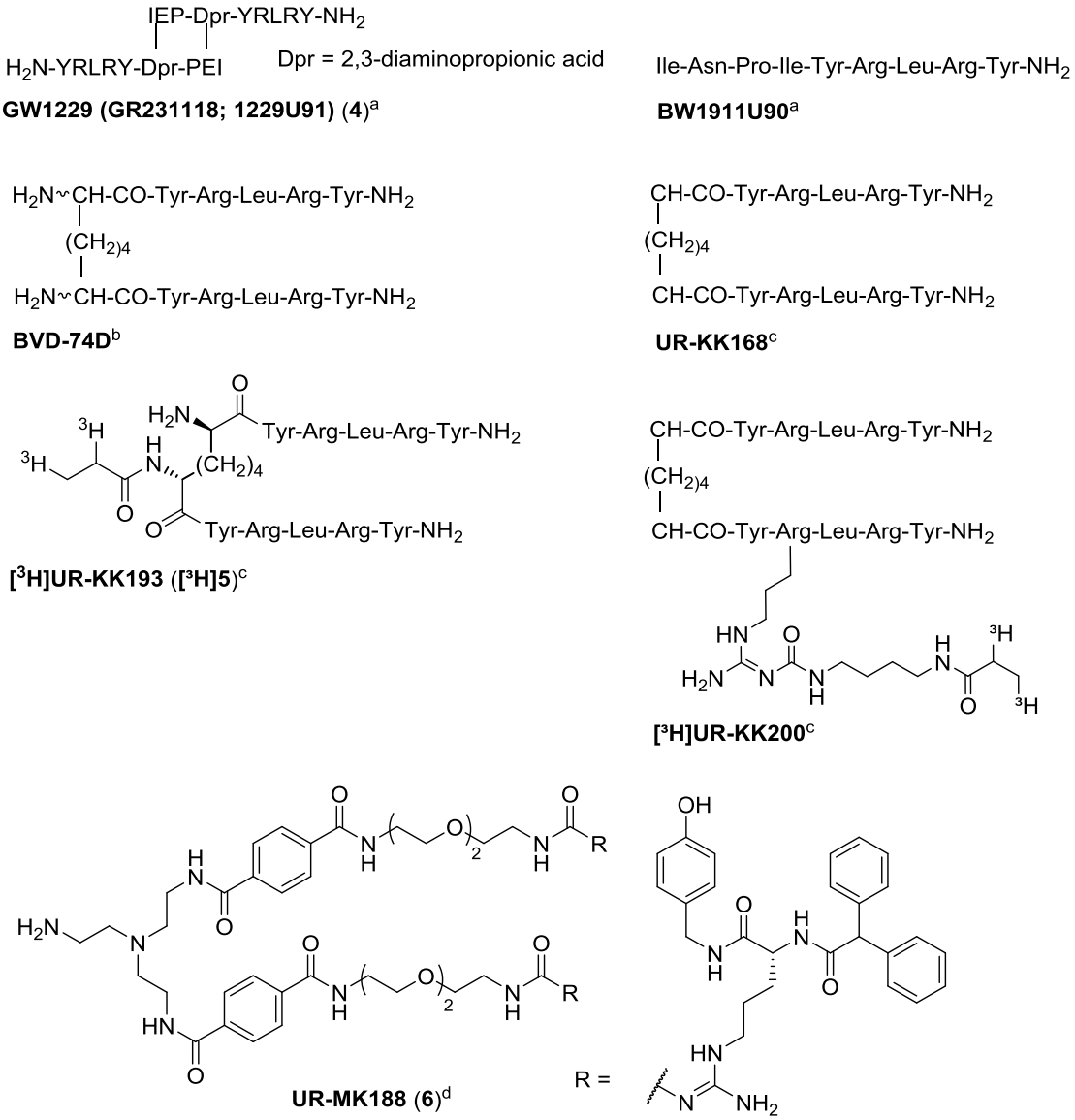

Figure 1.5. Structures of selected peptidic agonists and the non-peptidic antagonist UR-MK188. [a](Parker et al., 1998), [b](Balasubramaniam et al., 2006), [c](Kuhn et al., 2016), [d](Keller et al., 2013)

1.3 Sodium sensitivity of the NPY receptors

GPCR agonist binding and/or G-protein activation may depend on allosteric inhibition by sodium ions. In high-resolution structures of the human A_{2A} adenosine receptor (Liu et al., 2012), the ß$_1$ adrenergic receptor (Miller-Gallacher et al., 2014) and µ-opioid receptor (Huang et al., 2015) in the inactive state, Na^+ allosteric sites were identified. In case of NPY receptors, sensitivity of PP binding to sodium ions and to modulators of sodium transport was reported (Parker et al., 2002; Parker et al., 2000; Parker S.L., 2001; Parker et al., 2001; Parker and Parker, 2000a; b; Parker et al., 1999).

In functional studies, the effects of monovalent cations and anions were investigated using the steady-state GTPase assay at the hY_2R and hY_4R. At the hY_2R no effect of sodium was

observed, whereas the agonistic potency of GW1229 at the hY_4R was decreased by a factor of 8.4 in the presence of sodium (Pop et al., 2011). Very recent results from radioligand binding experiments support previous findings that the affinity of peptidic Y_4R agonists is considerably lower in the presence of sodium ions (Kuhn et al., 2016).

1.4 Tritium- and fluorescence-labeled NPY receptor ligands

1.4.1 Tritiated radioligands

In view of the long half-life and the convenient accessibility tritiated ligands are preferred in our laboratory. Labeling of amine precursors by conjugation with commercially available succinimidyl [^{3}H]propionate has been successfully performed in case of both, peptide agonists and nonpeptide antagonists. For instance, [^{3}H]propionyl-pNPY, acylated at Lys^4, has been used as a universal ligand of Y_1, Y_2 and Y_5 receptors in saturation and competition binding studies(Chang et al., 1988; Keller et al., 2015b; Kuhn et al., 2016; Widdowson and Halaris, 1990). Recently, in search for subtype-selective radioligands, different approaches afforded the tritiated ligands [^{3}H]UR-MK299 (Keller et al., 2015b), an antagonist at the Y_1R, the Y_2R antagonist [^{3}H]UR-PLN196 (Pluym et al., 2013) and the Y_4R selective agonist [^{3}H]UR-KK193 (Kuhn et al., 2016).

1.4.2 Fluorescent ligands for cellular investigations

Fluorescent ligands enable cellular investigations, which are, except for saturation and competition binding, complementary to studies with radioligands. Techniques such as flow cytometry enable the determination of binding affinities of compounds and the binding kinetics of the labeled ligand at the receptor. Furthermore, receptor localization and internalization can be visualized by confocal laser scanning microscopy, which is an indispensable tool for GPCR imaging. For such studies the selection of appropriate fluorophores is essential to optimize the signal-to-noise ratio. In the NPY receptor field, investigations with specifically bound fluorescent peptides, e.g. BODIPY®-NPY peptide analogs led to new insights in internalization and cellular trafficking processes (Dumont et al., 2005). The fluorescent peptide Cy5-pNPY (Schneider et al., 2006; Ziemek et al., 2006) was applied as a universal ligand for Y_1, Y_2 and Y_5 receptors, for example, for the determination of the NPY receptor subtype selectivity of novel compounds (Kaske, 2012; Pluym, 2011). Regarding the preferred synthesis of selective fluorescent ligands, the Py-1 labeled Y_1R antagonist UR-MK22 (Memminger et al., 2012; Schneider et al., 2007) and several Y_2R antagonists with various fluorophores (Pluym, 2011) were synthesized in our working group. For example, the expression of the Y_1R in MCF-7 cells was confirmed by the binding of UR-MK22. Selective Y_4R agonists such as Cy5-[Lys^4]hPP (Ziemek et al., 2007) and a sCy5

labeled fluorescent analog of BVD-74D (Liu et al., 2016) have been used for Y_4R imaging and binding studies.

1.5 References

Balasubramaniam, A.; Mullins, D. E.; Lin, S.; Zhai, W.; Tao, Z.; Dhawan, V. C.; Guzzi, M.; Knittel, J. J.; Slack, K.; Herzog, H.; Parker, E. M. (2006). Neuropeptide Y (NPY) Y4 Receptor Selective Agonists Based on NPY(32−36): Development of an Anorectic Y4 Receptor Selective Agonist with Picomolar Affinity. *Journal of Medicinal Chemistry* 49(8): 2661-2665.

Bard, J. A.; Walker, M. W.; Branchek, T. A.; Weinshank, R. L. (1995). Cloning and functional expression of a human Y4 subtype receptor for pancreatic polypeptide, neuropeptide Y, and peptide YY. *J. Biol. Chem.* 270(45): 26762-26765.

Baumeister, P. (2014). Molecular tools for G-protein coupled receptors: Synthesis, pharmacological characterization and [3H]-labeling of subtype-selective ligands for histamine H4 and NPY Y2 receptors Doctoral Thesis, University of Regensburg, Regensburg.

Beck-Sickinger, A. G.; Grouzmann, E.; Hoffmann, E.; Gaida, W.; Van Meir, E. G.; Waeber, B.; Jung, G. (1992). A novel cyclic analog of neuropeptide Y specific for the Y2 receptor. *Eur. J. Biochem.* 206(3): 957-964.

Berlicki, L.; Kaske, M.; Gutierrez-Abad, R.; Bernhardt, G.; Illa, O.; Ortuno, R. M.; Cabrele, C.; Buschauer, A.; Reiser, O. (2013). Replacement of Thr32 and Gln34 in the C-terminal neuropeptide Y fragment 25-36 by cis-cyclobutane and cis-cyclopentane beta-amino acids shifts selectivity toward the Y(4) receptor. *J. Med. Chem.* 56(21): 8422-8431.

Blomqvist, A. G.; Herzog, H. (1997). Y-receptor subtypes—how many more? *Trends Neurosci.* 20(7): 294-298.

Bonaventure, P.; Nepomuceno, D.; Mazur, C.; Lord, B.; Rudolph, D. A.; Jablonowski, J. A.; Carruthers, N. I.; Lovenberg, T. W. (2004). Characterization of N-(1-Acetyl-2,3-dihydro-1H-indol-6-yl)-3-(3-cyano-phenyl)-N-[1-(2-cyclopen tyl-ethyl)-piperidin-4yl]acrylamide (JNJ-5207787), a small molecule antagonist of the neuropeptide Y Y2 receptor. *J. Pharmacol. Exp. Ther.* 308(3): 1130-1137.

Bromee, T.; Sjodin, P.; Fredriksson, R.; Boswell, T.; Larsson, T. A.; Salaneck, E.; Zoorob, R.; Mohell, N.; Larhammar, D. (2006). Neuropeptide Y-family receptors Y6 and Y7 in chicken. Cloning, pharmacological characterization, tissue distribution and conserved synteny with human chromosome region. *The FEBS journal* 273(9): 2048-2063.

Brothers, S. P.; Saldanha, S. A.; Spicer, T. P.; Cameron, M.; Mercer, B. A.; Chase, P.; McDonald, P.; Wahlestedt, C.; Hodder, P. S. (2010). Selective and brain penetrant neuropeptide y y2 receptor antagonists discovered by whole-cell high-throughput screening. *Molecular Pharmacology* 77(1): 46-57.

Brothers, S. P.; Wahlestedt, C. (2010). Therapeutic potential of neuropeptide Y (NPY) receptor ligands. *EMBO Mol. Med.* 2(11): 429-439.

Burkert, K.; Zellmann, T.; Meier, R.; Kaiser, A.; Stichel, J.; Meiler, J.; Mittapalli, G. K.; Roberts, E.; Beck-Sickinger, A. G. (2016). A Deep Hydrophobic Binding Cavity is the Main Interaction for Different Y2 R Antagonists.

Burkhoff, A. M.; Linemeyer, D. L.; Salon, J. A. (1998). Distribution of a novel hypothalamic neuropeptide Y receptor gene and its absence in rat. *Mol. Brain Res.* 53(1–2): 311-316.

Cabrele, C.; Beck-Sickinger, A. G. (2000). Molecular characterization of the ligand-receptor interaction of the neuropeptide Y family. *J. Pept. Sci.* 6(3): 97-122.

Cabrele, C.; Langer, M.; Bader, R.; Wieland, H. A.; Doods, H. N.; Zerbe, O.; Beck-Sickinger, A. G. (2000). The first selective agonist for the neuropeptide YY5 receptor increases food intake in rats. *J. Biol. Chem.* 275(46): 36043-36048.

Cabrele, C.; Wieland, H. A.; Langer, M.; Stidsen, C. E.; Beck-Sickinger, A. G. (2001). Y-receptor affinity modulation by the design of pancreatic polypeptide/neuropeptide Y chimera led to Y(5)-receptor ligands with picomolar affinity. *Peptides* 22(3): 365-378.

Chang, R. S.; Lotti, V. J.; Chen, T. B. (1988). Specific [3H]propionyl-neuropeptide Y (NPY) binding in rabbit aortic membranes: comparisons with binding in rat brain and biological responses in rat vas deferens. *Biochem. Biophys. Res. Commun.* 151(3): 1213-1219.

Chronwall, B. M. (1985). Anatomy and physiology of the neuroendocrine arcuate nucleus. *Peptides* 6, Supplement 2: 1-11.

Criscione, L.; Rigollier, P.; Batzl-Hartmann, C.; Rueger, H.; Stricker-Krongrad, A.; Wyss, P.; Brunner, L.; Whitebread, S.; Yamaguchi, Y.; Gerald, C.; Heurich, R. O.; Walker, M. W.; Chiesi, M.; Schilling, W.; Hofbauer, K. G.; Levens, N. (1998). Food intake in free-feeding and energy-deprived lean rats is mediated by the neuropeptide Y5 receptor. *J. Clin. Invest.* 102(12): 2136-2145.

Criscione L, Y. Y., Mah R et al.,. Receptor Antagonists. 1997.

Della Zuana, O.; Sadlo, M.; Germain, M.; Feletou, M.; Chamorro, S.; Tisserand, F.; de Montrion, C.; Boivin, J. F.; Duhault, J.; Boutin, J. A.; Levens, N. (2001). Reduced food intake in response to CGP 71683A may be due to mechanisms other than NPY Y5 receptor blockade. *Int. J. Obes. Relat. Metab. Disord.* 25(1): 84-94.

Doods, H.; Gaida, W.; Wieland, H. A.; Dollinger, H.; Schnorrenberg, G.; Esser, F.; Engel, W.; Eberlein, W.; Rudolf, K. (1999). BIIE0246: a selective and high affinity neuropeptide Y Y(2) receptor antagonist. *Eur. J. Pharmacol.* 384(2-3): R3-5.

Dumont, Y.; Cadieux, A.; Doods, H.; Pheng, L. H.; Abounader, R.; Hamel, E.; Jacques, D.; Regoli, D.; Quirion, R. (2000). BIIE0246, a potent and highly selective non-peptide neuropeptide Y Y(2) receptor antagonist. *Br. J. Pharmacol.* 129(6): 1075-1088.

Dumont, Y.; Gaudreau, P.; Mazzuferi, M.; Langlois, D.; Chabot, J. G.; Fournier, A.; Simonato, M.; Quirion, R. (2005). BODIPY-conjugated neuropeptide Y ligands: new fluorescent tools to tag Y1, Y2, Y4 and Y5 receptor subtypes. *Br. J. Pharmacol.* 146(8): 1069-1081.

Erondu, N.; Gantz, I.; Musser, B.; Suryawanshi, S.; Mallick, M.; Addy, C.; Cote, J.; Bray, G.; Fujioka, K.; Bays, H.; Hollander, P.; Sanabria-Bohorquez, S. M.; Eng, W.; Langstrom, B.; Hargreaves, R. J.; Burns, H. D.; Kanatani, A.; Fukami, T.; MacNeil, D. J.; Gottesdiener, K. M.; Amatruda, J. M.; Kaufman, K. D.; Heymsfield, S. B. (2006). Neuropeptide Y5 receptor antagonism does not induce clinically meaningful weight loss in overweight and obese adults. *Cell Metab.* 4(4): 275-282.

Fetissov, S. O.; Kopp, J.; Hokfelt, T. (2004). Distribution of NPY receptors in the hypothalamus. *Neuropeptides* 38(4): 175-188.

Galli, S.; Naranjo, A.; Van Ryn, C.; Tilan, J. U.; Trinh, E.; Yang, C.; Tsuei, J.; Hong, S.-H.; Wang, H.; Izycka-Swieszewska, E.; Lee, Y.-C.; Rodriguez, O. C.; Albanese, C.; Kitlinska, J. (2016). Neuropeptide Y as a Biomarker and Therapeutic Target for Neuroblastoma. *The American Journal of Pathology* 186(11): 3040-3053.

Gerald, C.; Walker, M. W.; Vaysse, P. J.; He, C.; Branchek, T. A.; Weinshank, R. L. (1995). Expression cloning and pharmacological characterization of a human hippocampal neuropeptide Y/peptide YY Y2 receptor subtype. *J. Biol. Chem.* 270(45): 26758-26761.

Gotzsche, C. R.; Woldbye, D. P. (2016). The role of NPY in learning and memory. *Neuropeptides* 55: 79-89.

Grouzmann, E.; Meyer, C.; Burki, E.; Brunner, H. (2001). Neuropeptide Y Y2 receptor signalling mechanisms in the human glioblastoma cell line LN319. *Peptides* 22(3): 379-386.

He, C.; Zhang, J.; Gao, S.; Meng, F.; Bu, G.; Li, J.; Wang, Y. (2016). Molecular characterization of three NPY receptors (Y2, Y5 and Y7) in chickens: Gene structure, tissue expression, promoter identification, and functional analysis. *Gen. Comp. Endocrinol.* 236: 24-34.

Heilig, M.; Widerlov, E. (1995). Neurobiology and clinical aspects of neuropeptide Y. *Crit. Rev. Neurobiol.* 9(2-3): 115-136.

Hofliger, M. M.; Castejon, G. L.; Kiess, W.; Beck Sickinger, A. G. (2003). Novel cell line selectively expressing neuropeptide Y-Y2 receptors. *Journal of receptor and signal transduction research* 23(4): 351-360.

Holliday, N. D.; Michel, M. C.; Cox, H. M. (2004). NPY Receptor Subtypes and Their Signal Transduction. In *Neuropeptide Y and Related Peptides*, Michel, M. C., Ed. Springer Berlin Heidelberg: Berlin, Heidelberg, pp 45-73.

Huang, W.; Manglik, A.; Venkatakrishnan, A. J.; Laeremans, T.; Feinberg, E. N.; Sanborn, A. L.; Kato, H. E.; Livingston, K. E.; Thorsen, T. S.; Kling, R. C.; Granier, S.; Gmeiner, P.; Husbands, S. M.; Traynor, J. R.; Weis, W. I.; Steyaert, J.; Dror, R. O.; Kobilka, B. K. (2015). Structural insights into [micro]-opioid receptor activation. *Nature* 524(7565): 315-321.

Kaiser, A.; Muller, P.; Zellmann, T.; Scheidt, H. A.; Thomas, L.; Bosse, M.; Meier, R.; Meiler, J.; Huster, D.; Beck-Sickinger, A. G.; Schmidt, P. (2015). Unwinding of the C-Terminal Residues of Neuropeptide Y is critical for Y(2) Receptor Binding and Activation. *Angew. Chem. Int. Ed. Engl.* 54(25): 7446-7449.

Kanatani, A.; Hata, M.; Mashiko, S.; Ishihara, A.; Okamoto, O.; Haga, Y.; Ohe, T.; Kanno, T.; Murai, N.; Ishii, Y.; Fukuroda, T.; Fukami, T.; Ihara, M. (2001). A typical Y1 receptor regulates feeding behaviors: effects of a potent and selective Y1 antagonist, J-115814. *Mol. Pharmacol.* 59(3): 501-505.

Kanatani, A.; Ishihara, A.; Iwaasa, H.; Nakamura, K.; Okamoto, O.; Hidaka, M.; Ito, J.; Fukuroda, T.; MacNeil, D. J.; Van der Ploeg, L. H.; Ishii, Y.; Okabe, T.; Fukami, T.; Ihara, M. (2000). L-152,804: orally active and selective neuropeptide Y Y5 receptor antagonist. *Biochem. Biophys. Res. Commun.* 272(1): 169-173.

Kanatani, A.; Kanno, T.; Ishihara, A.; Hata, M.; Sakuraba, A.; Tanaka, T.; Tsuchiya, Y.; Mase, T.; Fukuroda, T.; Fukami, T.; Ihara, M. (1999). The novel neuropeptide Y Y(1) receptor antagonist J-104870: a potent feeding suppressant with oral bioavailability. *Biochem. Biophys. Res. Commun.* 266(1): 88-91.

Kaske, M. (2012). In search for potent and selective NPY Y4 receptor ligands: acylguanidines, argininamides and peptide analogs *Thesis*.

Keller, M.; Bernhardt, G.; Buschauer, A. (2011). [3H]UR-MK136: A Highly Potent and Selective Radioligand for Neuropeptide Y Y1 Receptors. *ChemMedChem* 6(9): 1566-1571.

Keller, M.; Kaske, M.; Holzammer, T.; Bernhardt, G.; Buschauer, A. (2013). Dimeric argininamide-type neuropeptide Y receptor antagonists: Chiral discrimination between Y1 and Y4 receptors. *Bioorg. Med. Chem.* 21(21): 6303-6322.

Keller, M.; Pop, N.; Hutzler, C.; Beck-Sickinger, A. G.; Bernhardt, G.; Buschauer, A. (2008). Guanidine−Acylguanidine Bioisosteric Approach in the Design of Radioligands: Synthesis of a Tritium-Labeled NG-Propionylargininamide ([3H]-UR-MK114) as a Highly Potent and Selective Neuropeptide Y Y1 Receptor Antagonist. *J. Med. Chem.* 51(24): 8168-8172.

Keller, M.; Schindler, L.; Bernhardt, G.; Buschauer, A. (2015a). Toward Labeled Argininamide-Type NPY Y1 Receptor Antagonists: Identification of a Favorable Propionylation Site in BIBO3304. *Arch. Pharm.* 348(6): 390-398.

Keller, M.; Weiss, S.; Hutzler, C.; Kuhn, K. K.; Mollereau, C.; Dukorn, S.; Schindler, L.; Bernhardt, G.; König, B.; Buschauer, A. (2015b). Nω-Carbamoylation of the Argininamide Moiety: An Avenue to Insurmountable NPY Y1 Receptor Antagonists and a Radiolabeled Selective High-Affinity Molecular Tool ([3H]UR-MK299) with Extended Residence Time. *J. Med. Chem.* 58(22): 8834-8849.

Kuhn, K. K.; Ertl, T.; Dukorn, S.; Keller, M.; Bernhardt, G.; Reiser, O.; Buschauer, A. (2016). High Affinity Agonists of the Neuropeptide Y (NPY) Y4 Receptor Derived from the C-Terminal Pentapeptide of Human Pancreatic Polypeptide (hPP): Synthesis, Stereochemical Discrimination, and Radiolabeling. *J. Med. Chem.* 59(13): 6045-6058.

Larhammar, D.; Wraith, A.; Berglund, M. M.; Holmberg, S. K.; Lundell, I. (2001). Origins of the many NPY-family receptors in mammals. *Peptides* 22(3): 295-307.

Liu, M.; Mountford, S. J.; Richardson, R. R.; Groenen, M.; Holliday, N. D.; Thompson, P. E. (2016). Optically Pure, Structural, and Fluorescent Analogues of a Dimeric Y4

Receptor Agonist Derived by an Olefin Metathesis Approach. *J. Med. Chem.* 59(13): 6059-6069.

Liu, W.; Chun, E.; Thompson, A. A.; Chubukov, P.; Xu, F.; Katritch, V.; Han, G. W.; Roth, C. B.; Heitman, L. H.; Ijzerman, A. P.; Cherezov, V.; Stevens, R. C. (2012). Structural Basis for Allosteric Regulation of GPCRs by Sodium Ions. *Science* 337: 232.

Lundell, I.; Blomqvist, A. G.; Berglund, M. M.; Schober, D. A.; Johnson, D.; Statnick, M. A.; Gadski, R. A.; Gehlert, D. R.; Larhammar, D. (1995). Cloning of a human receptor of the NPY receptor family with high affinity for pancreatic polypeptide and peptide YY. *J. Biol. Chem.* 270(49): 29123-29128.

Lynch, J. W.; Lemos, V. S.; Bucher, B.; Stoclet, J. C.; Takeda, K. (1994). A pertussis toxin-insensitive calcium influx mediated by neuropeptide Y2 receptors in a human neuroblastoma cell line. *J. Biol. Chem.* 269(11): 8226-8233.

Mäde, V.; Babilon, S.; Jolly, N.; Wanka, L.; Bellmann-Sickert, K.; Diaz Gimenez, L. E.; Morl, K.; Cox, H. M.; Gurevich, V. V.; Beck-Sickinger, A. G. (2014). Peptide modifications differentially alter G protein-coupled receptor internalization and signaling bias. *Angew. Chem. Int. Ed. Engl.* 53(38): 10067-10071.

Memminger, M.; Keller, M.; Lopuch, M.; Pop, N.; Bernhardt, G.; von Angerer, E.; Buschauer, A. (2012). The neuropeptide y y(1) receptor: a diagnostic marker? Expression in mcf-7 breast cancer cells is down-regulated by antiestrogens in vitro and in xenografts. *PLoS One* 7(12): e51032.

Merten, N.; Beck-Sickinger, A. G. (2006). Molecular ligand-receptor interaction of the NPY/PP peptide family. *NPY Family of Peptides in Neurobiology, Cardiovascular and Metabolic Disorders: from Genes to Therapeutics* (95): 35-62.

Michel, M. C.; Beck-Sickinger, A.; Cox, H.; Doods, H. N.; Herzog, H.; Larhammar, D.; Quirion, R.; Schwartz, T.; Westfall, T. (1998). XVI. International Union of Pharmacology recommendations for the nomenclature of neuropeptide Y, peptide YY, and pancreatic polypeptide receptors. *Pharmacol. Rev.* 50(1): 143-150.

Miller-Gallacher, J. L.; Nehmé, R.; Warne, T.; Edwards, P. C.; Schertler, G. F. X.; Leslie, A. G. W.; Tate, C. G. (2014). The 2.1 Å Resolution Structure of Cyanopindolol-Bound β1-Adrenoceptor Identifies an Intramembrane Na+ Ion that Stabilises the Ligand-Free Receptor. *PLOS ONE* 9(3): e92727.

Mittapalli, G. K.; Roberts, E. (2014). Ligands of the neuropeptide Y Y2 receptor. *Bioorg. Med. Chem. Lett.* 24(2): 430-441.

Moreno-Herrera, A.; Garcia, A.; Palos, I.; Rivera, G. (2014). Neuropeptide Y1 and Y5 Receptor Antagonists as Potential Anti-Obesity Drugs. Current Status. *Mini reviews in medicinal chemistry*.

Mörl, K.; Beck-Sickinger, A. G. (2015). Intracellular Trafficking of Neuropeptide Y Receptors. *Progress in molecular biology and translational science* 132: 73-96.

Müller, M.; Knieps, S.; Geßele, K.; Dove, S.; Bernhardt, G.; Buschauer, A. (1997). Synthesis and Neuropeptide Y Y1 Receptor Antagonistic Activity of N,N-Disubstituted ω-Guanidino- and ω-Aminoalkanoic Acid Amides. *Arch. Pharm.* 330(11): 333-342.

Parker, E. M.; Babij, C. K.; Balasubramaniam, A.; Burrier, R. E.; Guzzi, M.; Hamud, F.; Gitali, M.; Rudinski, M. S.; Tao, Z.; Tice, M.; Xia, L.; Mullins, D. E.; Salisbury, B. G. (1998). GR231118 (1229U91) and other analogues of the C-terminus of neuropeptide Y are potent neuropeptide Y Y1 receptor antagonists and neuropeptide Y Y4 receptor agonists. *Eur. J. Pharmacol.* 349(1): 97-105.

Parker, M. S.; Lundell, I.; Parker, S. L. (2002). Pancreatic polypeptide receptors: affinity, sodium sensitivity and stability of agonist binding. *Peptides* 23(2): 291-303.

Parker, M. S.; Wang, J. J.; Fournier, A.; Parker, S. L. (2000). Upregulation of pancreatic polypeptide-sensitive neuropeptide Y (NPY) receptors in estrogen-induced hypertrophy of the anterior pituitary gland in the Fischer-344 rat. *Mol. Cell. Endocrinol.* 164(1–2): 239-249.

Parker S.L., M. S. P., I. Lundell, M.M. Berglund. Pancreatic polypeptide receptors: correlations of agonist affinity, internalization, and sodium sensitivity. In *6th International Neuropeptide Y Meeting*, Pergamon, Sydney, Australia 2001.

Parker, S. L.; Kane, J. K.; Parker, M. S.; Berglund, M. M.; Lundell, I. A.; Li, M. D. (2001). Cloned neuropeptide Y (NPY) Y1 and pancreatic polypeptide Y4 receptors expressed in Chinese hamster ovary cells show considerable agonist-driven internalization, in contrast to the NPY Y2 receptor. *Eur. J. Biochem.* 268(4): 877-886.

Parker, S. L.; Parker, M. S. (2000a). FMRFamides exert a unique modulation of rodent pancreatic polypeptide sensitive neuropeptide Y (NPY) receptors. *Can. J. Physiol. Pharmacol.* 78(2): 150-161.

Parker, S. L.; Parker, M. S. (2000b). Ligand association with the rabbit kidney and brain Y1, Y2 and Y5-like neuropeptide Y (NPY) receptors shows large subtype-related differences in sensitivity to chaotropic and alkylating agents. *Regul. Pept.* 87(1–3): 59-72.

Parker, S. L.; Parker, M. S.; Crowley, W. R. (1999). Characterization of rabbit kidney and brain pancreatic polypeptide-binding neuropeptide Y receptors: differences with Y1 and Y2 sites in sensitivity to amiloride derivatives affecting sodium transport. *Regul. Pept.* 82(1–3): 91-102.

Pedragosa-Badia, X.; Sliwoski, G. R.; Dong Nguyen, E.; Lindner, D.; Stichel, J.; Kaufmann, K. W.; Meiler, J.; Beck-Sickinger, A. G. (2014). Pancreatic polypeptide is recognized by two hydrophobic domains of the human Y4 receptor binding pocket. *J. Biol. Chem.* 289(9): 5846-5859.

Pedragosa Badia, X.; Stichel, J.; Beck-Sickinger, A. (2013). Neuropeptide Y receptors: how to get subtype selectivity. *Frontiers in Endocrinology* 4(5).

Pluym, N. (2011). Application of the guanidine–acylguanidine bioisosteric approach to NPY Y2 receptor antagonists: bivalent, radiolabeled and fluorescent pharmacological tools. Doctoral Thesis, University of Regensburg, Regensburg.

Pluym, N.; Baumeister, P.; Keller, M.; Bernhardt, G.; Buschauer, A. (2013). [(3)H]UR-PLN196: a selective nonpeptide radioligand and insurmountable antagonist for the neuropeptide Y Y(2) receptor. *ChemMedChem* 8(4): 587-593.

Pluym, N.; Brennauer, A.; Keller, M.; Ziemek, R.; Pop, N.; Bernhardt, G.; Buschauer, A. (2011). Application of the guanidine-acylguanidine bioisosteric approach to argininamide-type NPY Y(2) receptor antagonists. *ChemMedChem* 6(9): 1727-1738.

Pop, N.; Igel, P.; Brennauer, A.; Cabrele, C.; Bernhardt, G.; Seifert, R.; Buschauer, A. (2011). Functional reconstitution of human neuropeptide Y (NPY) Y2 and Y4 receptors in Sf9 insect cells. *J. Recept. Signal Transduct. Res.* 31(4): 271-285.

Reichmann, F.; Holzer, P. (2016). Neuropeptide Y: A stressful review. *Neuropeptides* 55: 99-109.

Rose, P. M.; Lynch, J. S.; Frazier, S. T.; Fisher, S. M.; Chung, W.; Battaglino, P.; Fathi, Z.; Leibel, R.; Fernandes, P. (1997). Molecular genetic analysis of a human neuropeptide Y receptor. The human homolog of the murine "Y5" receptor may be a pseudogene. *J. Biol. Chem.* 272(6): 3622-3627.

Rudolf, K.; Eberlein, W.; Engel, W.; Wieland, H. A.; Willim, K. D.; Entzeroth, M.; Wienen, W.; Beck-Sickinger, A. G.; Doods, H. N. (1994). The first highly potent and selective non-peptide neuropeptide Y Y1 receptor antagonist: BIBP3226. *Eur. J. Pharmacol.* 271(2-3): R11-13.

Salaneck, E.; Larsson, T. A.; Larson, E. T.; Larhammar, D. (2008). Birth and death of neuropeptide Y receptor genes in relation to the teleost fish tetraploidization. *Gene* 409(1-2): 61-71.

Schneider, E.; Keller, M.; Brennauer, A.; Hoefelschweiger, B. K.; Gross, D.; Wolfbeis, O. S.; Bernhardt, G.; Buschauer, A. (2007). Synthesis and characterization of the first fluorescent nonpeptide NPY Y1 receptor antagonist. *Chembiochem* 8(16): 1981-1988.

Schneider, E.; Mayer, M.; Ziemek, R.; Li, L.; Hutzler, C.; Bernhardt, G.; Buschauer, A. (2006). A simple and powerful flow cytometric method for the simultaneous determination of multiple parameters at G protein-coupled receptor subtypes. *Chembiochem* 7(9): 1400-1409.

Selbie, L. A.; Darby, K.; Schmitz-Peiffer, C.; Browne, C. L.; Herzog, H.; Shine, J.; Biden, T. J. (1995). Synergistic interaction of Y1-neuropeptide Y and alpha 1b-adrenergic

receptors in the regulation of phospholipase C, protein kinase C, and arachidonic acid production. *J. Biol. Chem.* 270(20): 11789-11796.

Shigeri, Y.; Fujimoto, M. (1994). Y2 receptors for neuropeptide Y are coupled to three intracellular signal transduction pathways in a human neuroblastoma cell line. *J. Biol. Chem.* 269(12): 8842-8848.

Shoblock, J. R.; Welty, N.; Nepomuceno, D.; Lord, B.; Aluisio, L.; Fraser, I.; Motley, S. T.; Sutton, S. W.; Morton, K.; Galici, R.; Atack, J. R.; Dvorak, L.; Swanson, D. M.; Carruthers, N. I.; Dvorak, C.; Lovenberg, T. W.; Bonaventure, P. (2010). In vitro and in vivo characterization of JNJ-31020028 (N-(4-{4-[2-(diethylamino)-2-oxo-1-phenylethyl]piperazin-1-yl}-3-fluorophe nyl)-2-pyridin-3-ylbenzamide), a selective brain penetrant small molecule antagonist of the neuropeptide Y Y(2) receptor. *Psychopharmacology (Berl).* 208(2): 265-277.

Stanley, B. G.; Magdalin, W.; Seirafi, A.; Nguyen, M. M.; Leibowitz, S. F. (1992). Evidence for neuropeptide Y mediation of eating produced by food deprivation and for a variant of the Y1 receptor mediating this peptide's effect. *Peptides* 13(3): 581-587.

Sundler, F.; Böttcher, G.; Ekblad, E.; Håkanson, R. (1993). PP, PYY, and NPY. In *The Biology of Neuropeptide Y and Related Peptides*, Colmers, W. F.; Wahlestedt, C., Eds. Humana Press: Totowa, NJ, pp 157-196.

Tasan, R. O.; Verma, D.; Wood, J.; Lach, G.; Hormer, B.; de Lima, T. C.; Herzog, H.; Sperk, G. (2016). The role of Neuropeptide Y in fear conditioning and extinction. *Neuropeptides* 55: 111-126.

Tatemoto, K.; Carlquist, M.; Mutt, V. (1982). Neuropeptide Y--a novel brain peptide with structural similarities to peptide YY and pancreatic polypeptide. *Nature* 296(5858): 659-660.

Venkatakrishnan, A. J.; Deupi, X.; Lebon, G.; Tate, C. G.; Schertler, G. F.; Babu, M. M. (2013). Molecular signatures of G-protein-coupled receptors. *Nature* 494(7436): 185-194.

Verma, D.; Hormer, B.; Bellmann-Sickert, K.; Thieme, V.; Beck-Sickinger, A. G.; Herzog, H.; Sperk, G.; Tasan, R. O. (2016). Pancreatic polypeptide and its central Y4 receptors are essential for cued fear extinction and permanent suppression of fear. *Br. J. Pharmacol.* 173(12): 1925-1938.

von Hörsten, S.; Hoffmann, T.; Alfalah, M.; Wrann, C. D.; Karl, T.; Pabst, R.; Bedoui, S. (2004). PP, PYY and NPY: Synthesis, Storage, Release and Degradation. In *Neuropeptide Y and Related Peptides*, Michel, M. C., Ed. Springer Berlin Heidelberg: Berlin, Heidelberg, pp 23-44.

Wahlestedt, C.; Yanaihara, N.; Hakanson, R. (1986). Evidence for different pre-and post-junctional receptors for neuropeptide Y and related peptides. *Regul. Pept.* 13(3-4): 307-318.

Walker, M. W.; Wolinsky, T. D.; Jubian, V.; Chandrasena, G.; Zhong, H.; Huang, X.; Miller, S.; Hegde, L. G.; Marsteller, D. A.; Marzabadi, M. R.; Papp, M.; Overstreet, D. H.; Gerald, C. P.; Craig, D. A. (2009). The novel neuropeptide Y Y5 receptor antagonist Lu AA33810 [N-[[trans-4-[(4,5-dihydro[1]benzothiepino[5,4-d]thiazol-2-yl)amino]cycloh exyl]methyl]-methanesulfonamide] exerts anxiolytic- and antidepressant-like effects in rat models of stress sensitivity. *J. Pharmacol. Exp. Ther.* 328(3): 900-911.

Widdowson, P. S.; Halaris, A. E. (1990). A comparison of the binding of [3H]proprionyl-neuropeptide Y to rat and human frontal cortical membranes. *J. Neurochem.* 55(3): 956-962.

Wieland, H. A.; Engel, W.; Eberlein, W.; Rudolf, K.; Doods, H. N. (1998). Subtype selectivity of the novel nonpeptide neuropeptide Y Y1 receptor antagonist BIBO 3304 and its effect on feeding in rodents. *Br. J. Pharmacol.* 125(3): 549-555.

Yulyaningsih, E.; Zhang, L.; Herzog, H.; Sainsbury, A. (2011). NPY receptors as potential targets for anti-obesity drug development. *Br. J. Pharmacol.* 163(6): 1170-1202.

Ziemek, R. (2006). Development of binding and functional assays for the neuropeptide Y Y 2 and Y 4 receptors Doctoral Thesis, University of Regensburg, Regensburg.

Ziemek, R.; Brennauer, A.; Schneider, E.; Cabrele, C.; Beck-Sickinger, A. G.; Bernhardt, G.; Buschauer, A. (2006). Fluorescence- and luminescence-based methods for the

determination of affinity and activity of neuropeptide Y2 receptor ligands. *Eur. J. Pharmacol.* 551(1-3): 10-18.

Ziemek, R.; Schneider, E.; Kraus, A.; Cabrele, C.; Beck-Sickinger, A. G.; Bernhardt, G.; Buschauer, A. (2007). Determination of affinity and activity of ligands at the human neuropeptide Y Y4 receptor by flow cytometry and aequorin luminescence. *J. Recept. Signal Transduct. Res.* 27(4): 217-233.

Chapter 2

Scope and objectives

Binding and functional assays are indispensable for the characterization of GPCR ligands. One part of this thesis is aiming at establishing functional assays for the hY_2R and hY_4R. The [^{35}S]GTPγS binding assay and the luciferase gene reporter assay complement each other, since they provide different readouts. In the [^{35}S]GTPγS assay, receptor-mediated activation is measured directly at the G-protein level as a proximal effect of ligand binding without signal amplification. Moving down the signaling pathway, the activation (or inhibition) of transcription is the approach of the luciferase gene reporter assay, providing a convenient optical readout. For validation of the assays, a library of known Y_2R and Y_4R ligands including agonists and antagonists will be investigated at optimized assay conditions and compared with data reported in literature.

Several fluorescent or radiolabeled peptides have been used as pharmacological tools for the investigation of NPY receptor subtypes. However, there is a need especially for labeled Y_4R selective ligands. Previously, the fluorescent peptides Cy5- and S0586-[Lys^4]hPP (Ziemek et al., 2007) were synthesized and characterized in our working group and successfully used in flow cytometric saturation and competition binding assays. However, these peptides contain two methionine residues which are prone to oxidation during storage, resulting in mixtures of products (sulfoxides, sulfones). The consequences in terms of affinity and selectivity were unclear. Therefore, the aim is to obtain stable radiolabeled and fluorescent Y_4R ligands by derivatization of a [Lys^4]hPP analog, [Lys^4,Nle^{17,30}]hPP, containing norleucine instead of methionine. These molecular tools will be used for investigations at the Y_4R, e.g. in saturation, kinetic and competition binding assays. The applicability of the fluorescent ligand to flow cytometry and confocal microscopy will be explored, e. g. to investigate receptor internalization. Special attention will be paid to the investigation of the influence of the osmolarity and the composition of buffers on ligand binding and internalization.

Reference:

Ziemek, R.; Schneider, E.; Kraus, A.; Cabrele, C.; Beck-Sickinger, A. G.; Bernhardt, G.; Buschauer, A. (2007). Determination of Affinity and Activity of Ligands at the Human Neuropeptide Y Y4 Receptor by Flow Cytometry and Aequorin Luminescence. *J. Recept. Signal Transduct. Res.* 27(4): 217-233.

Chapter 3

Development of a [^{35}S]GTPγS binding assay for hY_2 and hY_4 receptors in Sf9 membranes

3.1 Introduction

Since binding assays provide only information about affinities, there is a need for functional assays to categorize ligands into agonists, inverse agonists and antagonists (Milligan, 2003). As all NPY receptor subtypes are coupling to $G_{i/o}$, stimulation of the receptors leads to an inhibition of adenylyl cyclase resulting in a decreased formation of cAMP. This effect is commonly used in assays based on the inhibition of forskolin-induced cAMP formation (Beck-Sickinger et al., 1992; Goumain et al., 2001). Furthermore, potencies of Y_2 and Y_4 receptor ligands can be determined by measuring tritium-labeled phosphoinositol accumulation, when COS-7 cells are co-transfected with YRs and chimeric G proteins (Merten et al., 2007). The mobilization of intracellular calcium in HEK293 cells can be measured fluorimetrically when the YR subtype of interest (Dautzenberg et al., 2005) is co-expressed with chimeric G-proteins such as Gq_{i5} to redirect the signal to the phospholipase C pathway. By analogy, aequorin-based bioluminescence can be used for the determination of ligand activity at the Y_2R and the Y_4R (Ziemek et al., 2006; Ziemek et al., 2007). In addition, the steady-state GTPase assay provides a proximal readout for functional studies on membrane preparations of Sf9 insect cells (Pop et al., 2011). Receptor-mediated activation is measured directly at the G-protein level as a proximal effect of agonist binding, which also holds for the [^{35}S]GTPγS assay (Dautzenberg et al., 2005). Figure 3.1 gives an overview of the principle of the [^{35}S]GTPγS assay.

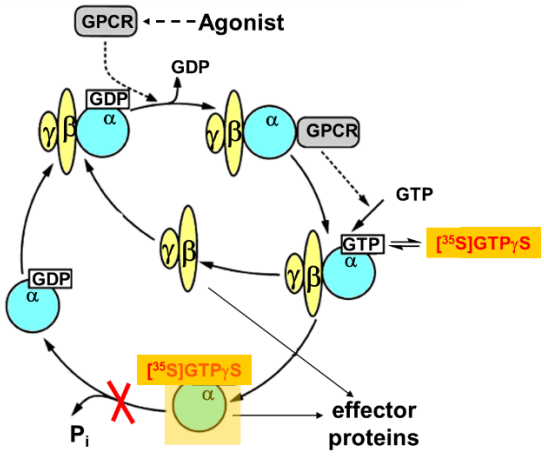

Figure 3.1. G protein activation/deactivation cycle after GPCR stimulation by an agonist (Hill et al., 2001); adapted from (Seifert and Wieland, 2005). Agonist binding to G protein-coupled receptors stimulates the exchange of GTP for GDP bound to the α subunit of coupled heterotrimeric GTP binding proteins. This causes the dissociation of the complex into the GPCR, the GTP- or [^{35}S]GTPγS-bound Gα-subunit and the Gβγ-dimer. The G protein subunits each activate effector proteins until the nucleotide is cleaved into GDP and inorganic phosphate (P_i) by GTPase. In the [^{35}S]GTPγS assay, the non-hydrolyzable GTP analog [^{35}S]GTPγS dissociates slowly from the Gα protein, so it accumulates. Association of GDP-bound Gα with the Gβγ-dimer is the termination of the cycle.

Hence, a [^{35}S]GTPγS assay for the hY$_2$R and the hY$_4$R (Dautzenberg et al., 2005) was established by analogy with the strategies described for other class A GPCRs heterologously expressed in Sf9 cells (Schneider and Seifert, 2010; Wieland and Seifert, 2006). Sf9 insect cells provide an excellent background due the absence of endogenous constitutively active receptors (Schneider and Seifert, 2010; Wieland and Seifert, 2006), making them suitable for investigations on constitutive GPCR activity. In contrast to the GTPase assay, there is no amplification of the signal in the [^{35}S]GTPγS assay. Functional activities of selected agonists and antagonists (see section 1.2.1) at the hY$_2$R were compared to results from GTPase (Pop et al., 2011) and calcium mobilization assays (Pluym, 2011; Shoblock et al., 2009). At the hY$_4$R the endogenous ligand hPP, [Lys^4]hPP and GW1229 were investigated and the effect of different sodium concentrations on receptor activation was studied.

3.2 Material and methods

3.2.1 Materials

The constructs of the human pVL1392-SF-Y$_2$R-His$_6$ and pVL1392-SF-Y$_4$R-His$_6$ vector were provided by Dr. N. Pop (Pop et al., 2011). The recombinant baculovirus encoding the G$_{αi2}$ subunit was kindly provided by Dr. A. G. Gilman (Department of Pharmacology, University of Southwestern Medical Centre, Dallas, TX USA), and the recombinant baculovirus encoding the unmodified version of the Gβ$_1$γ$_2$ subunits was a kind gift of Dr. P. Gierschik (Department of Pharmacology and Toxicology, University of Ulm, Ulm, Germany). BaculoGOLD transfection kit was from PharMingen (San Diego, CA). The peptides pNPY, hPP and [Lys^4]hPP were synthesized by Synpeptide (Shanghai, China). GW1229 (also designated GR231118 or 1229U91) was a gift from Dr. A. J. Daniels, Glaxo Wellcome Inc., USA. JNJ-31020028 (UR-KK54) (Shoblock et al., 2009) and [^{3}H]UR-KK200 (Kuhn et al., 2016) were synthesized by K. Kuhn (University of Regensburg, Germany), pNPY 22-36 was synthesized by Dr. M. Kaske (University of Regensburg, Germany). BIIE0246 (Doods et al., 1999) and UR-PLN75 were synthesized by Dr. Nikola Pluym in our research group as part of a doctoral project (Pluym, 2011). The chemical structures of the ligands are depicted in section 1.2.1. Peptides (1 mM) were dissolved in 10 mM HCl. BIIE0246 (10 mM), UR-PLN75 (10 mM) and JNJ-31020028 (10 mM) were dissolved in DMSO. Dilutions were prepared in binding buffer (75 mM Tris/HCl, 12.5 mM $MgCl_2$, 1 mM EDTA, pH 7.4).The amount of DMSO was adjusted to a final concentration of 2% in all assays. Coated reaction vessels (Sigmacote, Sigma Aldrich, Deisenhofen, Germany) were used for peptides. [^{35}S]GTPγS (≥ 1000 Ci/mmol, radiochemical purity > 95%) was from Hartmann Analytic (Braunschweig, Germany). All other reagents were from standard suppliers and of the highest purity available.

3.2.2 Cell culture, generation of recombinant baculoviruses, Sf9 cell membrane preparation

Cell culture and generation of high-titre recombinant baculovirus stocks as well as the co-infection of Sf9 cells with high-titre baculovirus stocks encoding $G\alpha_{i2}$, $G\beta_1\gamma_2$, and the hY_2R or the hY_4R were performed as described by Pop et al, 2011. Membrane preparations were performed according to Seifert et al. (1998) in the presence of 0.2 mM phenylmethylsulfonyl fluoride, 1 mM ethylenediaminetetraacetic acid (EDTA), 10 µg/mL leupeptin and 10 µg/mL benzamidine as protease inhibitors. Prepared membranes were re-suspended in binding buffer (75 mM Tris/HCl, 12.5 mM $MgCl_2$, 1 mM EDTA, pH 7.4) and stored at -80 °C in 0.5 or 1.0 mL aliquots.

3.2.3 [^{35}S]GTPγS binding assay at the hY_2R and the hY_4R

Membranes were thawed, centrifuged at 4 °C and 13,000 g for 10 min and carefully re-suspended in binding buffer. Experiments were performed in Primaria™ 96-well plates (Corning Life Sciences, Oneonta, NY) in a total volume of 100 µL per well. Each well contained 6-15 µg of protein, reaction buffer (binding buffer with 1 µM GDP, 0.05% (*w/v*) bovine serum albumin (BSA), 20 nCi of [^{35}S]GTPγS (0.2 nM)) and the ligand (10-fold concentrated) at concentrations as indicated in the results section. In the antagonist mode at the hY_2R, test compounds were incubated in the presence of pNPY (final concentration: 18 nM) at a final concentration of 2% DMSO. Nonspecific binding was determined in the presence of 10 µM unlabeled GTPγS. For optimization of the incubation period, membranes were incubated with [^{35}S]GTPγS in the presence (1 µM) and absence of pNPY in binding buffer containing 2% DMSO for 15, 30, 45, 60, 90 and 120 min. After incubation under shaking at 200 rpm at room temperature, bound [^{35}S]GTPγS was separated from free [^{35}S]GTPγS by filtration through glass microfibre filters using a 96-well Brandel harvester (Brandel Inc., Unterföhring, Germany). After three washing steps with binding buffer, for each well filter pieces were punched out and transferred into 96-well sample plates 1450-401 (Perkin Elmer, Rodgau, Germany). Each well was supplemented with 200 µL of scintillation cocktail (Rotiscint Eco plus, Roth, Karlsruhe, Germany) and incubated in the dark under shaking at 200 rpm. Radioactivity was measured with a Micro Beta2 1450 scintillation counter. At least two independent experiments (in triplicate) were performed and experiments were analyzed by four-parameter sigmoidal fits (GraphPad Prism 5.0, San Diego, CA). EC_{50}, K_b and α were calculated as means ± SEM. The maximal response to pNPY (hY_2R) and hPP (hY_4R), respectively, was set to 100% in the agonist mode. In the antagonist mode (hY_2R), the inhibition was referred to the response to pNPY (18 nM) in the presence of BIIE0246. To optimize the signal-to-noise ratio at the hY_4R, the effects of NaCl

(0, 50, 100, 150 mM) and $MgCl_2$ (1, 12.5, 20 mM) at different concentrations were investigated.

3.2.4 Radioligand binding at hY_4R Sf9 membranes

The experiments were performed in Primaria™ 96-well plates (Corning Life Sciences). Each well contained 60 µg of protein in a total volume of 200 µL. For saturation binding, membranes were incubated in buffer I (25 mM HEPES, 2.5 mM $CaCl_2$, 1 mM $MgCl_2$, pH 7.4) containing [^{3}H]UR-KK200 (0.15 - 5 nM) and 1% (w/v) BSA for 90 min at room temperature under shaking at 200 rpm. Nonspecific binding was determined in the presence of a 100-fold excess of [Lys^4]hPP. Filtration through glass microfibre filters (Whatman GF/C), pretreated with polyethylenimine 0.3% (w/v), using a Brandel 96 sample harvester separated unbound from membrane-associated [^{3}H]UR-KK200. After three washing steps with binding buffer for each well filter pieces were punched out and transferred into 96-well sample plates 1450-401 (Perkin Elmer). Each well was supplemented with 200 µL of scintillation cocktail (Rotiscint Eco plus) and incubated in the dark under shaking at 200 rpm. Radioactivity (dpm) was measured with a Micro Beta2 1450 scintillation counter.

Specific binding data from saturation experiments was plotted against the 'free' radioligand concentration and analyzed according to a two-parameter hyperbolic curve fit (Binding – Saturation: One site – Specific binding, GraphPad Prism 5.0).

3.3 Results and discussion

3.3.1 [^{35}S]GTPγS binding assay at the hY_2R

Monitoring the time course of [^{35}S]GTPγS binding in the presence and absence of pNPY, respectively, a plateau of bound [^{35}S]GTPγS in the presence of pNPY was reached after 90 min with a signal-to-noise ratio of approximately 3. Upon stimulation with pNPY, exchange of non-hydrolyzable [^{35}S]GTPγS (instead of GTP) for GDP at the Gα subunit occurs (Figure 3.2).

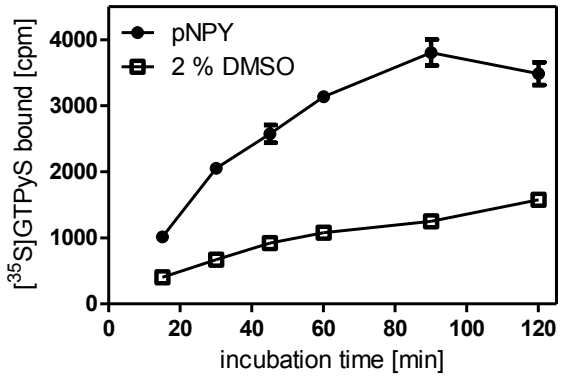

Figure 3.2. Representative time course of [^{35}S]GTPγS binding in the presence and absence of pNPY (1 µM). Two independent experiments were performed in triplicate.

Potencies (EC_{50}) and maximal effects (α) as well as antagonist activities (K_b) at the hY_2R in the [^{35}S]GTPγS-assay were determined by using selected agonists and antagonists, respectively (Figure 3.3 and Table 3.1). In literature, Dautzenberg et al. performed the [^{35}S]GTPγS-assay with membrane preparations of HEK293 cells expressing the hY_1, hY_2, hY_4 and mY_5R, respectively, and several ligands were tested at all subtypes (i.e. hY_2R: EC_{50}(hNPY) = 29 nM; EC_{50}(NPY3-36) = 61 nM; EC_{50}(NPY13-36) = 95 nM) (Dautzenberg et al., 2005). In the [^{35}S]GTPγS-assay performed with Sf9 membranes, the potency of pNPY was in good agreement with the EC_{50} values determined in a calcium mobilization assay and in the GTPase assay (Table 3.1). When tested in the agonist mode, antagonists such as the hY_2R standard antagonist BIIE0246 showed no inverse agonism. Therefore these ligands were tested in the antagonist mode. BIIE0246 and its acylguanidine analog UR-PLN75 behaved as full antagonists and the K_b values were in good agreement with reported data (Table 3.1). In literature, JNJ-31020028 is reported as a high affinity hY_2R antagonist with a K_b value of 9.1 nM determined in a calcium mobilization assay (Shoblock et al., 2009). Functional studies in the [^{35}S]GTPγS assay confirmed the antagonism of JNJ-31020028 at the hY_2R, and the determined K_b value of 10.0 nM was in good agreement with the published data. Except for UR-PLN75, radioligand binding data were in the same range as the respective K_b values from functional studies in the [^{35}S]GTPγS assay (Table 3.1).

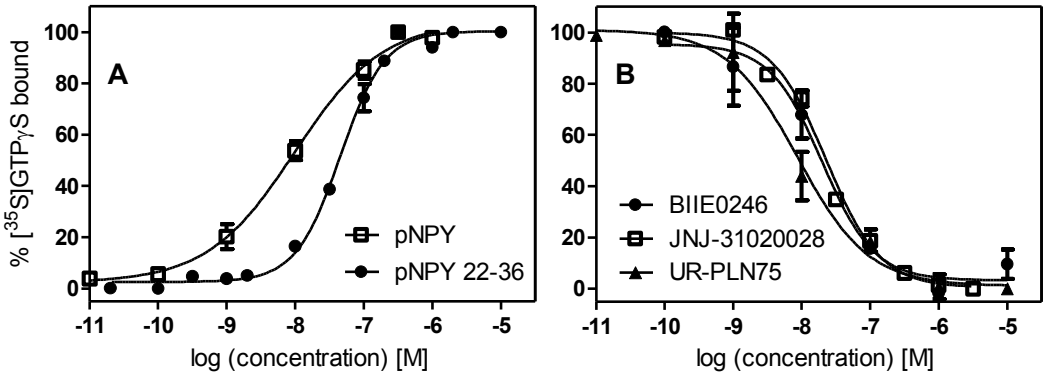

Figure 3.3. Concentration-response curves of agonists (**A**) and antagonists (**B**) investigated in the [^{35}S]GTPγS assay at the hY$_2$R. (**A**) In the agonist mode, the effect of pNPY22-36 is referred to the maximal response elicited by pNPY. (**B**) Antagonists were investigated versus pNPY (18 nM) as the agonist; maximal inhibition was determined in the presence of BIIE0246. Data represent mean values ± SEM from at least two independent experiments performed in triplicate.

Table 3.1. NPY hY$_2$R agonist potencies (EC_{50}) and intrinsic activities (α), antagonistic activities (K_b) of selected compounds.

	[^{35}S]GTPγS assay		Reference data	
Compound	EC_{50} or (K_b) [nM][a]	α	EC_{50} or (K_b) [nM]	K_i [nM][f]
pNPY	9.9 ± 1.1	1.00	11.7 ± 3.0[b]	1.72 ± 0.13
			16.9 ± 2.5[c]	
pNPY22-36	42 ± 5	0.99	n.d.	12.5 ± 1.8
BIIE0246	(5.5 ± 1.4)	-	(10.2 ± 1.8)[b]	24 ± 3
			(5.6 ± 0.4)[d]	
UR-PLN75	(3.3 ± 0.8)	-	(2.1 ± 0.4)[d]	31 ± 2
JNJ-31020028	(10.0 ± 2.6)	-	(9.1 ± 0.7)[e]	30 ± 2

[a] [^{35}S]GTPγS functional binding assays with membrane preparations of Sf9 cells expressing the hY$_2$R + G$_{αi2}$ + Gβ$_1$γ$_2$ + RGS4; the intrinsic activity (α) of pNPY was set to 1.00 and α values of other compounds were referred to this value in the agonist mode; the K_b values of antagonists were determined in the antagonist mode versus pNPY (18 nM) as the agonist; K_b values were calculated according to the Cheng-Prusoff equation (Cheng and Prusoff, 1973); mean values ± SEM (n = 2-3). [b] steady-state GTPase assay; data reported by Pop et al. 2011. [c-e] [Ca^{2+}]$_i$ mobilization in hY$_2$R-expressing cells; [c] (Ziemek et al., 2006); [d] (Pluym, 2011);.[e] (Shoblock et al., 2009). [f] hY$_2$R binding determined by displacement of [^{3}H]propionyl-pNPY (1 nM) from CHO cells, stably expressing the hY$_2$R; mean values ± SEM (n = 3-4).

3.3.2 [^{35}S]GTPγS binding assay at the hY$_4$R

Previously, membrane preparations (batch B75) of Sf9 cells expressing the hY$_4$R were successfully applied to establish a steady state GTPase assay (Pop et al., 2011). Therefore, the applicability to a [^{35}S]GTPγS assay was explored. Unfortunately, it was not possible to determine EC_{50} values of hPP as the response of the activated hY$_4$R almost equals the

bound [^{35}S]GTPγS in the absence of agonist. Therefore, new recombinant viruses encoding the hY_4 receptor were generated using the BaculoGOLD transfection kit according to the manufacture's protocol (Sf9 membranes, batch B171). The membranes were subjected to saturation binding experiments with [^{3}H]UR-KK200 to confirm the hY_4R expression (Figure 3.4). The radioligand [^{3}H]UR-KK200 was selected because this compound was characterized at CHO hY_4R cells to specifically bind to the hY_4R with a K_d value of 0.67 nM (Kuhn et al., 2016). Saturation binding of [^{3}H]UR-KK200 at the first batch of Sf9 membranes (B75) revealed a K_d value of 1.78 ± 0.04 nM which is in good agreement with experiments performed with CHO hY_4R cells (Figure 3.4A). Saturation binding experiments at the second batch of membranes (B171) failed (Figure 3.4B). Regardless of that, effort was spent to optimize the [^{35}S]GTPγS assay protocol using membrane batches B75 and B171.

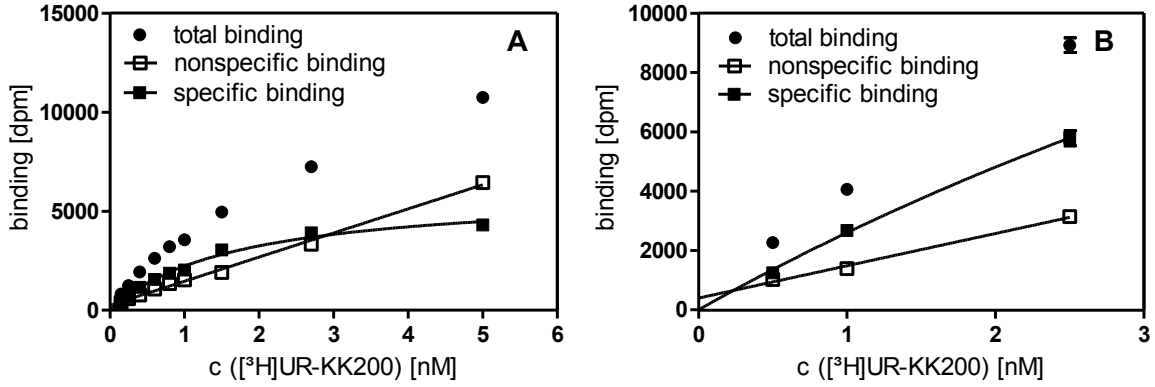

Figure 3.4. Saturation analysis of different membrane preparations of Sf9 insect cells expressing the hY_4R. (**A**) Representative saturation binding experiment with membrane batch B75 (n = 3); K_d = 1.78 ± 0.04 nM. (**B**) Binding experiment with membrane batch B171 (n = 2).

Mg^{2+} ions critically influence G protein function (Birnbaumer et al., 1990) and are indispensable for [^{35}S]GTPγS binding. Mg^{2+} ions increase the basal [^{35}S]GTPγS binding, but in particular enhance the signal upon agonist stimulation of a GPCR. Comparable concentration-response curves of hPP at the hY_4R were obtained in the presence of 12.5 mM (reported assay condition) and 20 mM $MgCl_2$, whereas a concentration of 1 mM $MgCl_2$ was obviously too low (Figure 3.5).

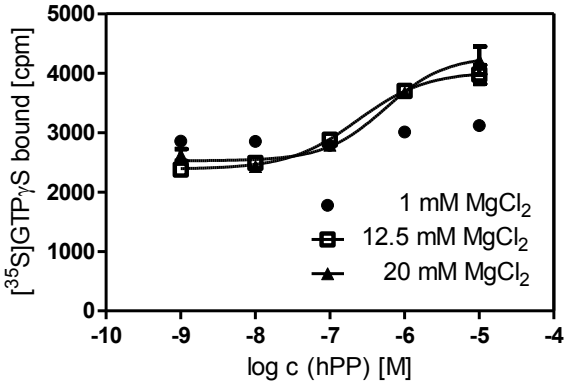

Figure 3.5. Representative concentration–response curves of hPP in the presence of 1, 12.5 and 20 mM $MgCl_2$; means ± SEM, assay performed in triplicate (n = 2).

As reported in literature, Na^+ acts as an allosteric inverse agonist at several $G_{i/o}$-coupled GPCRs and stabilizes the inactive state of the receptors (Schnell et al., 2010; Seifert and Wenzel-Seifert, 2001; 2002). The presence of Na^+ ions improves the agonist stimulated binding of [^{35}S]GTPγS relative to basal binding and hence the signal-to-noise ratio (Lazareno and Birdsall, 1993; Selley et al., 2000; Szekeres and Traynor, 1997; Tian et al., 1994). Na^+ ions are thought to bind to a conserved aspartate residue in transmembrane II of GPCRs (Horstman et al., 1990) and this facilitates uncoupling of the receptor-G protein complex and a decrease in basal [^{35}S]GTPγS binding. Therefore, concentration-response curves of the agonist hPP were performed in the presence of Na^+ ions at increasing concentrations (Figure 3.6A). Sodium induced a decrease in basal [^{35}S]GTPγS binding and a lower potency (EC_{50}) of hPP which was also reported for the GTPase assay (Pop et al., 2011). A decrease in the basal [^{35}S]GTPγS binding by 50% and of the maximum response by 30% was observed in the presence of 50 mM NaCl compared to the absence of NaCl. This is in good agreement with data determined in the GTPase assay at the hY_4R where the suppression of basal GTPase activity by 50 mM NaCl amounted to 47% (Pop et al., 2011). The signal-to-noise ratio was further improved to approximately 2:1 at higher NaCl concentrations. Furthermore, EC_{50} values of the agonists [Lys^4]hPP and GW1229 were determined in the presence (50 mM) and absence of NaCl for comparison with the effects of NaCl observed in the GTPase assay (Pop et al., 2011). Interestingly, for these ligands a lower potency by a factor of 4 ([Lys^4]hPP) and 3 (GW1229) was determined in the presence of 50 mM NaCl in the [^{35}S]GTPγS assay (Figure 3.6B, Table 3.2). Compared to the EC_{50} values in the GTPase assay, the activity of hPP was 19-fold lower and [Lys^4]hPP revealed 331 nM versus 143 nM. Most pronounced decrease in potency was observed for GW1229, which was 81- and 180-fold lower than reported for the GTPase assay in the absence and presence of NaCl (50 mM). The obvious discrepancies, including the rank order of the potencies of ligands, comparing [^{35}S]GTPγS and GTPase assay, are difficult to explain as in both cases receptor-mediated activation is measured at the G-protein level. Although a certain difference in the potency of agonists may be expected due to signal amplification in the GTPase assay, the

robustness of the data gained from the [^{35}S]GTPγS appears questionable. Functional studies at the hH_4R resulted in comparable pEC_{50} values of tested ligands such as histamine, thioperamide and UR-PI294 (Nordemann et al., 2013). One possible explanation could be the different composition of the used buffers which may result in a lower potencies especially at peptidergic GPCRs such as the hY_4R (see chapter 5; (Kuhn et al., 2016)).

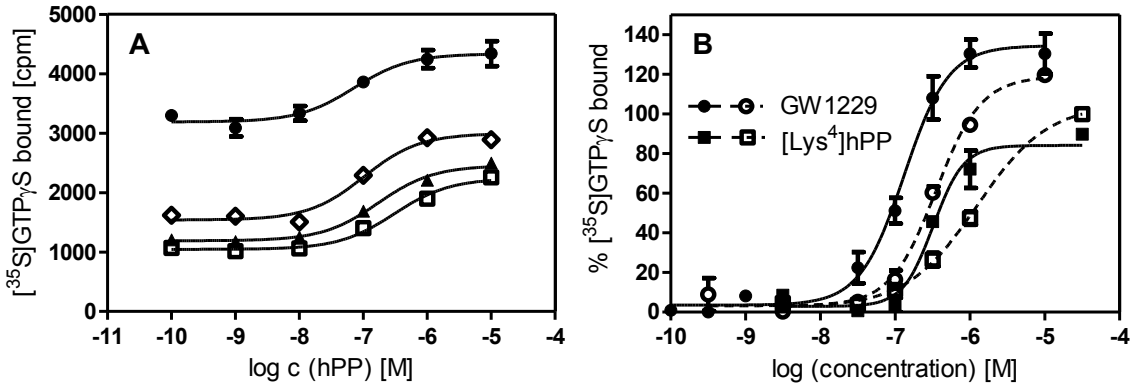

Figure 3.6. Selected ligands investigated in the [^{35}S]GTPγS assay at the hY_4R. (**A**) Representative concentration-response curves of hPP in the presence of 0 (●), 50 (◊), 100 (▲) and 150 (□) mM NaCl (n = 3). (**B**) Concentration-response curves of GW1229 and [Lys^4]hPP in the absence (solid line) and in the presence of 50 mM NaCl (dashed line). All curves are scaled with respect to a maximal hPP effect of 100%. Data represent mean values ± SEM; three independent experiments were performed in triplicate.

Table 3.2. hY_4R agonist potencies (EC_{50}) and intrinsic activities (α) of selected peptides and reference compound hPP, in the absence and presence of NaCl.

	[^{35}S]GTPγS binding assay		steady-state GTPase assay	
Compound	EC_{50} [nM][a]	α	EC_{50} [nM][b]	α
hPP	206 ± 30	1.00	11.0 ± 3.6	1.00
	4.5 ± 0.8[c]			
hPP + 50 mM NaCl	182 ± 38	1.00	28.3 ± 5.3	1.00
hPP + 100 mM NaCl	240 ± 3	1.00	n.d.	
hPP + 150 mM NaCl	367 ± 11	1.00	n.d.	
[Lys^4]hPP	331 ± 34	0.95	143 ± 24	1.02
[Lys^4]hPP + 50 mM NaCl	1230 ± 206	0.96	n.d.	
GW1229	99 ± 20	1.19	0.55 ± 0.15	0.82
GW1229 + 50 mM NaCl	334 ± 29	1.20	4.1 ± 0.2	0.97

[a] [^{35}S]GTPγS functional binding assays with membrane preparations of Sf9 cells expressing the hY_4R + Gα_{i2} + G$\beta_1\gamma_2$ +RGS4; the intrinsic activity (α) of hPP was set to 1.00 and α values of other compounds were referred to this value; mean values ± SEM (n = 3-4). [b] steady-state GTPase assay on membrane preparations expressing the hY_4R + Gα_{i2} + G$\beta_1\gamma_2$ + RGS4; data reported by Pop et al. 2011. [c] Data reported by Dautzenberg et al. 2005; [^{35}S]GTPγS assay with membrane preparations of HEK293 cells expressing the hY_4R.

3.4 Summary and conclusion

The baculovirus/Sf9 cell system is appropriate for the functional characterization of hY_2R ligands in the [^{35}S]GTPγS binding. Pharmacological data of reference compounds determined in this assay were in good agreement with functional studies in the steady-state GTPase assay and the calcium mobilization assay at the hY_2R.

The [^{35}S]GTPγS assay at the hY_4R revealed potencies of hPP and GW1229, which were lower by a factor 19 and 180, respectively, compared to reported data for the steady-state GTPase assay. Increasing Na^+ concentrations led to minor changes of the potency of hPP in the [^{35}S]GTPγS assay, whereas [Lys^4]hPP and GW1229 were markedly less potent in the presence of sodium. This is in agreement with the data from radioligand binding assays at the hY_4R (see section 5.3.3; (Kuhn et al., 2016)). Nevertheless, the [^{35}S]GTPγS assay is compromised by a low signal-to-noise ratio impairing the robustness of the data.

3.5 References

Beck-Sickinger, A. G.; Grouzmann, E.; Hoffmann, E.; Gaida, W.; Van Meir, E. G.; Waeber, B.; Jung, G. (1992). A novel cyclic analog of neuropeptide Y specific for the Y2 receptor. *Eur. J. Biochem.* 206(3): 957-964.

Birnbaumer, L.; Abramowitz, J.; Brown, A. M. (1990). Receptor-effector coupling by G proteins. *Biochimica et Biophysica Acta (BBA) - Reviews on Biomembranes* 1031(2): 163-224.

Cheng, Y.; Prusoff, W. H. (1973). Relationship between the inhibition constant (K1) and the concentration of inhibitor which causes 50 per cent inhibition (I50) of an enzymatic reaction. *Biochem. Pharmacol.* 22(23): 3099-3108.

Dautzenberg, F. M.; Higelin, J.; Pflieger, P.; Neidhart, W.; Guba, W. (2005). Establishment of robust functional assays for the characterization of neuropeptide Y (NPY) receptors: identification of 3-(5-benzoyl-thiazol-2-ylamino)-benzonitrile as selective NPY type 5 receptor antagonist. *Neuropharmacology* 48(7): 1043-1055.

Doods, H.; Gaida, W.; Wieland, H. A.; Dollinger, H.; Schnorrenberg, G.; Esser, F.; Engel, W.; Eberlein, W.; Rudolf, K. (1999). BIIE0246: a selective and high affinity neuropeptide Y Y(2) receptor antagonist. *Eur. J. Pharmacol.* 384(2-3): R3-5.

Goumain, M.; Voisin, T.; Lorinet, A. M.; Ducroc, R.; Tsocas, A.; Roze, C.; Rouet-Benzineb, P.; Herzog, H.; Balasubramaniam, A.; Laburthe, M. (2001). The peptide YY-preferring receptor mediating inhibition of small intestinal secretion is a peripheral Y(2) receptor: pharmacological evidence and molecular cloning. *Mol. Pharmacol.* 60(1): 124-134.

Hill, S. J.; Baker, J. G.; Rees, S. (2001). Reporter-gene systems for the study of G-protein-coupled receptors. *Curr. Opin. Pharmacol.* 1(5): 526-532.

Horstman, D. A.; Brandon, S.; Wilson, A. L.; Guyer, C. A.; Cragoe, E. J., Jr.; Limbird, L. E. (1990). An aspartate conserved among G-protein receptors confers allosteric regulation of alpha 2-adrenergic receptors by sodium. *J. Biol. Chem.* 265(35): 21590-21595.

Kuhn, K. K.; Ertl, T.; Dukorn, S.; Keller, M.; Bernhardt, G.; Reiser, O.; Buschauer, A. (2016). High Affinity Agonists of the Neuropeptide Y (NPY) Y4 Receptor Derived from the C-Terminal Pentapeptide of Human Pancreatic Polypeptide (hPP): Synthesis, Stereochemical Discrimination, and Radiolabeling. *J. Med. Chem.* 59(13): 6045-6058.

Lazareno, S.; Birdsall, N. J. M. (1993). Pharmacology characterization of guanine nucleotide exchange reactions in membranes from Cho cells stably transfected with human muscarinic receptors m1–m4. *Life Sci.* 52(5): 449-456.

Merten, N.; Lindner, D.; Rabe, N.; Rompler, H.; Mörl, K.; Schöneberg, T.; Beck-Sickinger, A. G. (2007). Receptor subtype-specific docking of Asp6.59 with C-terminal arginine residues in Y receptor ligands. *J. Biol. Chem.* 282(10): 7543-7551.

Milligan, G. (2003). Constitutive Activity and Inverse Agonists of G Protein-Coupled Receptors: a Current Perspective. *Mol. Pharmacol.* 64(6): 1271-1276.

Nordemann, U.; Wifling, D.; Schnell, D.; Bernhardt, G.; Stark, H.; Seifert, R.; Buschauer, A. (2013). Luciferase Reporter Gene Assay on Human, Murine and Rat Histamine H_4 Receptor Orthologs: Correlations and Discrepancies between Distal and Proximal Readouts. *PLoS ONE* 8(9): e73961.

Pluym, N. (2011). Application of the guanidine–acylguanidine bioisosteric approach to NPY Y2 receptor antagonists: bivalent, radiolabeled and fluorescent pharmacological tools. Doctoral Thesis, University of Regensburg, Regensburg.

Pop, N.; Igel, P.; Brennauer, A.; Cabrele, C.; Bernhardt, G.; Seifert, R.; Buschauer, A. (2011). Functional reconstitution of human neuropeptide Y (NPY) Y2 and Y4 receptors in Sf9 insect cells. *J. Recept. Signal Transduct. Res.* 31(4): 271-285.

Schneider, E. H.; Seifert, R. (2010). Sf9 cells: A versatile model system to investigate the pharmacological properties of G protein-coupled receptors. *Pharmacol. Ther.* 128(3): 387-418.

Schnell, D.; Burleigh, K.; Trick, J.; Seifert, R. (2010). No evidence for functional selectivity of proxyfan at the human histamine H3 receptor coupled to defined Gi/Go protein heterotrimers. *J. Pharmacol. Exp. Ther.* 332(3): 996-1005.

Seifert, R.; Wenzel-Seifert, K. (2001). Unmasking different constitutive activity of four chemoattractant receptors using Na+ as universal stabilizer of the inactive (R) state. *Receptors Channels* 7(5): 357-369.

Seifert, R.; Wenzel-Seifert, K. (2002). Constitutive activity of G-protein-coupled receptors: cause of disease and common property of wild-type receptors. *Naunyn. Schmiedebergs Arch. Pharmacol.* 366(5): 381-416.

Selley, D. E.; Cao, C.-C.; Liu, Q.; Childers, S. R. (2000). Effects of sodium on agonist efficacy for G-protein activation in μ-opioid receptor-transfected CHO cells and rat thalamus. *Br. J. Pharmacol.* 130(5): 987-996.

Shoblock, J. R.; Welty, N.; Nepomuceno, D.; Lord, B.; Aluisio, L.; Fraser, I.; Motley, S. T.; Sutton, S. W.; Morton, K.; Galici, R.; Atack, J. R.; Dvorak, L.; Swanson, D. M.; Carruthers, N. I.; Dvorak, C.; Lovenberg, T. W.; Bonaventure, P. (2009). In vitro and in vivo characterization of JNJ-31020028 (N-(4-{4-[2-(diethylamino)-2-oxo-1-phenylethyl]piperazin-1-yl}-3-fluorophenyl)-2-pyridin-3-ylbenzamide), a selective brain penetrant small molecule antagonist of the neuropeptide Y Y2 receptor. *Psychopharmacology (Berl).* 208(2): 265.

Szekeres, P. G.; Traynor, J. R. (1997). Delta Opioid Modulation of the Binding of Guanosine-5′-O-(3-[35S]thio)triphosphate to NG108–15 Cell Membranes: Characterization of Agonist and Inverse Agonist Effects *J. Pharmacol. Exp. Ther.* 283(3): 1276-1284.

Tian, W. N.; Duzic, E.; Lanier, S. M.; Deth, R. C. (1994). Determinants of alpha 2-adrenergic receptor activation of G proteins: evidence for a precoupled receptor/G protein state. *Mol. Pharmacol.* 45(3): 524-531.

Wieland, T.; Seifert, R. (2006). Methodological Approaches. In *G Protein-Coupled Receptors as Drug Targets*, Wiley-VCH Verlag GmbH & Co. KGaA: pp 81-120.

Ziemek, R.; Brennauer, A.; Schneider, E.; Cabrele, C.; Beck-Sickinger, A. G.; Bernhardt, G.; Buschauer, A. (2006). Fluorescence- and luminescence-based methods for the determination of affinity and activity of neuropeptide Y2 receptor ligands. *Eur. J. Pharmacol.* 551(1-3): 10-18.

Ziemek, R.; Schneider, E.; Kraus, A.; Cabrele, C.; Beck-Sickinger, A. G.; Bernhardt, G.; Buschauer, A. (2007). Determination of affinity and activity of ligands at the human neuropeptide Y Y4 receptor by flow cytometry and aequorin luminescence. *J. Recept. Signal Transduct. Res.* 27(4): 217-233.

Chapter 4

Development of luminescence based reporter gene assays for the human neuropeptide Y_2 and Y_4 receptor

4.1 Introduction

Because of their simplicity reporter gene assays are in widespread use for the study of ligand activity and potency and a convenient method for the measurement of functional response to $G\alpha_s$, $G\alpha_{i/o}$ and $G\alpha_q$ coupled GPCRs (Tang et al., 2004). A variety of reporters under control of specific responsive elements are in use for different classes of receptor and allow the quantification of agonist and antagonistic activity in living cells or cell lysates (Hill et al., 2001). Reporter gene assays are based on the modulation of transcription factors by GPCR signaling. The enhanced or repressed transcription of the gene is caused by the binding of these factors to regulatory elements in the promoter region of a target. The Y_2R and Y_4R couple to $G\alpha_{i/o}$ G-proteins, which mediate inhibition of the adenylyl cyclase (AC), resulting in a decrease in cAMP formation. Hence, the cAMP response element (CRE) has been preferably used. For the purpose of detection of a negative regulation of the AC, a stimulation of the AC is required to raise the cAMP level. This is accomplished by using the diterpene forskolin (see Figure 4.1) (Seamon and Daly, 1981).

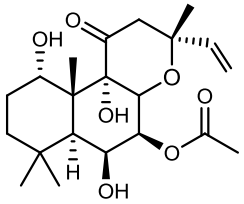

Figure 4.1. Chemical structure of the diterpene forskolin.

A scheme is given in Figure 4.2A which shows the Y_2R and Y_4R signaling pathway where a CRE-linked reporter gene is involved. Activation by an agonist of the respective receptor decreases forskolin stimulated luciferase activity, reflecting the inhibitory quality of the $G\alpha_{i/o}$ protein. Inverse agonists cause a shift of constitutively active receptors to an inactive conformation resulting in a decrease of the (constitutive) inhibition of the AC and in an increase in forskolin stimulated luciferase activity (see Figure 4.2B). K_b values of neutral antagonists are determined in the antagonist mode upon stimulation of the receptor by the respective agonist.

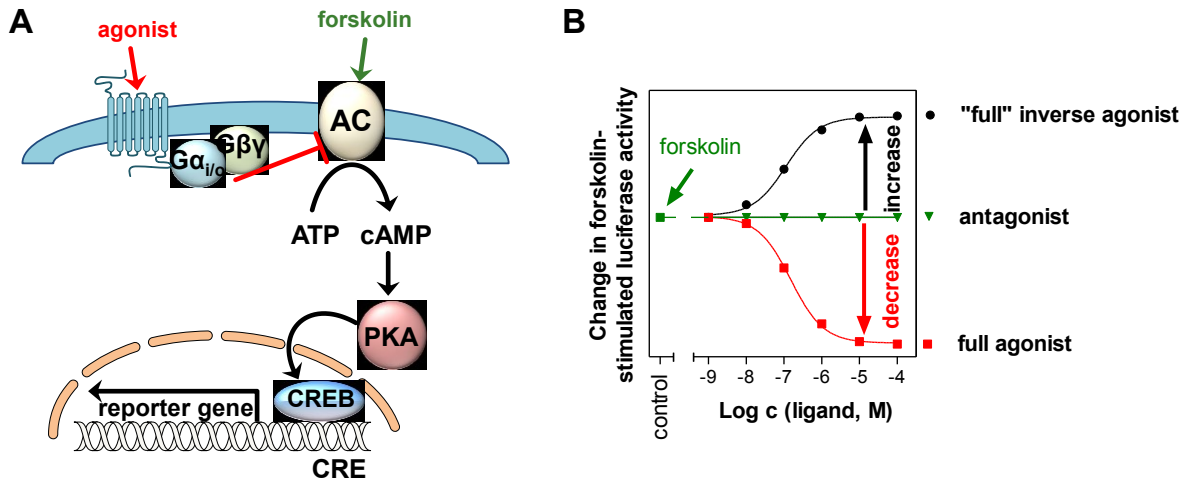

Figure 4.2. Schematic illustration of a CRE-controlled reporter gene assay (**A**). Activation of the $G_{i/o}$ coupled Y_2R and Y_4R by agonists implicates inhibition of the AC and, consequently, a decrease in transcription, whereas inverse agonists cause an increase in transcription. Neutral antagonists do not change the forskolin-stimulated luciferase activity. Forskolin-induced luciferase activity in cells in the presence and absence of agonist, inverse agonist and neutral antagonist (**B**).

In literature, the luciferase reporter gene assay in HEK293 cells was described for the human neuropeptide Y_5R (Beauverger et al., 2005). Functional activity of ligands at the Y_2R and Y_4R has been determined, for example, in the steady-state GTPase activity assay (Pop et al., 2011) and Ca^{2+} mobilization assay such as the aequorin and fura-2 assay (Ziemek et al., 2006; Ziemek et al., 2007).

The aim of this work was to develop a CRE-directed luciferase reporter gene assay in HEK293T cells, stably expressing the hY_2R or the hY_4R. Reporter gene assays provide a distal readout characterized by signal amplification. This may lead to increased agonist efficacy compared to more proximal readouts (George et al., 1997). Therefore, as far as possible, the data determined for a set of Y_2R and Y_4R ligands (for structures cf. section 1.2) in the luciferase assays were compared with results from functional assays on Sf9 cell membranes, such as the GTPase activity (Pop et al., 2011) or the [^{35}S]GTPγS binding assay (cf.chapter 3), and the arrestin recruitment assay for the hY_4R (cf. section 5.3.2). The potency of forskolin was determined to optimize assay sensitivity since the required concentration of forskolin for pre-stimulation depends on the cell type (Williams, 2004). Incubation periods of at least 4 – 6 h are indispensable taking into consideration the time course of transcription and translation. However, the risk of agonist mediated receptor desensitization raises with the duration of exposure, and this may result in a decrease in agonist potencies (Hill et al., 2001). In order to find the minimum incubation period required for appropriate signal strength, the time course of the luciferase reporter gene expression was determined. As peptidic (endogenous) ligands can be degraded by proteases under assay conditions, the stability of selected ligands and the effect of the protease inhibitor

bacitracin were investigated as well. As shown in Figure 4.3, the luciferase enzyme from the American firefly *Photinus pyralis* catalyzes in a multistep reaction the formation of oxyluciferin from the natural substrate D-luciferin, accompanied by emission of yellow/green light (560 nm). After injection of D-luciferin light is emitted, the intensity of which decreases during several seconds and reaches a plateau. The luciferase reaction is achieving a high signal-to-noise ratio, as cells or cell lysates normally do not emit interfering light (Bronstein et al., 1994; Shinde et al., 2006).

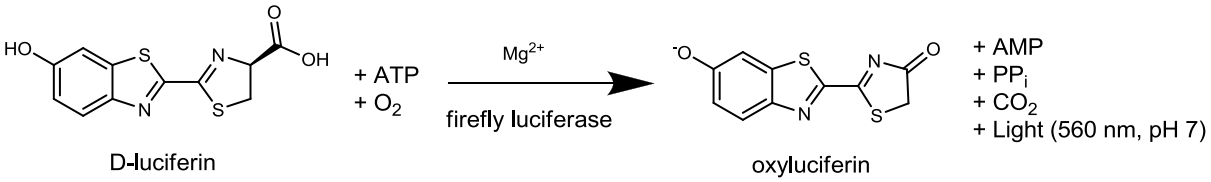

Figure 4.3. Conversion of D-luciferin by firefly luciferase to oxyluciferin (according to (Shinde et al., 2006)).

4.2 Materials and methods

4.2.1 Stable transfection of HEK293T-hY$_2$-CRE Luc and HEK293T-hY$_4$-CRE Luc cells with the pGL4.29[luc2P/CRE/Hygro] vector

HEK293T cells were stably co-transfected with the pGL4.29[luc2P/CRE/Hygro] plasmid (Promega, Mannheim, Germany) encoding hygromycin B resistance and the firefly luciferase, the transcription of which is controlled by the Camp responsive element (HEK293T-CRE Luc cells; (Nordemann et al., 2013)), and pcDNA3.1 hY$_2$ vector or pcDNA3.1 hY$_4$ vector (cDNA Resource Center; Bloomsberg, PA, USA), encoding the hY$_2$R (HEK293T-hY$_2$-CRE Luc cells) and hY$_4$R (HEK293T-hY$_4$-CRE Luc cells), respectively, and neomycin resistance. For transfection, the cells were seeded into a 24 well-plate (Becton Dickinson, Heidelberg, Germany), so that they reached 60–70% confluency on the next day. The transfection mixture containing 2 µg of the DNA and 8 µL of FuGene HD transfection reagent (Roche Diagnostics, Mannheim, Germany) was prepared according to the manufacturer's protocol and added to the cells, followed by an incubation period of 48 h at 37 °C and 5% CO_2 in a water-saturated atmosphere.

4.2.2 Cell culture

HEK293T–CRE-Luc cells stably expressing either the hY_2R or the hY_4R were cultured in Dulbecco`s Modified Eagle Medium (DMEM) (Sigma-Aldrich, Deisenhofen, Germany) containing L-glutamine (Sigma-Aldrich), 4500 mg/L glucose, 3.7 g/L $NaHCO_3$ (Merck, Darmstadt, Germany), 110 mg/L sodium pyruvate (Serva, Heidelberg, Germany), 10% fetal calf serum (FCS) (Biochrom, Berlin, Germany) and the selection antibiotics G418 (600 µg/mL) (Biochrom) and hygromycin b (300 µg/mL) (MoBiTec, Göttingen, Germany). Cells were maintained in culture flasks from Sarstedt (Nümbrecht, Germany) at 37 °C in water saturated atmosphere containing 5% CO_2 and diluted twice a week 1:10 with fresh medium after treatment with 0.05% trypsin / 0.02% EDTA (PAA, Pasching, Austria). The 10-fold concentrate of trypsin/EDTA was diluted with phosphate buffered saline (KCl 2.7 mM; KH_2PO_4 1.5 mM; NaCl 137 mM; Na_2HPO_4 5.6 mM; NaH_2PO_4 1.1 mM in Millipore water, pH 7.4, all chemicals were from Merck).

4.2.3 Saturation binding on HEK293T-CRE-Luc hY_2R and HEK293T-CRE-Luc hY_4R cells

For saturation binding experiments at HEK293T-CRE-Luc hY_2R cells, cells were grown to 80% - 100% confluency, detached from the culture flask and centrifuged at 300 *g* for 5 min. The culture medium was discarded, and the cells were re-suspended at a density of 10^6 cells/mL in buffer I (25 mM HEPES, 2.5 mM $CaCl_2$, 1 mM $MgCl_2$, pH 7.4) supplemented with 1% BSA and 0.1 mg/mL bacitracin. Experiments were performed in a final volume of 200 µL in Primaria™ 96-well plates (Corning Life Sciences, Oneonta, NY) in a concentration range of 0.25 - 20 nM with the radioligand [^{3}H]propionyl pNPY. Nonspecific binding was determined in the presence of a 150-fold excess of pNPY. Incubation period was 90 min. Bound and free radioligand were separated by filtration through 0.3% polyethyleneimine pre-treated GF/C filters (Whatman, Maidstone, UK) using a Brandel Harvester (Brandel, Gaithersburg, MD, USA). Filter pieces for each well were punched out and transferred into 96- well plates 1450-401 (PerkinElmer) and scintillation cocktail (200 µL, Rotiscint eco plus) was added. After incubation in the dark for 60 min, radioactivity (dpm) was measured with a MicroBeta2 plate counter (PerkinElmer).

The radioligand [^{3}H]UR-KK200 (Kuhn et al., 2016) was used for saturation binding experiments at intact HEK293T-hY_4-CRE Luc cells. Experiments were performed in a concentration range of 0.15 – 5 nM and nonspecific binding was determined in the presence of a 100-fold excess of [Lys^4, $Nle^{17,30}$]hPP. Experiments were performed as described above.

4.2.4 Luciferase reporter gene assay

4.2.4.1 Preparation of stock solutions and dilution series

Forskolin stock solution was prepared in 100% DMSO. Dilutions for concentration-response curves of forskolin were freshly made in DMEM without phenol red and 10% DMSO. The peptides pNPY, hPP, [Lys^4]hPP, [Lys^4, Nle^{17,30}]hPP, [Lys^4,Met(O)^{17,30}]hPP, [Lys^4,Met(O$_2$)^{17,30}] were synthesized by Synpeptide (Shanghai, China). JNJ-31020028 (UR-KK54) (Shoblock et al., 2010) was synthesized by K. Kuhn, pNPY 22-36 and M3 were synthesized by Dr. M. Kaske (University of Regensburg, Germany). The peptides pNPY2-36 and BW1911U90 were kindly provided by Prof. Dr. C. Cabrele (University of Salzburg, Austria). BIIE0246 (Doods et al., 1999), UR-PLN187 and UR-PLN208 were synthesized by Dr. Nikola Pluym in our research group as part of his doctoral project (Pluym, 2011). GW1229 (also designated GR231118 or 1229U91) was a gift from Dr. A. J. Daniels, Glaxo Wellcome Inc., USA. UR-MK188 was synthesized by Dr. M. Keller (Keller et al., 2013). For the synthesis of propionyl-[Lys^4]hPP, propionyl-[Lys^4,Nle^{17,30}]hPP and S0223[Lys^4,Nle^{17,30}]hPP cf. chapter 5. The chemical structures of the ligands are depicted in section 1.2.1. Peptides (1 mM) were dissolved in 10 mM HCl. BIIE0246 (10 mM), UR-PLN187 (10 mM), UR-PLN208 (10 mM), JNJ-31020028 (10 mM) and UR-MK188 (10 mM) were dissolved in DMSO. Dilution series of the compounds were prepared in DMEM without phenol red and 0.5% BSA. The amount of DMSO was adjusted to a final concentration of 0.2% in all assays performing the antagonist mode and 0.02% performing the agonist mode. Coated reaction vessels were used for peptides (Sigmacote, Sigma-Aldrich).

4.2.4.2 Preparation of the cells and determination of bioluminescence

The luciferase assay was performed on HEK293T-hY$_2$-CRE Luc cells and HEK293T-hY$_4$-CRE Luc cells, respectively. One day prior to the experiment, the cells were adjusted to a density of approximately 800,000 per mL in DMEM without phenol red supplemented with 5% FCS. Cells were seeded in a volume of 160 µL per well into Primaria™ 96-well plates and allowed to attach at 37 °C, 5% CO_2 in a water-saturated atmosphere overnight. A stock solution (10 mM) of forskolin (Sigma) in DMSO was used to prepare feed solutions in DMEM without phenol red (final DMSO concentration in the assay was 0.02% in the agonist mode and 0.2% in the antagonist mode, respectively). After addition of 20 µL of forskolin solution (final concentration 2 µM), 20 µL of a 10-fold concentrated solution of the respective test compound were added in the agonist mode. For assays performed in the antagonist mode, the forskolin solution was supplemented with 15 nM of pNPY (final concentration 1.5 nM) at the Y$_2$R and with 22 nM of [Lys^4, Nle^{17,30}]hPP (final concentration 2.2 nM) at the Y$_4$R, respectively. The cells were incubated at 37 °C in water saturated atmosphere containing 5%

CO_2 for 4.5 h. Afterwards, the medium was discarded, and 80 µL of lysis solution (25 mM Tricine, 10% (v/v) Glycerol, 2 mM EGTA, 1% (v/v) Triton™ X-100, 5 mM $MgSO_4 \cdot 7\ H_2O$, 1 mM DTT; pH 7.8) were added to each well. The plates were shaken at 600 rpm for 30 min. Afterwards, 40 µL of the lysate were transferred into white 96-well plates (Greiner, Frickenhausen, Germany). Luminescence was measured with a GENios Pro microplate reader. Light emission was induced by injecting 80 µL of the luciferase assay buffer (25 mM Gly-Gly; 15 mM $MgSO_4 \cdot 7\ H_2O$; 15 mM KH_2PO_4; 4 mM EGTA; 2 mM ATP disodium salt; 2 mM DTT; 0.2 mg/mL D-luciferin potassium salt (Synchem, Felsberg, Germany); pH was adjusted to 7.8 with hydrochloric acid). Luminescence [RLU] was measured for 10 s. All data are presented as means ± SEM from at least two independent experiments performed in triplicate. Concentration-response curves from the luciferase assay were analyzed by four parameter sigmoidal fits (GraphPad Prism 5.0, San Diego, CA). Agonist potencies are given as EC_{50} values, maximal responses (efficacies) are expressed as α value referred to the effect of 300 nM pNPY (α = 1.0) or 300 nM hPP (α = 1.0), respectively. Antagonist activities are given as K_b values.

4.2.4.3 Effect of the solvent on luciferase activity

The stock solution of forskolin (10 mM) was prepared in DMSO or DMF, respectively. A volume of 20 µL of a forskolin solution (final concentration: 2 µM) and DMSO or DMF in a volume of 20 µL were added at increasing concentrations to 160 µL of cell culture medium per well. Luciferase assay was performed as described above.

4.2.4.4 Determination of the optimal forskolin concentration

A volume of 20 µL of a 10-fold concentrated forskolin solution (containing 10% DMSO) was added to 180 µL of cell culture medium per well. The cells were incubated for 4.5 h at 37 °C and 5% CO_2 in a water saturated atmosphere. Forskolin was investigated at concentrations up to 100 µM to determine the optimal concentration. For measurement of luminescence cf. 4.2.4.2.

4.2.4.5 Effects of different forskolin concentrations on the concentration-response curves of pNPY and [Lys^4, Nle^{17,30}]hPP

A volume of 20 µL of forskolin solution (final concentration 1 µM, 1.5 µM, 2 µM, 3 µM, 4 µM) and 20 µL of a 10-fold concentrated solution of pNPY and [Lys^4, Nle^{17,30}]hPP, respectively,

were added to 160 µL of cell culture medium per well, and the assay was performed as described above.

4.2.4.6 Effect of bacitracin on the stability of pNPY and [Lys^4, Nle^{17,30}]hPP

The stock solution of bacitracin (100 mg/mL) was prepared in water. For a final concentration of 0.1 mg/mL in the assay, bacitracin was added to the forskolin solution 10-fold concentrated. Luciferase assay was performed as described above. EC_{50} values of pNPY and [Lys^4, Nle^{17,30}]hPP were determined in the absence and in the presence of bacitracin (0.1 mg/mL).

4.2.4.7 Monitoring the time course of luciferase expression

A forskolin solution (20 µL, 20 µM) was added to 180 µL of cell culture medium per well. The luminescence was measured after 0.0, 1.0, 2.0, 3.0, 4.0, 5.0, 4.5, 5.0, 8.0, 9.0, 22 and 23 h. The basal luminescence was subtracted from each signal and the obtained values were plotted against the time.

4.2.4.8 Control experiments using HEK293T-CRE-Luc cells devoid of hY$_2$R and hY$_4$R

The procedure was the same as described in section 4.2.4.2, but HEK293T-CRE-Luc cells devoid of hY$_2$R and hY$_4$R, respectively, were used. All RLUs were referred to the luciferase activity at 2 µM forskolin which was used for pre-stimulation and set to 100%.

4.3 Results and discussion

4.3.1 Reporter gene assay for the human neuropeptide Y$_2$ receptor

4.3.1.1 Saturation binding assay using HEK293T-hY$_2$-CRE Luc cells

Due to the poor adherence of the HEK293T cells (Lieb et al., 2016), the assay was performed by using cells in suspension. The bound radioligand [^{3}H]propionyl-pNPY was separated from the free radioligand by filtration. Unfortunately, the nonspecific binding was high, and binding was not saturable (Figure 4.4). The hY$_2$R expression could not be confirmed by saturation binding assays.

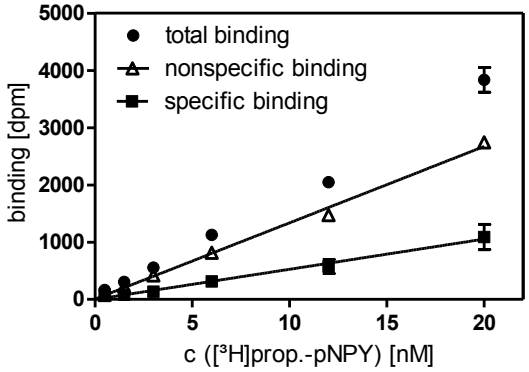

Figure 4.4. Representative binding experiment on HEK293T-CRE-Luc hY_2R cells. Nonspecific binding of [^{3}H]prop.-pNPY was determined in the presence of a 150-fold excess of pNPY. Two independent experiments were performed in triplicate.

4.3.1.2 Effects of the solvent on the luciferase activity

The effects of DMSO and DMF (Figure 4.5) on the luciferase signal were investigated, as DMSO can negatively effect bioluminescence (Plank, 2016).

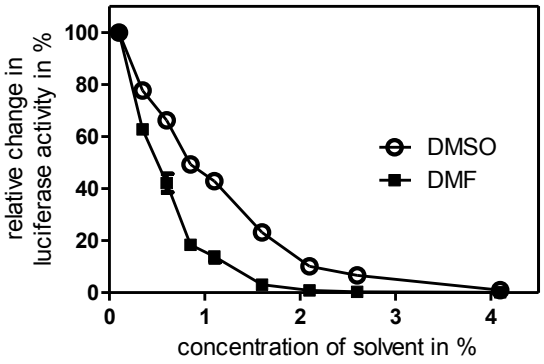

Figure 4.5. Impact of DMSO and DMF on the luciferase signal. Cells were incubated with buffer containing the respective solvent. The luciferase activity induced by 2 µM forskolin was set to 100%. Data are means ± SEM of three independent experiments, each performed in triplicate.

DMSO at a concentration of 1.1% reduced the maximum luciferase signal by approximately 58%, whereas in the presence of 2.5% DMSO the signal was almost completely suppressed. The effect of DMF was investigated as an alternative to DMSO. Interestingly, at a final concentration of 0.6% DMF the reduction of the luminescence signal was comparable to a DMSO concentration of 1.1%. In the presence of 1.6% DMF the signal was almost completely suppressed. Therefore, DMSO should not be replaced by DMF as solvent, if the concentration of these solvents exceeds the standard value of 0.2%.

4.3.1.3 Optimization of stimulation with forskolin

In literature, the concentration of forskolin used in reporter gene assays for $G\alpha_{i/o}$ coupled GPCRs ranges from 500 nM (Kemp et al., 1999) to 10 µM (Liu et al., 2001). HEK293T-hY_2-CRE Luc cells were incubated with increasing forskolin concentrations in 1% DMSO or 1% DMF, respectively (Figure 4.6). In a concentration dependent manner, forskolin stimulated luciferase expression up to a concentration of 10 µM. Higher forskolin

concentrations caused a decrease in luciferase expression as already described for several cell types expressing the luciferase gene reporter (George et al., 1997; Kemp et al., 2002; Stroop et al., 1995). All respective dilutions were freshly prepared for every assay to exclude precipitation of forskolin.

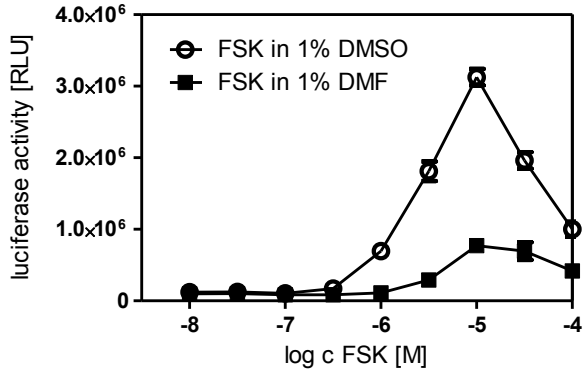

Figure 4.6. Forskolin-stimulated luciferase expression in HEK293T-hY_2-CRE Luc cells. "Bell-shaped" concentration-response curve in 1% DMSO and 1% DMF. Data represent mean values ± SEM of at least three independent experiments performed in triplicate.

The "bell-shaped" concentration-response curve showed a maximum at 10 µM of forskolin. Hence, only the ascending part of the curve was considered for the determination of the EC_{50} value of forskolin (2 µM). The decrease in luciferase expression at higher concentrations of forskolin may be interpreted as a hint to endogenous cAMP dependent ICER activity in HEK293T cells which was shown for CHO cells (Kemp et al., 2002). Stimulation with 2 µM of forskolin turned out to be suitable to perform the reporter gene assay with HEK293T-hY_2-CRE Luc cells.

4.3.1.4 Optimization of the period of incubation

According to the literature, the preferred incubation period for luciferase reporter gene assays ranges from 4 h (Kemp et al., 1999) to 8 h (Li et al., 2007). For optimization of the assay, the time course of the luciferase expression in HEK293T-hY_2-CRE Luc cells was investigated. Luciferase gene transcription was stimulated with 2 µM of forskolin, and the cells were lysed after various incubation periods as shown in Figure 4.7. The maximum of expression was reached after a period of 9 h, after 23 h the luciferase activity amounted to 46% of the maximal response. An incubation period of 4.5 h appeared to be sufficient, as 74% of the maximum expression were reached.

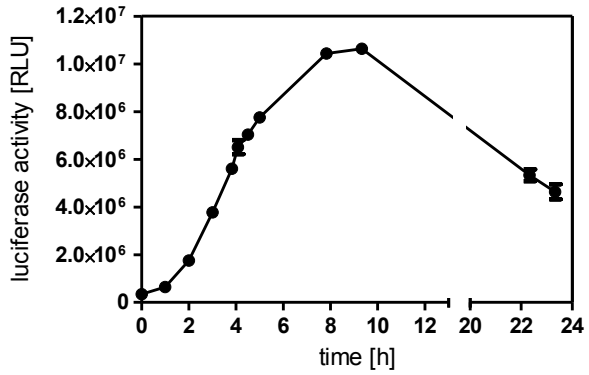

Figure 4.7. Time course of luciferase expression in HEK293T-hY_2-CRE Luc cells after stimulation with 2 µM of forskolin. Luciferase activity was determined after the indicated incubation periods (mean values ± SEM; n = 2).

4.3.1.5 Effects of different forskolin concentrations on pNPY concentration-response curves

Concentration-response curves of pNPY in the presence of different forskolin concentrations revealed comparable EC_{50} values (0.17 – 0.41 nM). As shown in Figure 4.8, the amplitude of the concentration-response curves (903,000 - 1,012,000 RLU) remains nearly unchanged with increasing forskolin concentrations.

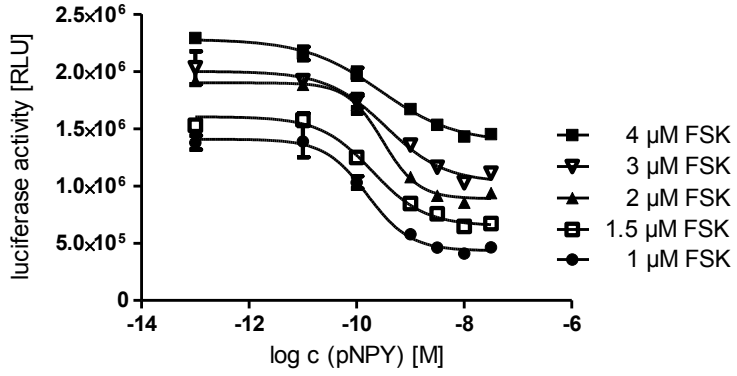

Figure 4.8. Representative concentration-response curves of pNPY in the presence of different forskolin concentrations. Data represent means ± SEM (performed in triplicate).

4.3.1.6 Effect of bacitracin on the stability of pNPY

Bacitracin, an antibiotic containing a mixture of related cyclic peptides, is also known as protease inhibitor and commonly used in peptide research (Wang and Adrian, 1995). As enzymatic cleavage under assay conditions cannot be precluded, concentration-response curves of the peptide pNPY were constructed in the absence and presence of bacitracin (0.1 mg/mL) (Figure 4.9). Surprisingly, the curves and the determined EC_{50} values were identical, that is, pNPY was stable under these assay conditions and bacitracin can be omitted.

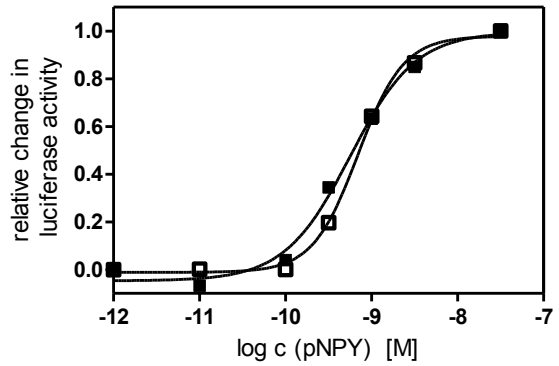

Figure 4.9. Concentration-response curves of pNPY at HEK293T-hY$_2$-CRE Luc cells in the absence (■) and presence (□) of bacitracin (0.1 mg/mL). Data are means ± SEM of a representative experiment performed in triplicate.

4.3.1.7 Control experiments on cells devoid of the hY$_2$R

In principle, changes in CRE-controlled luciferase activity can be caused by off-target effects independent of the GPCR of interest (Atwood et al., 2011). Therefore, control experiments with HEK293T-CRE-Luc cells devoid of the hY$_2$R were performed. The cells were stimulated with 2 µM forskolin and co-incubated with the agonist pNPY or the antagonist BIIE0246 (Figure 4.10). Changes in luciferase activity were not detected, that is, the effects depicted in Figure 4.11 are Y$_2$R-mediated.

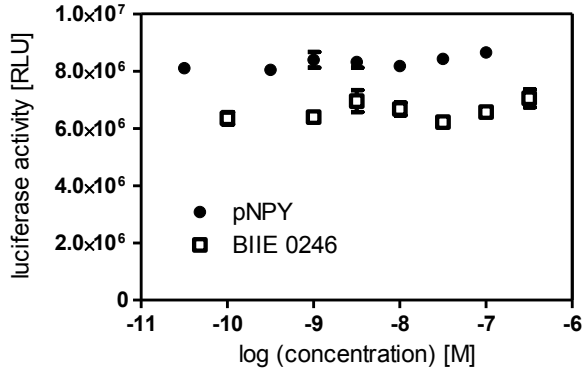

Figure 4.10. Luciferase activity in the presence of the agonist pNPY (final c(DMSO) = 0.02%) and the antagonist BIIE0246 (final c(DMSO) = 0.2%) in the reporter gene assay using HEK293T-CRE Luc cells devoid of Y$_2$R expression. Data are means ± SEM of a representative experiment performed in triplicate.

4.3.1.8 Functional activities of selected ligands at the hY$_2$R

Selected ligands including agonists and antagonists (cf. section 1.2.1), were investigated for their ability to change forskolin (2 µM) stimulated luciferase activity in HEK293T-hY$_2$-CRE Luc cells. All antagonists behaved as neutral antagonists in the agonist mode (data not shown). The determined EC_{50} values or K_b values were compared, as far as possible, with results from functional studies using more proximal readouts in G-protein mediated signal transduction, e.g. the functional [^{35}S]GTPγS binding assay (cf. chapter 3) and the steady-state GTPase activity assay (Pop et al., 2011), which were both performed on membrane

preparations of Sf9 cells expressing the hY_2R. The obtained results as well as the reported data are summarized in Table 4.1. NPY and its analogs pNPY2-36 and pNPY22-36 acted as full agonists on HEK293T-hY_2-CRE Luc cells (Figure 4.11A, Table 4.1). The EC_{50} values of these agonists were in the same range as reported binding data, determined in a radioligand binding assay with [³H]propionyl-pNPY (Table 4.1). Although the EC_{50} values were lower compared to EC_{50} values from other functional assays, the rank order of potencies and affinities (pNPY > pNPY2-36 > pNPY22-36) was identical (Table 4.1). In the antagonist mode, BIIE0246 antagonized the pNPY induced decrease in luciferase activity with a K_b value of 1.08 nM, which was lower compared to the results determined in the GTPase and [^{35}S]GTPγS assay (cf. section 3.3.1). In agreement with data from the Ca^{2+} mobilization and the [^{35}S]GTPγS binding assay, the derivatives of BIIE0246, namely UR- PLN187 and UR-PLN208, proved to be full antagonists.

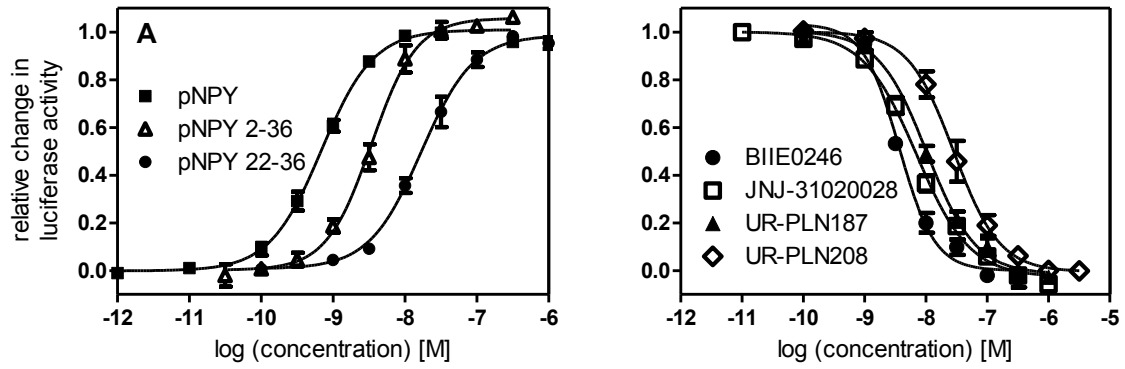

Figure 4.11. Concentration-response curves of pNPY, pNPY2-36, pNPY22-36, BIIE0246, UR-PLN187, UR-PLN208 and JNJ-31020028 in the luciferase assay on HEK293T-hY_2-CRE Luc cells. (**A**) Agonist mode, maximum change of 1 is defined as full agonism and referred to the effect of pNPY (α = 1.0). (**B**) Antagonist mode, maximum change is defined as full antagonism and referred to the effect of 1 µM BIIE0246. Data points shown are the mean values ± SEM of at least three independent experiments performed in triplicate.

In summary, agonistic and antagonistic activities at the hY_2R were determined on genetically engineered HEK293T cells (HEK293T-hY_2-CRE Luc cells) co-expressing the hY_2R and a CRE controlled luciferase reporter gene. The agonistic potencies of the investigated Y_2R ligands were in accordance with the K_i values determined in radioligand binding studies. Except for UR-PLN208, all antagonists showed higher activities compared to functional studies in other assays. In case of agonists, it should be kept in mind that potential differences may be masked in assays with a distal readout due to signal amplification in the second messenger cascade downstream from G-protein activation.

Table 4.1. NPY hY_2R agonist potencies (EC_{50}), intrinsic activities (α) and affinities of selected peptides and reference compound pNPY.

Compound	EC_{50} [nM] or (K_b) [nM][a]	α	EC_{50} [nM] or (K_b) [nM]	K_i [nM][i]
pNPY	0.58 ± 0.07	1.0	11.7 ± 3.0[b]	1.72 ± 0.13
			16.9 ± 2.5[d]	
pNPY2-36	3.7 ± 0.4	1.07	n.d.	5.8 ± 1.1
pNPY22-36	18.0 ± 2.3	0.99	42 ± 5[h]	12.5 ± 1.8
BIIE0246	(1.0 ± 0.1)		(10.2 ± 1.8)[b]	24.4 ± 3
			(5.6 ± 0.4)[e]	
UR-PLN187	(3.0 ± 0.1)		(6.8 ± 1.9)[f]	101 ± 13
UR-PLN208	(7.9 ± 1.9)		(8.2 ± 0.4)[e]	19.5 ± 3.7
			(8.3 ± 0.5)[c]	
JNJ-31020028	(1.9 ± 0.3)		(10.0 ± 2.6)[h]	29.8 ± 2.2
			(9.1 ± 0.7)[g]	

[a] CRE-luciferase reporter gene assay on HEK293T cells stably expressing the hY_2R. Y_2R agonist potency was determined from the inhibition of forskolin (2 µM) stimulated luciferase activity; in the agonist mode, the intrinsic activity (α) of pNPY was set to 1.0 and α values of other compounds were referred to this value; maximum change of 1 indicates full agonism; the K_b values of neutral antagonists were determined in the antagonist mode versus pNPY (1.5 nM) as the agonist; K_b values were calculated according to the Cheng-Prusoff equation (Cheng and Prusoff, 1973); mean values ± SEM, at least three independent experiments were performed in triplicate. [b-c] Steady-state GTPase assay on membrane preparations expressing the hY_2R + $G\alpha_{i2}$ + $G\beta_1\gamma_2$ + RGS4; [b] data reported by (Pop et al., 2011); [c] (Baumeister, 2014). [d-g] Calcium mobilization assay on CHO cells, stably expressing the hY_2R; [d] data reported by (Ziemek, 2006); [e] (Pluym et al., 2013); [f] (Pluym, 2011); [g](Shoblock et al., 2010). [h] [^{35}S]GTPγS functional binding assay with membrane preparations of Sf9 cells expressing the hY_2R + $G\alpha_{i2}$ + $G\beta_1\gamma_2$ +RGS4 (see section 3.3.1). [i] Radioligand binding assay performed with [^{3}H]prop.-NPY (c = 1 nM) at CHO hY_2R cells; mean values ± SEM, at least three independent experiments were performed in triplicate.

4.3.2 Reporter gene assay for the human neuropeptide Y_4 receptor

4.3.2.1 Saturation binding assay using HEK293T-hY_4-CRE Luc cells

Receptor expression was confirmed by saturation binding assays using whole cells. The quantitative analysis of the saturation binding of [^{3}H]UR-KK200 resulted in around 100,000 receptors per cell for the HEK293T-hY_4-CRE Luc cells (Figure 4.12). The determined K_d value of 0.48 ± 0.13 nM was in the same range as data determined on CHO cells, stably expressing the hY_4R (0.67 nM; (Kuhn et al., 2016)).

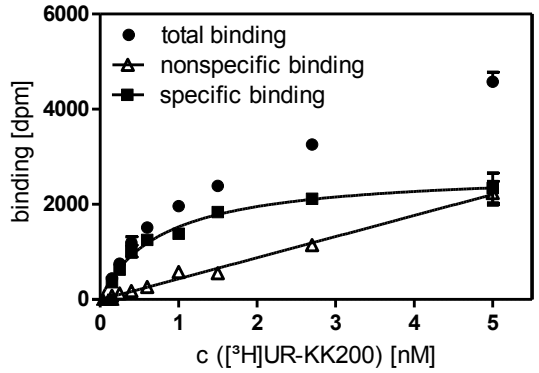

Figure 4.12. Representative saturation binding experiment with [^{3}H]UR-KK200 on HEK293T-CRE-Luc hY$_4$R cells. Nonspecific binding was determined in the presence of a 100-fold excess of [Lys^4, Nle^{17,30}]hPP; K_d = 0.48 ± 0.13 nM; experiment performed in triplicate.

4.3.2.2 Effect of the solvent on the luciferase activity

The effects of DMSO and DMF were investigated as described for the hY$_2$R (section 4.3.1.2, Figure 4.13).

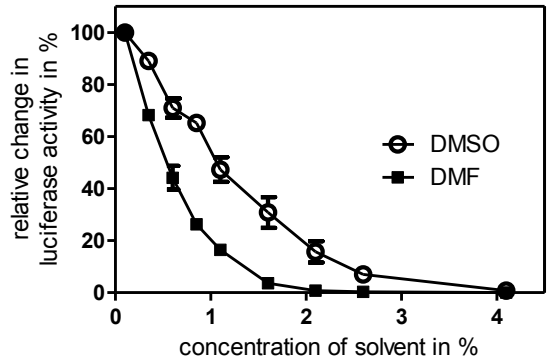

Figure 4.13. Impact of DMSO and DMF on the luciferase signal. Cells were incubated with buffer containing the respective solvent. The luciferase activity induced by 2 µM forskolin (0.02% DMSO or 0.02% DMF) was set to 100%. Data are means ± SEM of three independent experiments, each performed in triplicate.

DMSO at a concentration of 1.1% reduced the maximum luciferase signal by approximately 53%, whereas in the presence of 2.5% DMSO the signal was almost completely suppressed. The effect of DMF was investigated with respect to a possible alternative to DMSO. Reduction of the maximum luminescence signal is comparable to results for the hY$_2$R (see section 4.3.1.2). Therefore, DMSO should not be replaced by DMF as solvent, if the concentration exceeds the standard value of 0.2%.

4.3.2.3 Optimization of stimulation with forskolin

HEK293T-hY$_4$-CRE Luc cells were incubated with increasing forskolin (FSK) concentrations in the presence of 1% DMSO or 1% DMF (Figure 4.14). In a concentration dependent manner, forskolin stimulated luciferase expression up to a concentration of 10 µM.

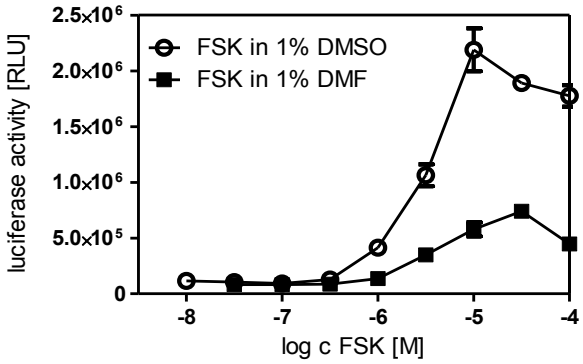

Figure 4.14. Forskolin-stimulated luciferase expression in HEK293T-hY$_4$-CRE Luc cells. "Bell-shaped" concentration-response curve in the presence of 1% DMSO and 1% DMF. Data points are mean values ± SEM of at least three independent experiments performed in triplicate.

The "bell-shaped" concentration-response curve showed a maximum at 10 µM (1% DMSO) and 30 µM (1% DMF) of forskolin, respectively. Hence, the ascending part of the curve was considered for the determination of the EC_{50} value (2 µM in the presence of DMSO) of forskolin. The low level of the luciferase activity in 1% DMF is also shown in section 4.3.2.2.

4.3.2.4 Optimization of the incubation time

For optimization of the assay conditions, the time course of the luciferase expression in HEK293T-hY$_2$-CRE Luc cells was investigated. Luciferase gene transcription was stimulated with 2 µM of forskolin, and the cells were lysed after various incubation periods as shown in Figure 4.15. Maximum expression was reached after a period of 9 h. The signal decreased to 47% after 23 h. Therefore, an incubation period of 4.5 h, when 73% of the maximum expression were reached, appeared to be sufficient.

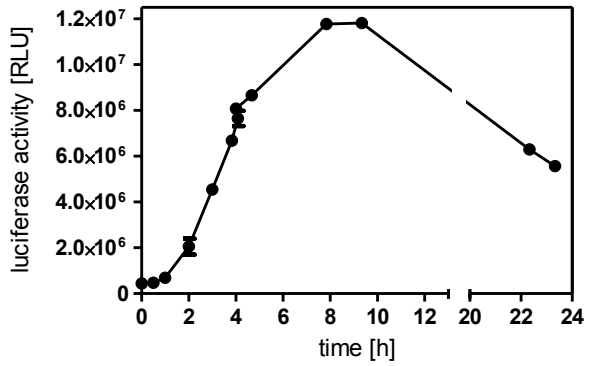

Figure 4.15. Time course of luciferase expression in HEK293T-hY$_4$-CRE Luc cells after stimulation with 2 µM of forskolin. Luciferase activity was determined after the indicated incubation periods (mean values ± SEM; n = 2).

4.3.2.5 Effects of different forskolin concentrations on the concentration-response curve of [Lys^4, Nle^{17,30}]hPP

Concentration-response curves of [Lys^4, Nle^{17,30}]hPP in the presence of different forskolin concentrations revealed comparable EC_{50} values (0.24 — 0.96 nM). As shown for

representative experiments in Figure 4.16 the amplitude of luciferase activity was almost the same (2,260,000 – 2,850,000 RLU) irrespective of increasing forskolin concentrations.

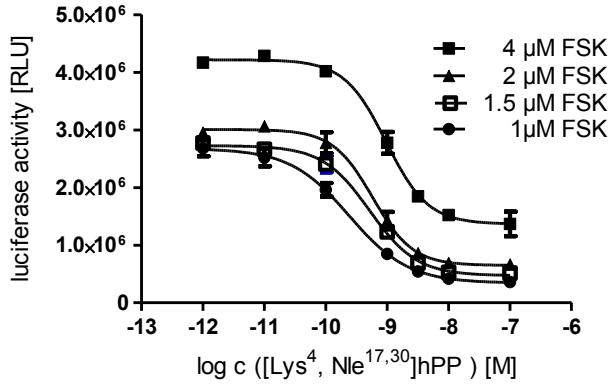

4.16. Representative concentration-response curves of [Lys^4, Nle^{17,30}]hPP in the presence of different forskolin (FSK) concentrations. Data represent means ± SEM (performed in triplicate).

4.3.2.6 Effect of bacitracin on the stability of [Lys^4, Nle^{17,30}]hPP

As also described above for pNPY at the hY$_2$R (cf. section 4.3.1.6), no effect of bacitracin was observed in case of [Lys^4, Nle^{17,30}]hPP (Figure 4.17). Hence, [Lys^4, Nle^{17,30}]hPP is stable under these assay conditions and bacitracin can be omitted.

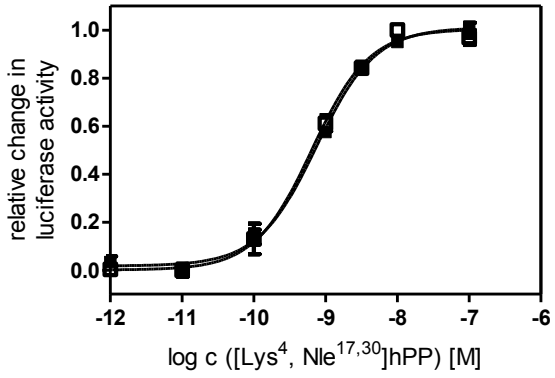

Figure 4.17. Concentration-response curves of [Lys^4, Nle^{17,30}]hPP at HEK293T-hY$_4$-CRE Luc cells in the absence (■) and presence (□) of bacitracin (0.1 mg/mL). Data are means ± SEM of representative experiments, each performed in triplicate.

4.3.2.7 Control experiments on cells devoid of the hY$_4$R

In control experiments, HEK293T-CRE-Luc cells devoid of the hY$_4$R were stimulated with 2 µM forskolin and co-incubated with the agonist hPP (see Figure 4.18). Changes in luciferase activity were not detected, confirming that the effects of the investigated Y$_4$R ligands shown in Figure 4.19 are receptor mediated.

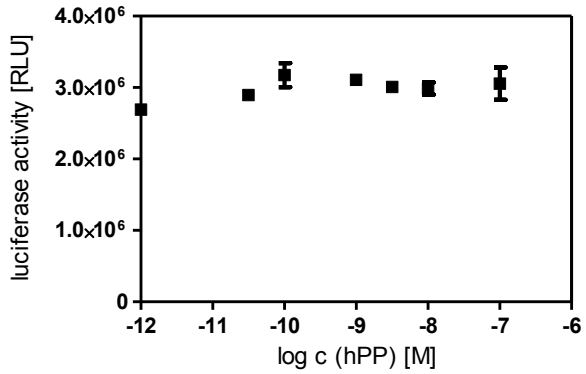

Figure 4.18. Luciferase activity in the reporter gene assay at HEK293T-CRE Luc cells devoid of the Y_4R using hPP as agonist. Stimulation with forskolin (2 µM). Data are means ± SEM of a representative experiment performed in triplicate.

4.3.2.8 Functional activities of selected ligands at the hY_4R

Selected ligands including agonists and antagonists (for structures cf. sections 1.2.2 and 5.1) were investigated for their ability to change forskolin (2 µM) stimulated luciferase activity in HEK293T-hY_4-CRE Luc cells. The determined EC_{50} values or K_b values were compared, as far as possible, with results from functional studies using more proximal readouts, e.g. the arrestin recruitment assay on HEK293T-ARRB1-Y_4R and HEK293T-ARRB2-Y_4R cells (T.Littmann, personal communication), and the steady-state [^{33}P]GTPase activity assay (Pop, 2011), which was performed on membrane preparations of Sf9 cells expressing the hY_4R. The obtained results as well as the reported data are summarized in Table 4.2.

The peptide hPP and its analogs [Lys^4]hPP and [Lys^4, Nle^{17,30}]hPP acted as full agonists on HEK293T-hY_4-CRE Luc cells (Figure 4.19). The potencies of these agonists were in accordance with reported binding data, determined in a radioligand binding assay with [^{3}H]propionyl-[Lys^4, Nle^{17,30}]hPP in buffer I (25 mM HEPES, 2.5 mM $CaCl_2$, 1 mM $MgCl_2$, pH 7.4) (see section 5.3.5). Although, the EC_{50} values were lower compared to the K_i values and EC_{50} values of other functional assays such as the arrestin recruitment assay, the rank order of potencies and affinities (hPP > [Lys^4, Nle^{17,30}]hPP > [Lys^4]hPP) was identical, which is in agreement with binding and functional data from different assays. In literature, GW1229 was reported both as a partial (Berglund et al., 2003b; Ziemek et al., 2007) and a full agonist (Berglund et al., 2003a; Parker et al., 1998). Interestingly, in the luciferase assay GW1229 was a full agonist and nearly 100 times more potent (EC_{50} = 5.5 nM) than in the β-arrestin-1 recruitment assay (EC_{50} = 413 nM). The replacement of Arg^{25} in the Y_4R partial agonist [cpen^{34}]pNPY(25-36) by a functionalized arginine building block resulted in the ligand M3 (Ac-Arg(N^{ω}-Ahx)-HYINLITR-cpen-RY-NH_2) which was investigated in our working group (Kaske, 2012). M3 acted as partial agonist at the hY_4R which was in agreement with results from the GTPase activity assay (Kaske, 2012). In case of BW1911U90, there are discrepancies regarding the intrinsic activity in different assays. Whereas BW1911U90 acted as a full agonist in the GTPase assay (Pop et al., 2011) and the cAMP assay (Parker et al.,

1998), the hY$_4$R was only partially activated in the luciferase reporter gene assay (α = 0.51). UR-MK188 antagonized the [Lys^4, Nle^{17,30}]hPP induced decrease in luciferase activity. The determined K_b value of 30 nM was in good agreement with results from the Ca^{2+} mobilization assay (K_b = 20 nM; (Keller et al., 2013).

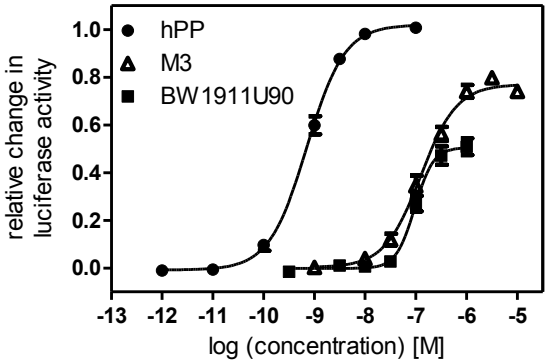

Figure 4.19. Potencies and efficacies of hPP, M3 and BW1911U90 in HEK293T-hY$_4$-CRE Luc cells. Agonist mode, maximum change is referred to the maximal response to hPP (α = 1.0). Data points shown are the mean values ± SEM of at least three independent experiments, each performed in triplicate.

Table 4.2. NPY hY$_4$R agonist potencies (EC_{50}) and intrinsic activities (α) of selected peptides and reference compound hPP.

Compound	EC_{50} [nM] or (K_b) [nM][a]	α	EC_{50} [nM][d] or (K_b) [nM]	α	β-arrestin isoform
hPP	0.6 ± 0.1[a]	1.0	4.4 ± 0.02	1.0	1
			3.1 ± 0.01	1.0	2
[Lys^4]hPP	1.5 ± 0.2[a]	0.99	7.3 ± 0.03	0.75	1
			5.0 ± 0.03	0.88	2
Propionyl-[Lys^4]hPP	3.5 ± 0.4[a]	0.97	15 ± 0.08	0.81	1
			10 ± 0.04	0.89	2
[Lys^4,Met(O)^{17,30}]hPP	4.2 ± 0.3[a]	1.02	42 ± 0.18	0.72	1
			27 ± 0.12	0.79	2
[Lys^4,Met(O$_2$)^{17,30}]hPP	1.9 ± 0.4[a]	0.99	10 ± 0.05	0.71	1
			6.4 ± 0.02	0.80	2
[Lys^4,Nle^{17,30}]hPP	0.9 ± 0.1[a]	1.00	15 ± 0.05	0.74	1
			10 ± 0.03	0.86	2
Prop.-[Lys^4,Nle^{17,30}]hPP	1.0 ± 0.1[a]	0.99	14 ± 0.09	0.79	1
			9.2 ± 0.04	0.83	2
S0223[Lys^4,Nle^{17,30}]hPP	3.1 ± 0.9[a]	1.00	19 ± 0.12	0.84	1
			13 ± 0.10	0.89	2
GW1229	5.5 ± 0.8[a]	1.01	413 ± 2	0.53	1
			236 ± 2	0.63	2
BW1911U90	107 ± 13[a]	0.51	n.d.		
	8.9 ± 1.5[b]	1.28			
M3	130 ± 17[a]	0.77	n.d.		
	38 ± 8.8[b]	0.67			
UR-MK188	(30 ± 2.4)[a]		55 ± 22		1
			(46 ± 18)		2

[a] CRE-luciferase reporter gene assay on HEK293T cells stably co-expressing the hY$_4$R and the CRE-controlled luciferase gene reporter. Y$_4$R agonist potency was determined from the inhibition of forskolin (2 µM) stimulated luciferase activity; the intrinsic activity (α) of hPP was set to 1.00 and α values of other compounds were referred to this value, maximum change of 1 indicates full agonism; the K_b values of neutral antagonists were determined in the antagonist mode versus [Lys^4,Nle^{17,30}]hPP (2.2 nM) as the agonist; K_b values were calculated according to the Cheng-Prusoff equation (Cheng and Prusoff, 1973); mean values ± SEM (n = 3 - 9). [b-c] Steady-state GTPase assay on membrane preparations expressing the hY$_4$R + Gα_{i2} + G$\beta_1\gamma_2$ + RGS4; [b] data reported by Pop et al. (Pop et al., 2011); [c] data reported by (Kaske, 2012). [d] Arrestin recruitment assay on HEK293T-ARRB1-Y$_4$R and HEK293T-ARRB2-Y$_4$R cells (see section 5.3.2; T. Littmann, personal communication). The maximal response (intrinsic activity, α) is referred to the effect of hPP set to α = 1.0; K_b value of UR-MK188 was determined in the antagonist mode versus hPP (3 nM) as the agonist and calculated according to the Chen-Prusoff equation; data represent mean values ± SEM from at least two independent experiments performed in triplicate.

In summary, agonistic and antagonistic activities at the hY_4R were determined on genetically engineered HEK293T cells (HEK293T-hY_4-CRE Luc cells) co-expressing the hY_4R and a CRE controlled luciferase reporter gene. Activation of hY_4R in the luciferase assay resulted in higher agonist potencies compared to functional assays providing more proximal readouts such as the GTPase or the β-arrestin recruitment assay. This may be interpreted as a hint to signal amplification. K_i values determined in radioligand binding studies in buffer I were in good agreement with the EC_{50} values determined in the luciferase assay.

4.4 Summary and conclusion

Agonistic and antagonistic activity can be determined in HEK293T cells, stably expressing the human Y_2 and Y_4 receptor, respectively, by using a CRE-controlled luciferase reporter gene assay. Non-Y_2R and -Y_4R mediated (off-target) effects were not detected in cells of the same genetic background, that is, HEK293T-CRE-Luc cells devoid of Y_2R or Y_4R. An optimal incubation period of 4.5 h was determined by monitoring the time course of the luciferase expression which was nearly identical for the Y_2R and Y_4R expressing cells. A 'bell-shaped' concentration-response curve of forskolin became obvious, presumably, caused by activation of ICER at high cAMP concentrations. The optimum concentration of 2 µM of forskolin was used throughout in the luciferase assay. As the concentration-response curves of peptide agonists remained unchanged in the presence of bacitracin, the addition of a protease inhibitor appears unnecessary. Furthermore, a tremendous impact of solvents on luciferase activity became obvious by investigating DMSO and DMF as possible solvents for water-insoluble compounds. DMSO should be preferred to DMF, however, at the concentrations required to keep forskolin and test compounds in solution, the inhibitory solvent effect was negligible. The determined potencies of selected Y_2R and Y_4R ligands at the respective receptor were generally higher compared to data determined in other functional assays.

4.5 References

Baumeister, P. (2014). Molecular tools for G-protein coupled receptors: Synthesis, pharmacological characterization and [3H]-labeling of subtype-selective ligands for histamine H4 and NPY Y2 receptors Doctoral Thesis, University of Regensburg, Regensburg.

Beauverger, P.; Rodriguez, M.; Nicolas, J.-P.; Audinot, V.; Lamamy, V.; Dromaint, S.; Nagel, N.; Macia, C.; Léopold, O.; Galizzi, J.-P.; Caignard, D.-H.; Aldana, I.; Monge, A.; Chomarat, P.; Boutin, J. A. (2005). Functional characterization of human neuropeptide Y receptor subtype five specific antagonists using a luciferase reporter gene assay. *Cell. Signal.* 17(4): 489-496.

Berglund, M. M.; Schober, D. A.; Esterman, M. A.; Gehlert, D. R. (2003a). Neuropeptide Y Y4 receptor homodimers dissociate upon agonist stimulation. *J. Pharmacol. Exp. Ther.* 307(3): 1120-1126.

Berglund, M. M.; Schober, D. A.; Statnick, M. A.; McDonald, P. H.; Gehlert, D. R. (2003b). The use of bioluminescence resonance energy transfer 2 to study neuropeptide Y receptor agonist-induced beta-arrestin 2 interaction. *J. Pharmacol. Exp. Ther.* 306(1): 147-156.

Bronstein, I.; Fortin, J.; Stanley, P. E.; Stewart, G. S.; Kricka, L. J. (1994). Chemiluminescent and bioluminescent reporter gene assays. *Anal. Biochem.* 219(2): 169-181.

Cheng, Y.; Prusoff, W. H. (1973). Relationship between the inhibition constant (K1) and the concentration of inhibitor which causes 50 per cent inhibition (I50) of an enzymatic reaction. *Biochem. Pharmacol.* 22(23): 3099-3108.

Doods, H.; Gaida, W.; Wieland, H. A.; Dollinger, H.; Schnorrenberg, G.; Esser, F.; Engel, W.; Eberlein, W.; Rudolf, K. (1999). BIIE0246: a selective and high affinity neuropeptide Y Y(2) receptor antagonist. *Eur. J. Pharmacol.* 384(2-3): R3-5.

George, S. E.; Bungay, P. J.; Naylor, L. H. (1997). Evaluation of a CRE-Directed Luciferase Reporter Gene Assay as an Alternative to Measuring cAMP Accumulation. *Journal of Biomolecular Screening* 2(4): 235-240.

Hill, S. J.; Baker, J. G.; Rees, S. (2001). Reporter-gene systems for the study of G-protein-coupled receptors. *Curr. Opin. Pharmacol.* 1(5): 526-532.

Kaske, M. (2012). In search for potent and selective NPY Y4 receptor ligands: acylguanidines, argininamides and peptide analogs Doctoral Thesis, University of Regensburg, Regensburg.

Keller, M.; Kaske, M.; Holzammer, T.; Bernhardt, G.; Buschauer, A. (2013). Dimeric argininamide-type neuropeptide Y receptor antagonists: Chiral discrimination between Y1 and Y4 receptors. *Bioorg. Med. Chem.* 21(21): 6303-6322.

Kemp, D. M.; George, S. E.; Bungay, P. J.; Naylor, L. H. (1999). Partial agonism at serotonin 5-HT1B and dopamine D2L receptors using a luciferase reporter gene assay. *Eur. J. Pharmacol.* 373(2-3): 215-222.

Kemp, D. M.; George, S. E.; Kent, T. C.; Bungay, P. J.; Naylor, L. H. (2002). The effect of ICER on screening methods involving CRE-mediated reporter gene expression. *J. Biomol. Screen* 7(2): 141-148.

Kuhn, K. K.; Ertl, T.; Dukorn, S.; Keller, M.; Bernhardt, G.; Reiser, O.; Buschauer, A. (2016). High Affinity Agonists of the Neuropeptide Y (NPY) Y4 Receptor Derived from the C-Terminal Pentapeptide of Human Pancreatic Polypeptide (hPP): Synthesis, Stereochemical Discrimination, and Radiolabeling. *J. Med. Chem.* 59(13): 6045-6058.

Li, X.; Shen, F.; Zhang, Y.; Zhu, J.; Huang, L.; Shi, Q. (2007). Functional characterization of cell lines for high-throughput screening of human neuromedin U receptor subtype 2 specific agonists using a luciferase reporter gene assay. *Eur. J. Pharm. Biopharm.* 67(1): 284-292.

Lieb, S.; Michaelis, S.; Plank, N.; Bernhardt, G.; Buschauer, A.; Wegener, J. (2016). Label-free analysis of GPCR-stimulation: The critical impact of cell adhesion. *Pharmacol. Res.* 108: 65-74.

Liu, C.; Ma, X.; Jiang, X.; Wilson, S. J.; Hofstra, C. L.; Blevitt, J.; Pyati, J.; Li, X.; Chai, W.; Carruthers, N.; Lovenberg, T. W. (2001). Cloning and pharmacological characterization of a fourth histamine receptor (H(4)) expressed in bone marrow. *Mol. Pharmacol.* 59(3): 420-426.

Nordemann, U.; Wifling, D.; Schnell, D.; Bernhardt, G.; Stark, H.; Seifert, R.; Buschauer, A. (2013). Luciferase Reporter Gene Assay on Human, Murine and Rat Histamine H_4 Receptor Orthologs: Correlations and Discrepancies between Distal and Proximal Readouts. *PLoS ONE* 8(9): e73961.

Parker, E. M.; Babij, C. K.; Balasubramaniam, A.; Burrier, R. E.; Guzzi, M.; Hamud, F.; Gitali, M.; Rudinski, M. S.; Tao, Z.; Tice, M.; Xia, L.; Mullins, D. E.; Salisbury, B. G. (1998). GR231118 (1229U91) and other analogues of the C-terminus of neuropeptide Y are potent neuropeptide Y Y1 receptor antagonists and neuropeptide Y Y4 receptor agonists. *Eur. J. Pharmacol.* 349(1): 97-105.

Plank, N. (2016). Dimeric histamine H2 receptor agonists as molecular tools and genetically engineered HEK293T cells as an assay platform to unravel signaling pathways of hH1R and hH2R. Doctoral Thesis, University of Regensburg, Regensburg.

Pluym, N. (2011). Application of the guanidine–acylguanidine bioisosteric approach to NPY Y2 receptor antagonists: bivalent, radiolabeled and fluorescent pharmacological tools. Doctoral Thesis, University of Regensburg, Regensburg.

Pluym, N.; Baumeister, P.; Keller, M.; Bernhardt, G.; Buschauer, A. (2013). [3H]UR-PLN196: A Selective Nonpeptide Radioligand and Insurmountable Antagonist for the Neuropeptide Y Y2 Receptor. *ChemMedChem* 8(4): 587-593.

Pop, N.; Igel, P.; Brennauer, A.; Cabrele, C.; Bernhardt, G.; Seifert, R.; Buschauer, A. (2011). Functional reconstitution of human neuropeptide Y (NPY) Y2 and Y4 receptors in Sf9 insect cells. *J. Recept. Signal Transduct. Res.* 31(4): 271-285.

Seamon, K. B.; Daly, J. W. (1981). Forskolin: a unique diterpene activator of cyclic AMP-generating systems. *J. Cyclic Nucleotide Res.* 7(4): 201-224.

Shinde, R.; Perkins, J.; Contag, C. H. (2006). Luciferin Derivatives for Enhanced in Vitro and in Vivo Bioluminescence Assays. *Biochemistry* 45(37): 11103-11112.

Shoblock, J. R.; Welty, N.; Nepomuceno, D.; Lord, B.; Aluisio, L.; Fraser, I.; Motley, S. T.; Sutton, S. W.; Morton, K.; Galici, R.; Atack, J. R.; Dvorak, L.; Swanson, D. M.; Carruthers, N. I.; Dvorak, C.; Lovenberg, T. W.; Bonaventure, P. (2010). In vitro and in vivo characterization of JNJ-31020028 (N-(4-{4-[2-(diethylamino)-2-oxo-1-phenylethyl]piperazin-1-yl}-3-fluorophe nyl)-2-pyridin-3-ylbenzamide), a selective brain penetrant small molecule antagonist of the neuropeptide Y Y(2) receptor. *Psychopharmacology (Berl.)* 208(2): 265-277.

Stroop, S. D.; Kuestner, R. E.; Serwold, T. F.; Chen, L.; Moore, E. E. (1995). Chimeric human calcitonin and glucagon receptors reveal two dissociable calcitonin interaction sites. *Biochemistry* 34(3): 1050-1057.

Tang, Y.; Luo, J.; Fleming, C. R.; Kong, Y.; Olini, G. C., Jr.; Wildey, M. J.; Cavender, D. E.; Demarest, K. T. (2004). Development of a sensitive and HTS-compatible reporter gene assay for functional analysis of human adenosine A2a receptors in CHO-K1 cells. *Assay and drug development technologies* 2(3): 281-289.

Wang, Q. J.; Adrian, T. E. (1995). Effect of protease inhibitors on peptide-stimulated amylase secretion from dispersed pancreatic acini. *Int. J. Pancreatol.* 17(3): 261-269.

Williams, C. (2004). cAMP detection methods in HTS: selecting the best from the rest. *Nat. Rev. Drug Discov.* 3(2): 125-135.

Ziemek, R. (2006). Development of binding and functional assays for the neuropeptide Y Y 2 and Y 4 receptors Doctoral Thesis, University of Regensburg, Regensburg.

Ziemek, R.; Brennauer, A.; Schneider, E.; Cabrele, C.; Beck-Sickinger, A. G.; Bernhardt, G.; Buschauer, A. (2006). Fluorescence- and luminescence-based methods for the determination of affinity and activity of neuropeptide Y2 receptor ligands. *Eur. J. Pharmacol.* 551(1-3): 10-18.

Ziemek, R.; Schneider, E.; Kraus, A.; Cabrele, C.; Beck-Sickinger, A. G.; Bernhardt, G.; Buschauer, A. (2007). Determination of affinity and activity of ligands at the human neuropeptide Y Y4 receptor by flow cytometry and aequorin luminescence. *J. Recept. Signal Transduct. Res.* 27(4): 217-233.

Chapter 5

Fluorescence- and radiolabeling of [Lys^4,Nle^{17,30}]hPP yields molecular tools for the NPY Y_4 receptor

Note: Prior to the submission of this thesis, parts of this chapter were submitted to publication in cooperation with partners:

Timo Littmann, Max Keller, Kilian Kuhn, Chiara Cabrele, Paul Baumeister, Günther Bernhardt, and Armin Buschauer

The following experimental work was performed/supported by co-authors:

Timo Littmann: Characterization of compounds in the β-arrestin 1 and β-arrestin 2 assay
Max Keller: Support in the synthesis of [^{3}H]**12**, **13** and [^{3}H]propionyl-pNPY and investigation of chemical stability
Chiara Cabrele: Synthesis of the peptides pNPY, hPP, **7** and **11**
Paul Baumeister: Support in the synthesis of [^{3}H]**8** and [^{3}H]propionyl-pNPY

5.1 Introduction

The neuropeptide Y (NPY) family comprises the 36-amino acid peptides neuropeptide Y (NPY), peptide YY (PYY), and pancreatic polypeptide (PP). In humans, the biological effects of these peptides are mediated by four functionally expressed receptor subtypes, designated Y_1, Y_2, Y_4 and Y_5 receptors (Y_1R, Y_2R, Y_4R, Y_5R) (Zhang et al., 2011). Among the NPY receptors the Y_4R is unique, as it prefers PP over NPY and PYY as the endogenous ligand. PP is predominantly expressed in an endocrine cell type (PP cells) of the pancreas (Wang et al., 2013), and is, for example, considered to be involved in satiety signaling, the regulation of food intake and energy metabolism. Therefore, Y_4R agonists are discussed as potential anti-obesity drugs (Kamiji and Inui, 2007; Li et al., 2010; Yulyaningsih et al., 2011). For the characterization of Y_4R ligands, pharmacological tools are indispensable. Affinity data are usually determined in radioligand binding assays using membranes or homogenates of Y_4R expressing cells and [^{125}I]-labeled rPP (Walker et al., 1997; Yan et al., 1996), hPP (**3**) (Berglund et al., 2001; Eriksson et al., 1998; Parker et al., 2002; Parker et al., 2005), GR231118 (syn. GW1229) (**4**) (Dumont and Quirion, 2000) PYY (Dautzenberg et al., 2005), or [Leu^{31},Pro^{34}]PYY (Gehlert et al., 1997) (Figure 5.1) as tracers, which are obtained by iodination of tyrosine residues. An alternative to [^{125}I]-labeling is [^{3}H]propionylation of a non-essential primary amino group in analogs of appropriate peptides or non-peptides containing, e. g., lysine or “arginysine”, an amino-functionalized arginine-derived building block (Keller et al., 2016). Dimeric analogs of the C-terminal pentapeptide of PP, previously identified as potent Y_4R agonists (Balasubramaniam et al., 2006), were recently structurally optimized to obtain [^{3}H]-labeled and fluorescent tools (Kuhn et al., 2016; Liu et al., 2016a; Liu et al., 2016b).

In principle, labeling of the ε-amino group in lysine is a convenient way to synthesize structurally uniform radioligands as well as fluorescent derivatives of the same precursor. Porcine NPY (**2**) (pNPY), which differs from the human peptide by a Leu residue instead of Met in position 17 and is comparable to hNPY (**1**) regarding affinity and potency, is usually preferred due to higher chemical stability (Clark et al., 1987; Martel et al., 1990). Previously described cyanine-labeled pNPY and [Lys^{4}]hPP (**7**) enabled flow cytometric binding assays under equilibrium conditions on the Y_1R (Schneider et al., 2006), and the Y_4R (Ziemek et al., 2007), respectively. By analogy with tritium-labeling of pNPY (Keller et al., 2015), a corresponding tritiated Y_4R ligand should be easily accessible and useful to complement the arsenal of molecular tools. Unfortunately, during storage in buffer, oxidation of the methionine residues in **7** and derivatives was detected by HPLC-MS analysis. Aiming at more stable full length labeled hPP analogs, we selected [Lys^{4},Nle^{17,30}]hPP (**11**) as a template, as the methionine residues in position 17 and 30 in **7** are prone to oxidation (Scheme 5.1). For comparison, we included the oxidized analogs of **7**, [Lys^{4},Met(O)^{17,30}]hPP

(**9**) and [Lys^4,Met(O$_2$)^{17,30}]hPP (**10**), in the present study because the impact of the sulfoxide and sulfone groups on biological activity and binding at the Y$_4$R was unknown. [^{3}H]propionyl-[Lys^4]hPP ([^{3}H]**8**), [^{3}H]propionyl-[Lys^4,Nle^{17,30}]hPP ([^{3}H]**12**) and the cyanine-labeled fluorescent peptide S0223[Lys^4,Nle^{17,30}]hPP (**13**) (Scheme 5.1) were synthesized and characterized in saturation and kinetic Y$_4$R binding experiments, in functional studies and with respect to NPY receptor subtype selectivity. The labeled compounds were also used to determine the affinities of unlabeled compounds in competition binding assays.

Endogenous peptides

YPSKPDNPGEDAPAEDMARYYSALRHYINLITRQRY-NH$_2$ hNPY (**1**)

YPSKPDNPGEDAPAEDLARYYSALRHYINLITRQRY-NH$_2$ pNPY (**2**)

APLEPVYPGDNATPEQMAQYAADLRRYINMLTRPRY-NH$_2$ hPP (**3**)

Y$_4$R agonists

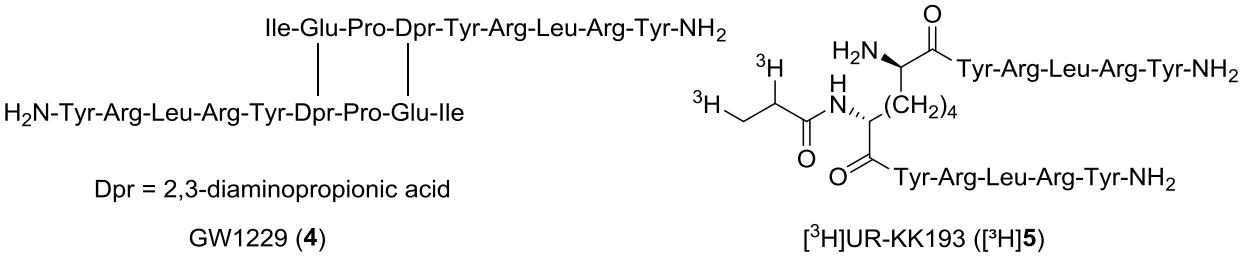

Y$_4$R antagonist

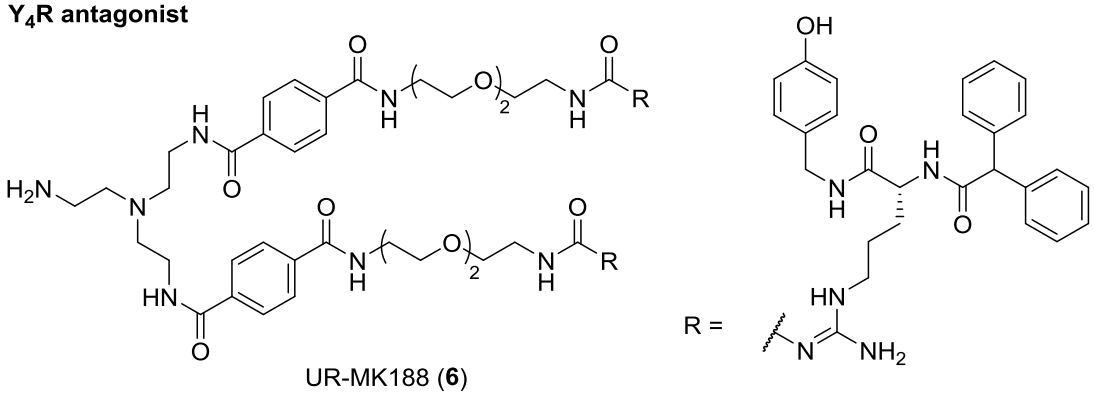

Figure 5.1. Amino acid sequences of the peptide agonists hNPY (**1**), pNPY (**2**), hPP (**3**) and structures of the Y$_1$R antagonist/Y$_4$R agonist GW1229 (**4**), the radiolabeled Y$_4$R agonist [^{3}H]UR-KK193 ([^{3}H]**5**), and the Y$_1$R/Y$_4$R antagonist UR-MK188 (**6**). Amino acids in pNPY and hPP which differ from the hNPY sequence are highlighted in blue.

Previously, experiments performed with the radioligand [^{3}H]UR-KK193 ([^{3}H]**5**, Figure 5.1) (Kuhn et al., 2016) in different buffers revealed that the discrepancies between binding data are, at least in part, caused by the absence or presence of sodium ions. A ‘sodium effect’ in agonist binding was also described for other GPCRs such as the adenosine and the δ-opioid receptor (Liu et al., 2012). Therefore, special attention was paid to the influence of the

sodium ion concentration and isotonic vs. hypotonic conditions on the hY_4R binding characteristics of the labeled and unlabeled ligands.

Scheme 5.1. Structures of [Lys^4]hPP (**7**), [Lys^4,Nle^{17,30}]hPP (**11**), oxidation products and derivatives obtained by conjugation at Lys^4 with tritiated or unlabeled propionic acid or fluorescent dye.

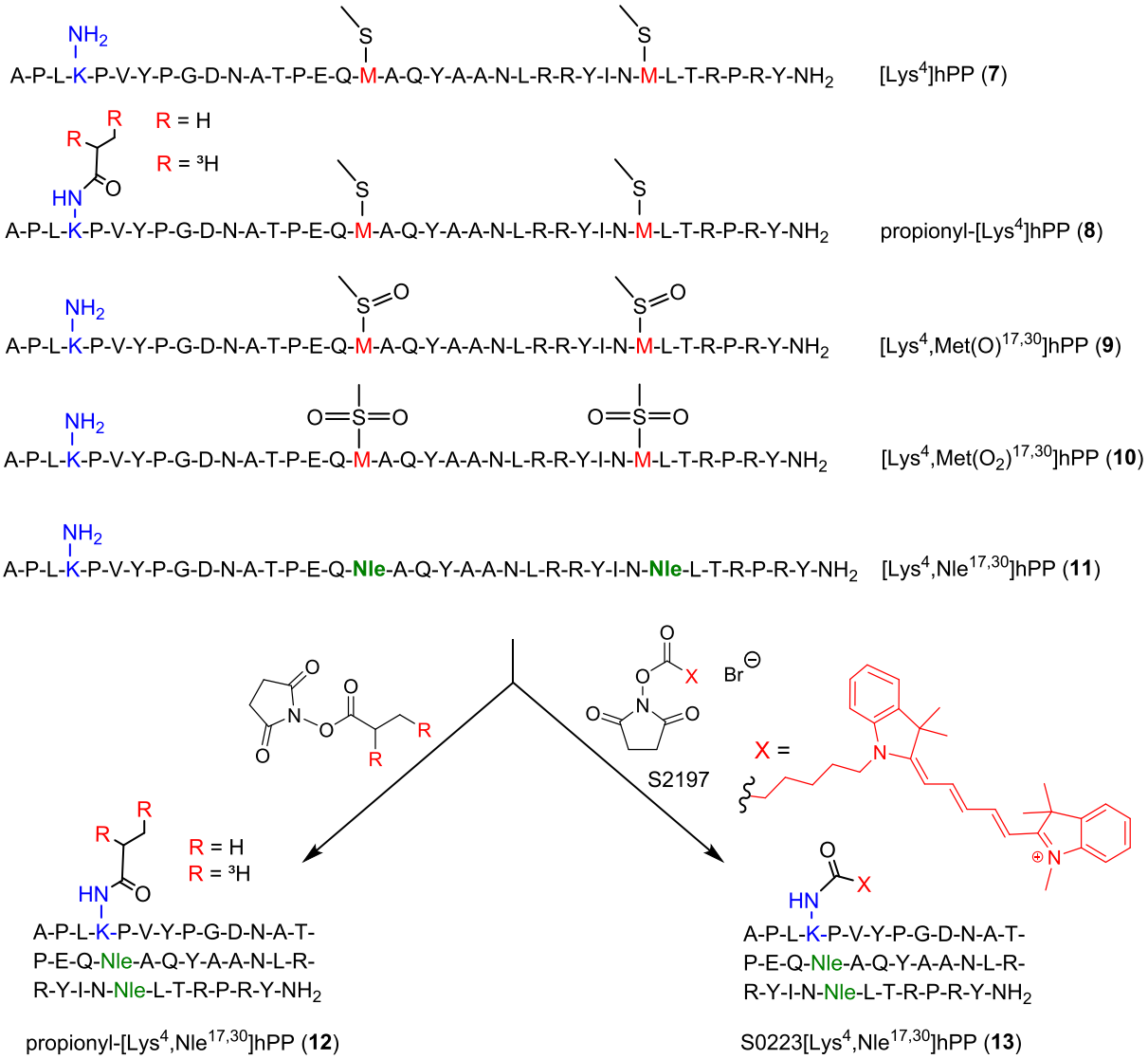

5.2 Materials and methods

5.2.1 General experimental conditions

Chemicals and solvents were from commercial suppliers and used without further purification unless otherwise indicated. Na_2CO_3, $NaHCO_3$ for buffer preparation and acetonitrile (MeCN) for HPLC (gradient grade) were from Merck (Darmstadt, Germany). DMF for peptide synthesis was from Acros Organics/Fisher Scientific (Nidderau, Germany). The succinimidyl

ester (S0223-NHS) of the fluorescent dye S2197 was from FEW Chemicals (Bitterfeld-Wolfen, Germany). Glycine was from Thermo Fisher Scientific (Darmstadt, Germany), trifluoroacetic acid (TFA), ethanol, Sigmacote and Triton X-100 were from Sigma-Aldrich (Deisenhofen, Germany), *N,N*-diisopropylethylamine (DIPEA) (99%) was from ABCR (Karlsruhe, Germany). Bovine serum albumin (BSA) and bacitracin were from Serva (Heidelberg, Germany). Human pancreatic polypeptide (hPP), **7**, **11** and porcine neuropeptide Y (pNPY) were synthesized by solid-phase peptide synthesis (SPPS). Chemicals for SPPS: N^{α}-Fmoc amino acids (side-chain protecting groups: tBu for Thr, Tyr, Asp, Glu; Trt for Asn and Gln; Boc for Lys; Pbf for Arg), DMF, 1-methyl-2-pyrrolidinone (NMP), dichloromethane (DCM), diethyl ether (Et_2O), and DIPEA were from Iris Biotech GmbH (Marktredwitz, Germany). The Fmoc-Rink amide MBHA resin (0.45 mmol/g) was from Novabiochem (Merck Millipore Darmstadt, Germany). 1-Hydroxybenzotriazole (HOBt), 2-(1*H*-benzotriazol-1-yl)-1,1,3,3-tetramethyluronium hexafluorophosphate (HBTU), TFA and piperidine were obtained from Biosolve (Valkenswaard, The Netherlands). All chemicals and solvents were of peptide-synthesis grade. Triisopropylsilane (TIS), 1,2-ethanedithiol (EDT) and thioanisole (TIA) were from Sigma-Aldrich. Compounds **9** and **10** were from Synpeptide (Shanghai, P.R. China). Naphthalene-1-sulfonic acid {*trans*-4-[(4-aminoquinazolin-2-ylamino)methyl] cyclohexyl-methyl}amide (Criscione et al., 1998) was synthesized as described previously (Li et al., 2003). Compound **4** was a gift from Dr. A. J. Daniels (Glaxo Wellcome, NC, USA). The synthesis of compound **6** was previously described (Keller et al., 2013). Stock solutions (1 mM) of the peptides were prepared with 10 mM HCl and stored at –20 °C. The solids and stock solutions of hPP, **7**-**10** were stored under an argon atmosphere. Millipore water was used throughout for the preparation of buffers and HPLC eluents. Polypropylene reaction vessels (1.5 or 2 mL) with screw caps (Süd-Laborbedarf, Gauting, Germany) were used for the synthesis of the radioligands [^{3}H]**8**, [^{3}H]**12** and [^{3}H]propionyl-pNPY, for small scale reactions (e.g. the preparation of the `cold´ analogs) and for the storage of stock solutions. Sigmacote was used for coating the polypropylene reaction vessels to prevent adsorption of the peptides.

High-resolution mass spectrometry (HRMS) analysis was performed on an Agilent 6540 UHD Accurate-Mass Q-TOF LC/MS system (Agilent Technologies, Santa Clara, CA) using an ESI source. Preparative HPLC was performed on a system from Knauer (Berlin, Germany) consisting of two K-1800 pumps and a K-2001 detector using mixtures of acetonitrile and 0.1% aqueous TFA solution as mobile phase (flow rate 15 mL/min). A detection wavelength of 220 nm was used throughout. The collected fractions were lyophilized using an alpha 2-4 LD apparatus (Martin Christ, Osterode am Harz, Germany) equipped with a RZ 6 rotary vane vacuum pump (vacuubrand, Wertheim, Germany). Analytical HPLC analysis of compounds **12**, **13** was performed with a system from Thermo Separation Products composed of a

SN400 controller, a P4000 pump, a degasser (Degassex DG-4400, Phenomenex), an AS3000 autosampler and a SpectraFOCUS forward optical scanning detector. A YMC-Triart C 8 (250 x 4.6 mm, 5 µm; YMC Europe, Dinslaken, Germany) served as RP-column at a flow rate of 0.8 mL/min. Mixtures of acetonitrile (A) and 0.05% aq TFA (B) were used as mobile phase. An injection volume of 100 µL and a detection wavelength of 220 nm (additionally 630 nm for **13**) were used throughout. Analytical HPLC analysis of 'cold' **8** was performed with a HPLC system from Waters (Eschborn, Germany) consisting of two 510 pumps, a pump control module, and a 486 UV/VIS detector. A Synergi Hydro-RP (250 x 4.6 mm, 4 µm; Phenomenex, Aschaffenburg, Germany) was used as stationary phase at a flow rate of 0.8 mL/min. Solutions for injection (concentrations in the two-digit µM range) were prepared in a mixture of A and B corresponding to the composition of the eluent at the start of the gradient.

5.2.2 Chemistry: experimental protocols and analytical data

Compound 12 pentakis(hydrotrifluoroacetate). Compound **11** (2.8 mg, 0.68 µmol) was dissolved in 3% DIPEA in anhydrous DMF (80 µL). A solution of succinimidyl propionate in anhydrous DMF (1.4 mg/mL) was added in small portions (a total of 40 µL (0.34 µmol)). To prevent two-fold acylation, the reaction was monitored by HPLC. The mixture was acidified by addition of 10% aqueous TFA (14 µL). The product was purified by preparative HPLC (column: YMC-Actus-Triart C8 250 x 20 mm ID, S 5 µm,12 nm; gradient: MeCN/0.1% aq TFA: 0–21 min: 10:90 – 38:62, 21–40 min: 38:62 – 46:54, 40–48 min: 95:5. t_R = 25.8 min). Lyophilisation of the eluate afforded **12** as a white fluffy solid (1.0 mg, 0.21 µmol). HRMS (m/z): $[M+5H]^{5+}$ calcd. for $C_{191}H_{305}N_{54}O_{53}$, 840.6561; found, 840.6587. RP-HPLC (220 nm): 99% (column: YMC-Triart C 8 (250 x 4.6 mm, 5 µm; gradient: MeCN/0.1% aq TFA: 0–30 min: 15:85 – 42:58, 30–40 min: 95:5. t_R = 26.9 min, k = 8.6). $C_{191}H_{300}N_{54}O_{53} \cdot C_{10}H_5F_{15}O_{10}$ (4200.76 + 570.10).

Synthesis of the radioligand [^{3}H]12. A solution of succinimidyl [^{3}H]propionate (500 µL = 2.5 mCi; 32 nmol; specific activity: 80 Ci/mmol (2.96 TBq/mmol), purchased from American Radiolabeled Chemicals, St. Louis, MO via Hartman Analytics, Braunschweig, Germany) in hexane/EtOAc (9:1) was transferred from the delivered ampoule into a 1.5 mL reaction vessel with screw cap, and the solvent was removed in a vacuum concentrator (30 °C, 30 min). A solution of **11** (0.5 mg, 109 nmol, in 0.1 M $NaHCO_3$ (pH 9.2) containing 35% DMF) (145 µL) was added, and the vessel was vigorously shaken at rt for 2 h. The mixture was acidified by addition of 2% aqueous TFA (87 µL) followed by addition of MeCN/H_2O (10:90; 368 µL). [^{3}H]**12** was purified using a HPLC system from Waters (Eschborn, Germany) consisting of two 510 pumps, a pump control module, a 486 UV/VIS

detector and a Flow-one beta series A-500 radiodetector (Packard, Meriden, USA). A Synergi Hydro-RP (250 x 4.6 mm, 4 µm) was used as stationary phase at a flow rate of 0.8 mL/min. Acetonitrile supplemented with 0.04% TFA (A) and 0.05% aq TFA (B) were used as mobile phase. The following linear gradient was applied: A/B: 0–25.5 min: 5:95 – 40.5:59.5, 25.5–29 min: 40.5:59.5, 29–33 min: 40.5:59.5–46:54, 33–34 min: 46:54 – 95:5, 34–42 min: 95:5. For the purification of the radiolabeled peptide four HPLC runs were performed. The radioligand was collected in 2-mL reaction vessels with screw caps, the volumes of the combined eluates were reduced by evaporation to 450 µL, and 50 µL of ethanol were added to obtain a solution containing 10% (v/v) ethanol for storage at 4 °C (stock solution). For the quantification of the radioligand [^{3}H]**12**, two samples were prepared by diluting 2 µL of the radioligand solution with 128 µL MeCN/0.05% aq TFA (10:90). By five-point calibration with **12** (0.1, 0.2, 0.35, 0.5 and 0.75 µM; injection volume: 100 µL, UV-detection: 220 nm) a concentration of 8.13 µM of [^{3}H]**12** was determined in the stock by HPLC. The following linear gradient was applied: A/B: 0–30 min: 15:85 – 45:55, 30–39 min: 95:5. To quantify the radioactivity, 3 µL of each sample were counted in 3 mL of liquid scintillator (Rotiszint eco plus, Carl Roth, Karlsruhe, Germany) with a LS 6500 liquid scintillation counter (Beckman Coulter, Krefeld, Germany) in pentuplicate. To determine the radiochemical purity and to prove the identity of the radioligand, a solution of the radiolabeled peptide (100 µL, 0.15 µM), spiked with 'cold' **12** (final concentration: 25 µM, t_R = 29.3 min), was analyzed by HPLC with combined UV/radiochemical detection (Rotiszint eco plus/acetonitrile, 85:15 (v/v), flow rate: 4.0 mL/min). The radiochemical purity was 92%. Calculated specific activity: 41.42 Ci/mmol (1.532 TBq/mmol). Chemical yield: penta(hydrotrifluoroacetate) of [^{3}H]**12**: 18.9 µg, 4.1 nmol, 12.8%. Radiochemical yield: 0.168 mCi (6.22 MBq) in 500 µL, 6.7%. Analysis of the radioligand (100 µL, 0.10 µM) after storage at 4 °C for 7 months revealed a radiochemical purity of 88%.

Synthesis of the fluorescent ligand 13. A solution of S2197 (S0223-NHS; 0.7 mg, 1.06 µmol, 0.8 eq) in 30 µL DMF was added to a solution of **11** [1.53 mg, 0.33 µmol, 1 eq) in buffer (81.6% 0.5 M $NaHCO_3$, 18.4% 0.5 M Na_2CO_3, pH 9.4) containing 23% DMF. After 45 min a reaction control was performed by analytical HPLC, another portion (0.4 eq) of the active ester was added, and additional 1.5 eq were added after 30 and 60 min. The reaction was stopped by addition of 10% aq. TFA (40 µL) after a total incubation period of 3 h at room temperature. The product was purified by analytical HPLC (8 injections). Chemical yield: **13** hexakis(hydrotrifluoroacetate): 0.96 mg, 0.206 µmol; RP-HPLC (220 nm): 96% (YMC-Triart C 8 (250 x 4.6 mm, 5 µm); gradient: MeCN 0.04% TFA/0.05% TFA: 0–30 min: A/B 20:80–50:50, 30–31 min: 50:50–95:5, 31–40 min: 95:5; t_R = 27.3 min, k = 8.8, 220 nm; t_R = 27.7 min, 630 nm); HRMS (m/z): $[M+6H]^{6+}$ calcd. for $C_{200}H_{333}N_{56}O_{53}$, 768.7593; found, 768.7575. $C_{200}H_{333}N_{56}O_{53} \cdot C_{12}H_6F_{18}O_{12}$ (4610.34 + 684.12).

5.2.3 Fluorescence spectroscopy and determination of quantum yields

Fluorescence quantum yields of **13** were determined in PBS (pH 7.4) and PBS containing 1% BSA with a Cary Eclipse spectro-fluorimeter and a Cary 100 UV/VIS photometer (Varian Inc., Mulgrave, Victoria, Australia) according to a previously described procedure using acryl cuvettes (10 mm × 10 mm, Sarstedt, ref. 67.755) and cresyl violet perchlorate as quantum yield standard (Keller et al., 2011b). Emission spectra were recorded at the slit adjustments (ex./em.) 10/5 nm and 10/10 nm, and the quantum yields obtained for these slit combinations were averaged (cf. Supporting Information, Figure S9, Table S1).

5.2.4 Investigation of the chemical stability of the peptides in buffer

The chemical stability of hPP, **7**, **8**, **11**, **12** and **13** was investigated in autoclaved buffer I at 22 ± 1 °C. The incubation was started by addition of 9 µL (hPP, **7**, **9**, **10**, **11**) and 4.5 µL (**8**, **12**) of a 1 mM solution to the buffer (82 µL or 85.5 µL) to give final concentrations of 50 µM (hPP, **7**-**11**) and 25 µM (**8**, **12**), respectively. Compound **13** was dissolved in buffer I (100 µL) to give a final concentration of 40 µM. After 0, 4, 12 and 48 h, aliquots (20 µL) were taken, and 20 µL of MeCN/ 0.2% aq TFA (2:8 v/v) were added. Analytical HPLC analysis was performed with a system from Agilent Technologies composed of a 1290 Infinity binary pump equipped with a degasser, a 1290 Infinity autosampler, a 1290 Infinity thermostated column compartment, a 1260 Infinity diode array detector, and a 1260 Infinity fluorescence detector. A Kinetex-XB C18, 2.5 µm, 100 mm×3 mm (Phenomenex), served as stationary phase at a flow rate of 0.6 mL/min. Mixtures of acetonitrile (A) and 0.04% aq TFA (B) were used as mobile phase. The following linear gradients were applied. Compounds hPP, **7**-**12**: 0–12 min: A/B 10:90 – 45:55, 12–16 min: 45:55– 95:5, 16–20 min: 95:5; **13**: 0–12 min: A/B 10:90 – 60:40, 12–16 min: 60:40– 95:5, 16–20 min: 95:5. The oven temperature was 25 °C, and the injection volume was 20 µL. Detection was performed at 220 nm throughout and additionally at 645 nm in case of **13**. For chemical stabilities of hPP and **7**-**11** cf. Supporting Information Figures S3-S8.

5.2.5 Cell culture

The HEC-1B human endometrial cancer cell line and the MCF-7 (HTB 22) human breast cancer cells were from the American Type Culture Collection (Rockville, MD). A subclone of the MCF-7 cell line with high Y_1R expression was established in our laboratory and used for binding experiments (Keller et al., 2011a). Human embryonal kidney cells (HEK-293T cells) and Chinese hamster ovarian (CHO) cells were from Deutsche Sammlung für Mikroorganismen und Zellkulturen (DSMZ, Braunschweig, Germany). Routinely performed

examinations for mycoplasma contamination using the Venor GeM Mycoplasma Detection Kit (Minerva Biolabs, Berlin, Germany) were negative for all cell types.

Cells were cultured in 25- or 75-cm^2 flasks (Sarstedt, Nümbrecht, Germany) in a humidified atmosphere (95% air, 5% CO_2) at 37 °C. MCF-7-Y_1 cells,(Keller et al., 2011a) CHO-hY_2-G_{qi5}-mtAEQ cells (Ziemek et al., 2006) and CHO-hY_4-G_{qi5}-mtAEQ cells (Ziemek et al., 2007), HEK293T-hY_4-CRE Luc (Kuhn et al., 2016) cells and HEC-1B cells expressing the human Y_5R (Moser, 2000) were cultured as previously described.

5.2.6 Buffers used in binding and functional experiments

Buffer I. A sodium-free, hypo-osmotic HEPES buffer (25 mM HEPES, 2.5 mM $CaCl_2$, 1 mM $MgCl_2$, pH 7.4) was used in binding experiments at the Y_2R and Y_4R. For binding experiments at the Y_5R, buffer I was supplemented with glycine (final concentration 0.3 M) to reach iso-osmotic conditions as hypotonic conditions were not tolerated by HEC-1B cells expressing the human Y_5R. Buffer II. Binding experiments at the Y_1R, Y_2R, Y_4R and Y_5R were performed in a buffer containing 10 mM HEPES, 150 mM NaCl, 25 mM $NaHCO_3$, 2.5 mM $CaCl_2 \cdot 2\ H_2O$, 1.2 mM KH_2PO_4, 1.2 mM $MgSO_4 \cdot 7\ H_2O$ and 5 mM KCl. Binding buffer. The respective buffer containing 1% BSA and 0.1 g/L bacitracin was used for dilutions of the compounds and in binding experiments.

5.2.7 Radioligand binding assay

Radioligand binding assays were performed at 22 ± 1 °C. Cells (200 µL suspension per well) were seeded into 96-well plates with clear bottom (Corning Incorporated Life Sciences, Tewksbury, MA; cat. no. 3610).

Y_1R binding. Competition binding experiments with the radioligand [^{3}H]propionyl-pNPY (K_d = 6.6 nM, c = 5 nM) were performed at intact MCF-7-Y_1 cells as previously described (Kuhn et al., 2016). In saturation binding experiments, a concentration range of 0.25 - 60 nM of the radioligand was covered in buffer I supplemented with 0.3 M glycine and buffer II, respectively. Nonspecific binding was determined in the presence of a 200-fold excess of BIBP3226 (N2-(diphenylacetyl)-N-[(4-hydroxyphenyl)methyl]-D-arginine amide) (Rudolf et al., 1994). Incubation period was 90 min. After incubation, the cells were processed as previously described (Kuhn et al., 2016).

Y_2R binding. Binding experiments were performed at CHO-hY_2R-G_{qi5}-mtAEQ cells (Ziemek et al., 2006) with [^{3}H]propionyl-pNPY as previously described (Kuhn et al., 2016). Saturation binding experiments were performed in a concentration range of 0.25 - 18 nM of the

radioligand, when using buffer I, 0.5 – 60 nM when using buffer I supplemented with 0.3 M glycine and 0.3 M sucrose, respectively, or 2.5 - 200 nM when using buffer II. Nonspecific binding was determined in the presence of a 100-fold excess of pNPY. The samples were processed as previously described (Kuhn et al., 2016).

Y_4R binding. All binding assays with [^{3}H]**8** and [^{3}H]**12** were performed at intact CHO-hY_4R-G_{qi5}-mtAEQ cells (Ziemek et al., 2007) as previously described for the CHO Y_2R cells, which were attached to the plate (Kuhn et al., 2016). Saturation binding experiments of [^{3}H]**8** were performed in buffer II with following modifications: One day prior to the experiment, the cells (500 µL suspension per well) were seeded into Primaria™ 24-well plates (Corning Life Sciences, Oneonta, NY). The cells were allowed to attach at 37 °C, 5 % CO_2 in a water-saturated atmosphere overnight. On the day of the experiment, confluency of the cells was approximately 90 %. The culture medium was removed by suction, the cells were washed with 500 µL of buffer II and covered with 200 µL of the binding buffer per well. Saturation binding experiments with [^{3}H]**8** were performed in a concentration range of 0.1 - 30 nM. Nonspecific binding was determined in the presence of a 200-fold excess of [Lys^4]hPP. After 90 min of incubation, the solution was removed by suction, and the cells were washed twice with buffer II (500 µL, 4 °C) followed by the addition of lysis solution (200 µL). The lysis solution was transferred into 6-mL scintillation vials filled with scintillator (3 mL). The vials were gently shaken and kept in darkness for at least 1 h prior to counting.

Competition binding experiments were performed in the 96-well format with increasing concentrations of unlabeled compounds using the radioligand [^{3}H]**8** at a concentration of 5 nM in buffer II as previously described for the CHO Y_2R cells (Kuhn et al., 2016). Nonspecific binding was determined in the presence of a 100-fold excess of hPP. Kinetic experiments were performed with a radioligand concentration of 10 nM in BD Primaria™ 24-well plates as described for saturation binding experiments. Nonspecific binding was determined in the presence of **7** (1 µM). For association experiments, the incubation of the cells was stopped after different periods of time (2 – 150 min) by removing the radioligand-containing medium, and cells were washed twice with ice-cold buffer (200 µL). In case of dissociation experiments, cells were pre-incubated with [^{3}H]**8** (10 nM) for 90 min. The solution was removed by suction, and the cells were covered with binding buffer (200 µL) containing a 100-fold excess of **7**. After different periods of time (5 – 140 min) the cells were washed with ice-cold buffer. The solution was removed by suction, and the cells were washed with buffer (500 µL, 4 °C) followed by the addition of lysis solution (200 µL). The lysis solution was transferred into 6-mL scintillation vials filled with scintillator (3 mL). The vials were gently shaken and kept in darkness for at least 1 h prior to counting.

Binding assays with the radioligand [^{3}H]**12** were performed at intact CHO-hY_4R-G_{qi5}-mtAEQ cells (Ziemek et al., 2007) as previously described for the CHO Y_2R cells (Kuhn et al., 2016).

All experiments were performed in binding buffer I (sodium-free HEPES buffer) and binding buffer II, respectively. Saturation binding experiments were performed in a concentration range of 0.1 - 18 nM (buffer I) or 0.5 – 120 nM (buffer II). For investigations of the "sodium effect", buffer I was supplemented with glycine (final concentration 0.3 M) or with sodium chloride at different concentrations (final concentrations: 50 mM, 100 mM) in saturation binding experiments. Additionally, buffer I containing 50 mM NaCl was adjusted with glycine (final concentration 0.19 M) to obtain iso-osmotic conditions. Competition binding experiments were performed with increasing concentrations of unlabeled compounds using the radioligand [^{3}H]**12** at a concentration of 1 nM in buffer I or 5 nM in buffer II. Nonspecific binding was determined in the presence of a 100-fold excess of **11**. The incubation period was 90 min. Kinetic experiments were performed with radioligand concentrations of 1 nM in buffer I and 5 nM in buffer II. The cells were adjusted to a density of approximately 170,000 per mL in Ham's F12 (Sigma Aldrich) supplemented with 10% FCS. The cells were allowed to attach overnight at 37 °C, 5% CO_2 in a water-saturated atmosphere. On the day of the experiment, confluency of the cells was approximately 90%. The culture medium was removed by suction, the cells were washed with 200 µL of the respective buffer and covered with 80 µL of the respective binding buffer per well. Nonspecific binding was determined in the presence of **11**. For association experiments, incubation of the cells was stopped after different periods of time (2 – 220 min) by removing the radioligand-containing medium, and cells were washed twice with ice-cold buffer (200 µL). In case of dissociation experiments, cells were pre-incubated with [^{3}H]**12** for 120 min. The solution was removed by suction, and the cells were covered with binding buffer (100 µL) containing a 100-fold excess of **11**. After different periods of time (5 – 260 min) the cells were washed with ice-cold buffer. The solution was removed by suction, and the cells were washed with the respective ice-cold buffer (1 × 200 µL) followed by the addition of lysis solution (25 µL). The plates were shaken for 30 min followed by the addition of 200 µL of liquid scintillator (Optiphase Supermix). The plates were sealed and handled as described (Kuhn et al., 2016).

Y_5R binding. Competition binding experiments were performed at HEC-1B-hY_5R cells (Moser, 2000) with [^{3}H]propionyl-pNPY (buffer I: K_d = 24.5 nM; c = 4 nM; buffer II: K_d = 11.0 nM, c = 4 nM) and [^{3}H]**12** (buffer I: K_d = 16.4 nM; c = 10 nM; buffer II: K_d = 11.4 nM, c = 10 nM). The cells were processed as previously described (Kuhn et al., 2016). In saturation binding experiments, a concentration range of 0.5 - 120 nM ([^{3}H]propionyl-pNPY) and 0.25 - 80 nM ([^{3}H]**12**) of the respective radioligand was covered. Nonspecific binding was determined in the presence of a 100-fold excess of pNPY. The plates were handled as described previously (Kuhn et al., 2016). In saturation binding experiments with [^{3}H]**8**, performed in the 24-well format in buffer II, a concentration range of 0.5 - 30 nM of the radioligand was covered. Nonspecific binding was determined in the presence of a 200-fold

excess of CGP 71683A. The plates were processed as previously described for 24-well plates.

5.2.8 Flow cytometric binding assay at the Y_4R and the Y_5R

The flow cytometric Y_4R binding assays on CHO-hY_4-G_{qi5}-mtAEQ cells and Y_5R saturation binding assays on HEC-1B-hY_5R cells using **13** as fluorescent ligand were performed as previously described for Cy5-[Lys^4]hPP on a FACSCalibur flow cytometer (Becton Dickinson), equipped with an argon laser (488 nm) and a red diode laser (635 nm) (settings: FSC: E-1, SSC: 280 V, Fl-4:700−750 V) (Ziemek et al., 2007). The cell density in the respective binding buffer was 10^6 cells/mL. The samples were incubated in 1.5 mL reaction vessels in the dark at rt for 90 min. The dissociation constant (K_d value) of **13** was determined in saturation experiments applying concentrations from 0.75 to 140 nM (buffer I and buffer I containing 0.3 M glycine) and 0.75 to 180 nM (buffer II), respectively. Nonspecific binding was determined in the presence of a 100-fold excess of hPP. The K_d value of **13** at the Y_5R was determined in saturation experiments applying concentrations from 0.75 to 290 nM (buffer II). Nonspecific binding was determined in the presence of an 80-fold excess of CGP 71683A. Data acquisition was stopped after counting of 10,000 − 15,000 gated events. For competition binding studies at the Y_4R (c(**13**) = 10 nM), nonspecific binding was determined by addition of hPP (final concentration: 1 µM). Association kinetics was determined by incubation of the cells with **13** at a constant concentration (10 nM). Samples were taken at different time periods and measured. Nonspecific binding was measured in the presence of a 100-fold excess of **11**. For dissociation experiments cells were pre-incubated with the labeled ligand (10 nM) for 60 min in the respective binding buffer. For nonspecific binding, pre-incubation was performed in the presence of a 100-fold excess of **7**. Afterwards, cells were centrifuged (3.5 min, 2000 rpm) and resuspended in the respective binding buffer containing **7** (80-fold excess). Samples were taken at different time periods and measured.

5.2.9 Luciferase assay

The Luciferase assay was performed on HEK293T-hY_4-CRE Luc cells as previously described (cf section 4.3.2; (Kuhn et al., 2016)).

5.2.10 Arrestin recruitment assay

The β-arrestin recruitment was quantified via a split-luciferase complementation assay as described for the H_1 histamine receptor (Lieb et al., 2016). In brief, one day before the

experiment, HEK293T-ARRB1-Y_4R and HEK293T-ARRB2-Y_4R cells were trypsinized (0.05% trypsin, 0.02% EDTA in PBS) and centrifuged (400 *g*, 5 min). The cells were resuspended in DMEM without phenol red (Sigma, Steinheim, Germany) supplemented with 5% FCS, and 90 µL of the cell suspension were seeded in white, TC-treated, flat bottom 96-well microtiter plates (VWR, Ismaning, Germany) at a density of approximately 100,000 cells/well. The cells were cultivated at 37 °C overnight in a water-saturated atmosphere containing 5% CO_2. Shortly before the experiment, the cells were removed from the incubator and allowed to equilibrate to room temperature, and 10 µL of agonist solution were added per well. The plates were shaken at 25 °C for 60 min. At the end of the incubation period, 50 µL of medium were replaced by 50 µL of Bright-Glo luciferase assay reagent (Promega, Mannheim, Germany). The plates were vigorously shaken (800 rpm) for 5 min. Bioluminescence was recorded for 1 s per well using a GENios Pro microplate reader (Tecan, Salzburg, Austria).

5.2.11 Confocal microscopy

Two days prior to the experiment CHO-hY_4-G_{qi5}-mtAEQ cells were trypsinized and seeded in an ibiTreat µ-slide chamber with 8 wells (Ibidi, Martinsried, Germany) in Ham's F12 and 5% FCS. On the day of the experiment, confluency of the cells was 30 - 60%. The culture medium was removed, and the cells were washed twice with the respective buffer (buffer I, buffer I containing 0.3 M glycine, buffer II; 400 µL). The cells were covered with 3.5 µg/mL Hoechst 33342 staining solution (Invitrogen, Karlsruhe, Germany) (150 µL) as nuclear counterstain and incubated for 10 min protected from light. After incubation the staining solution was removed, the cells were washed twice (400 µL) and covered with the respective buffer (200 µL) containing the fluorescent ligand **13** (10 nM) were added for total binding. Nonspecific binding was determined in the presence of hPP (1 µM). Images were acquired after an incubation period of 2 – 120 min. Confocal microscopy was performed with a Leica SP8 microscope. An HC PL APO CS2 63x/1.40 oil immersion objective was used. Hoechst 33342 was excited at 405 nm (laser transmission: 1%), and emission was detected in the range of 415 – 470 nm. The fluorescent ligand **13** was excited at 633 nm (laser transmission: 5%), and emission was detected in the range of 645 nm – 768 nm. Accordingly, fluorescence crosstalk could be excluded.

5.2.12 Data analysis

All data are presented as mean ± SEM from at least two independent experiments performed in triplicate, in case of flow cytometric experiments in duplicate. Concentration response curves from the luciferase assay and displacement curves from radioligand binding

experiments were analyzed by four-parameter sigmoidal fits (GraphPad Prism 5.0, San Diego, CA). Agonist potencies are given as EC_{50} values, maximal responses (efficacies) are expressed as α value referred to the effect of 1 µM hPP (α = 1.0). K_i values were calculated from IC_{50} values using the Cheng-Prusoff equation (Cheng and Prusoff, 1973). Specific binding data from saturation binding experiments was plotted against the 'free' radioligand concentration and analyzed according to a two-parameter hyperbolic curve fit (Binding – Saturation: One site – Specific binding, GraphPad Prism 5.0, San Diego, CA, USA). The resulting B_{max} value was used to calculate the number of binding sites per cell. Specific binding data from association experiments were analyzed with an equation describing a two-parameter exponential rise to a maximum (GraphPad Prism 5.0), giving the observed association constant k_{obs}. Specific binding data from dissociation experiments were fitted according to a one-phase exponential decay (GraphPad Prism 5.0). Kinetically derived dissociation constants $K_{d(kin)}$ were calculated from the association rate constant k_{on} and k_{off} (k_{on} = (k_{obs}-k_{off})/[L]; $K_{d(kin)}$ = k_{off}/k_{on}).

5.3 Results and discussion

5.3.1 Synthesis of the tritiated and fluorescently labeled peptides

For the preparation of [³H]propionyl-[Lys⁴]hPP ([³H]**8**) the precursor [Lys⁴]hPP (**7**) was treated with succinimidyl [³H]propionate (Scheme 5.1, Supporting Information). After purification by RP-HPLC, the radioligand [³H]**8** was obtained in a radiochemical purity of 90% (Supporting Information Figure S1). After storage in EtOH/10 mM HCl 2:98 (v/v) at 4 °C an increasing amount of decomposition products became obvious in the radiochromatogram, and after two years, only approximately 5% of [³H]**8** were left (Supporting Information Figure S2). [³H]propionyl-[Lys⁴,Nle^{17,30}]hPP ([³H]**12**) was prepared in the same way as [³H]**8** from [Lys⁴,Nle^{17,30}]hPP (**11**) (cf. Supporting Information) and succinimidyl [³H]propionate affording the radioligand with a specific activity of 1.532 TBq/mmol in a radiochemical purity of 92%. Unlike [³H]**8**, [³H]**12** showed excellent chemical stability when stored in 10% ethanol at 4 °C (Figure 5.2A, B). No decomposition was observed after an incubation period of 48 h, when the 'cold' analogs, **12** (Figure 5.3A) and **8** (cf. Supporting Information, Figure S5), both prepared by analogy with the radioligands, and [Lys⁴,Met(O)^{17,30}]hPP (**9**) were investigated for stability in a HEPES buffer (buffer I, pH 7.4). In case of **9** a small peak was observed with the same retention time as that of [Lys⁴,Met(O_2)^{17,30}]hPP (**10**) (t_R = 7.9 min; <1%) after 48 h (cf. Supporting Information, Figures S6 and S7).

The fluorescent ligand S0223[Lys⁴,Nle^{17,30}]hPP (**13**) was prepared by treating an 1.3-fold excess of amine precursor **11** with the succinimidyl ester of the cyanine dye S0223 (S2197)

(Scheme 5.1). The fluorescent ligand **13** was isolated by RP-HPLC and obtained in a chemical yield of 62% and high purity (Figure 5.2C). The compound proved to be sufficiently stable during incubation in buffer I for up to 48 h (Figure 5.3B).

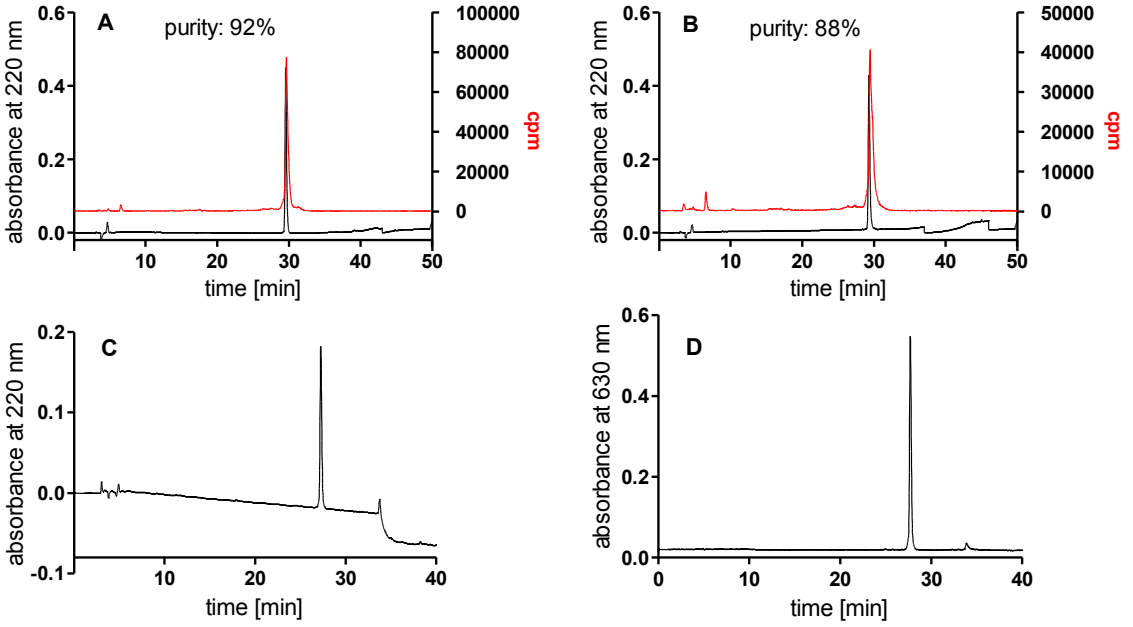

Figure 5.2. Purity, identity and long-term stability of the radiolabeled peptide [^{3}H]**12** and the fluorescent ligand **13** determined by HPLC. (**A**) HPLC analysis of [^{3}H]**12** (ca. 0.15 µM) spiked with 'cold' **12** (25 µM). Radiochemical purity: 92%. (**B**) HPLC analysis of [^{3}H]**12** (ca. 0.10 µM) spiked with 'cold' **12** (25 µM), analyzed after 7 months of storage at 4 °C in EtOH/H_2O (10:90); injection volume: 100 µL. Radiochemical purity: 88%. The minor differences in t_R result from serial detection of the UV and radiometric signals. (**C**) HPLC analysis of **13** 1 day after synthesis at 220 nm, chemical purity: 96%. (**D**) HPLC analysis of **13** 1 day after synthesis at 630 nm.

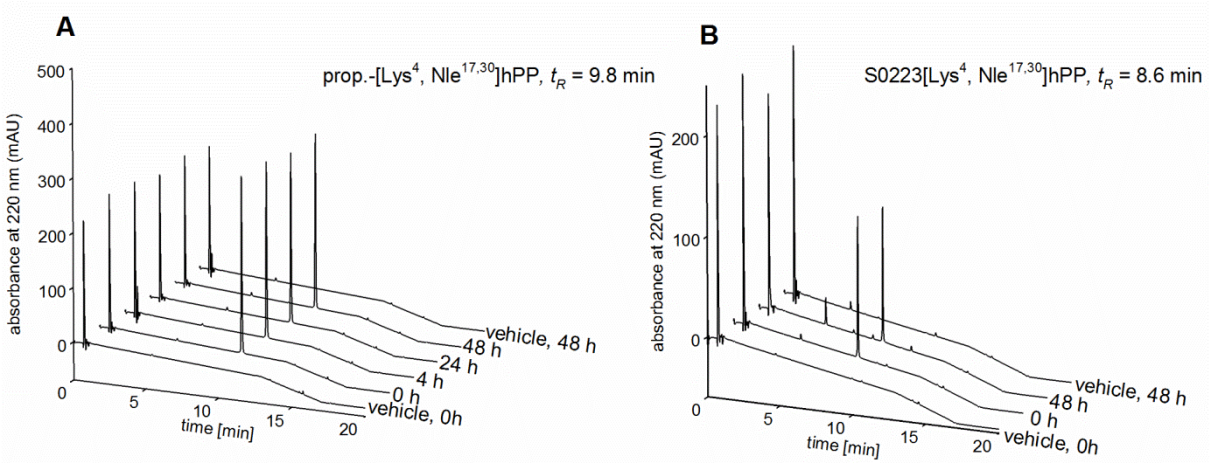

Figure 5.3. HPLC analysis of 'cold' **12** (**A**) and the fluorescent peptide **13** (**B**) after incubation in buffer I (HEPES buffer, sodium-free, pH 7.4) for up to 48 h. Compound **12** showed no decomposition, whereas in case of **13** two small additional peaks (t_R = 6.6 min, t_R = 8.0 min) corresponding to <3.5% of the peak areas were detected after 48 h of incubation. For **13** a different gradient was applied. Peaks between 0 and 6 min correspond to buffer components.

5.3.2 Functional studies at the hY_4R

The peptides were investigated for Y_4R agonism in a luciferase gene reporter assay on HEK293T cells expressing the hY_4R as well as in β-arrestin1 and β-arrestin2 recruitment assays (split luciferase complementation assays) by using HEK293T-ARRB1-Y_4R and HEK293T-ARRB2-Y_4R cells (data T.Littmann, personal communication).

Table 5.1. NPY hY_4R agonist potencies (EC_{50}) and intrinsic activities (α) of selected peptides and reference compound hPP.

Compound	Luciferase assay		Arrestin assay		β-arrestin isoform
	EC_{50} [nM][a]	α	EC_{50} [nM][b]	α	
hPP	0.6 ± 0.1	1.0	4.4 ± 0.02	1.0	1
			3.1 ± 0.01	1.0	2
4	5.5 ± 0.8	1.01	413 ± 2	0.53	1
			236 ± 2	0.63	2
7	1.5 ± 0.2	0.99	7.3 ± 0.03	0.75	1
			5.0 ± 0.03	0.88	2
8	3.5 ± 0.4	0.97	15 ± 0.08	0.81	1
			10 ± 0.04	0.89	2
9	4.2 ± 0.3	1.02	42 ± 0.18	0.72	1
			27 ± 0.12	0.79	2
10	1.9 ± 0.4	0.99	10 ± 0.05	0.71	1
			6.4 ± 0.02	0.80	2
11	0.9 ± 0.1	1.00	15 ± 0.05	0.74	1
			10 ± 0.03	0.86	2
12	1.0 ± 0.1	0.99	14 ± 0.09	0.79	1
			9.2 ± 0.04	0.83	2
13	3.1 ± 0.9	1.00	19 ± 0.12	0.84	1
			13 ± 0.10	0.89	2

[a]CRE-luciferase reporter gene assay on HEK293T cells stably co-expressing the hY_4R and the CRE-controlled luciferase gene reporter. Y_4R agonist potency was determined by the inhibition of forskolin (2 µM) stimulated luciferase activity. [b]Arrestin recruitment assay on HEK293T-ARRB1-Y_4R and HEK293T-ARRB2-Y_4R cells. The maximal response (intrinsic activity, α) is referred to the effect of hPP set to α = 1.0. Data represent mean values ± SEM from at least two independent experiments performed in triplicate.

All investigated peptides were full agonists in the gene reporter assay. The potencies were essentially comparable, regardless of the oxidation state of the sulfur atoms, the replacement

of methionine by norleucine and the derivatization of the lysine in both, **7** and **11**. As differences between agonist potencies and intrinsic activities may be masked due to signal amplification in assays with distal readouts such as gene reporter assays, the peptides were also tested in a β-arrestin recruitment assay, a system with a rather proximal readout. In this assay, the rank order of potencies was similar compared to that determined in the luciferase assay, but the EC_{50} values were higher. A slight preference for the isoform 2 of β-arrestin became obvious. Contrary to the gene reporter assay, all peptides showed partial agonism with intrinsic activities between 0.7 and 0.9. In literature, **4** was reported both, as a partial (Berglund et al., 2003b; Ziemek et al., 2007) and a full Y_4R agonist (Berglund et al., 2003a; Parker et al., 1998). Compared to the luciferase assay, **4** turned out to be 40-75 times less potent and a partial Y_4R agonist in the β-arrestin assay, achieving 50-60% of the maximal response, that is, the difference between data from both assays was most pronounced in case of compound **4**. Regardless of being aware of the different extent of signal amplification in luciferase gene reporter and split luciferase complementation assay, this discrepancy may reflect G protein bias.

5.3.3 Y_4R binding of the radiolabeled and fluorescence labeled compounds **8**, **12** and **13**

More detailed binding studies were performed on intact CHO-hY_4-G_{qi5}-mtAEQ cells in a hypotonic sodium-free buffer (buffer I, HEPES) (compounds [^{3}H]**12** and **13**) and an isotonic buffer (buffer II, HEPES, 150 mM sodium) (compounds **8**, [^{3}H]**12** and **13**). The radioactive form of propionyl-[Lys^4]hPP was characterized by saturation and kinetic binding experiments (cf. Supporting Information Figures S10 and S11) within 4 months after purification. Saturation binding studies with [^{3}H]propionyl-[Lys^4]hPP at live CHO cells expressing the hY_4R revealed a K_d value of 6.0 nM. The number of specific binding sites per cell amounted to approximately 252,000 and was in the same range as previously reported (Kuhn et al., 2016). At concentrations around the K_d value, nonspecific binding amounted to 5 % of the total binding. Association to the receptor was complete after 100 min (k_{obs} = 0.0293 min^{-1}). Dissociation from the receptor was monophasic with a k_{off} of 0.0118 min^{-1}. The kinetically derived K_d (k_{off}/k_{on} = 25.5 nM) was in the same order of magnitude as the K_d from saturation binding experiments. To investigate the impact of sodium ions on the K_d value of [^{3}H]**12**, buffer I was supplemented with sodium chloride at different concentrations. An increasing sodium concentration in buffer I led to higher K_d values (Figure 5.4). To investigate whether this effect was sodium dependent or related to the hypotonic character of buffer I, the osmolarity was adjusted by addition of glycine (concentration: 0.3 M in the absence of NaCl and 0.19 M in the presence of 50 mM NaCl; Figure 5.4; cf. Supporting Information Table S2,

Figure S12). Saturation binding studies with [^{3}H]**12** at live CHO cells expressing the hY$_4$R revealed a 20-fold higher K_d value of 20.9 nM (buffer II) in comparison to saturation binding performed in buffer I (K_d = 1.1 nM) (Figure 5.4, Table 5.2). At concentrations around the K_d value, nonspecific binding amounted to 2% of the total binding in buffer I and 5% in buffer II. Association to the receptor was complete after 130 min (buffer I: k_{obs} = 0.0169 min^{-1}; Figure 5.5A) and 70 min (buffer II: k_{obs} = 0.0387 min^{-1}, Figure 5.5C), respectively. Dissociation from the receptor was monophasic (Figure 5.5B and Figure 5.5D) with a k_{off} of 0.0110 min^{-1} (buffer I) and 0.0292 min^{-1} (buffer II), respectively. After 250 minutes, the residual specific binding of the tritiated compound amounted to approximately 13% (buffer I) and 31% (buffer II), respectively, suggesting in part (pseudo)irreversible binding. The kinetically derived K_d (buffer I: k_{off}/k_{on} = 1.9 nM; buffer II: 15.4 nM) was in excellent agreement with the K_d from saturation binding experiments (buffer I: 1.1 nM; buffer II: 20.9 nM).

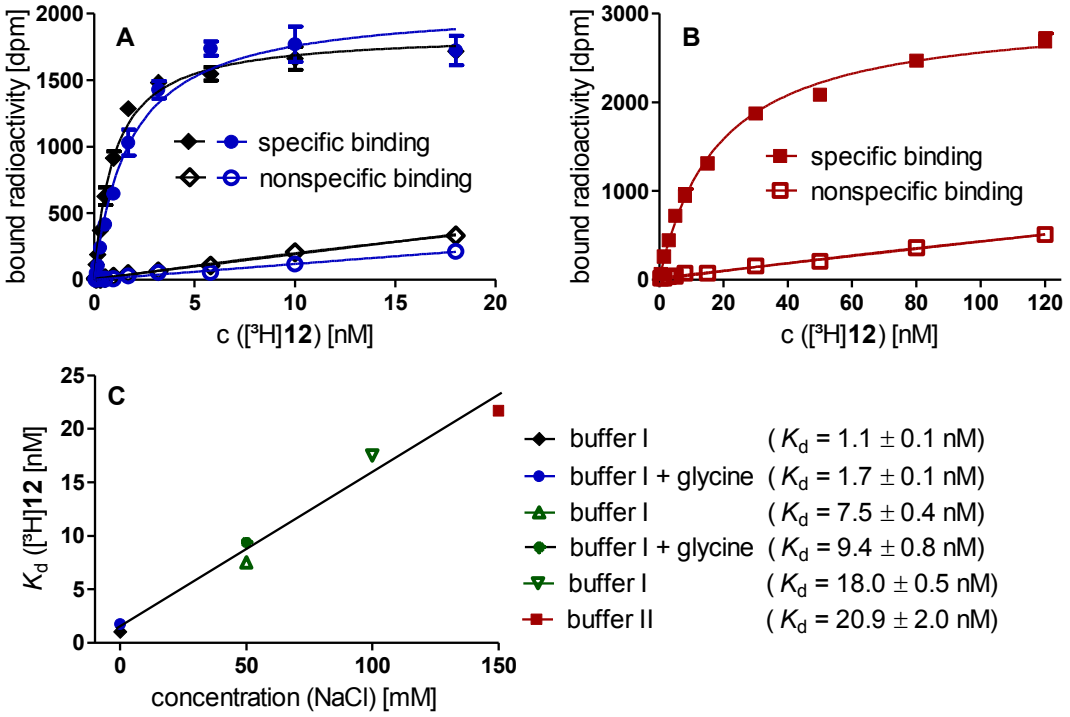

Figure 5.4. Y$_4$R saturation binding of the radioligand [^{3}H]**12** depending on NaCl content and hypotonicity. Data determined at CHO-hY$_4$-G$_{qi5}$-mtAEQ cells at 22 °C in buffer I, buffer I supplemented with 0.3 M glycine or with sodium chloride at different concentrations (0 mM, 50 mM, 100 mM), buffer I supplemented with 50 mM sodium chloride and 0.19 M glycine for iso-osmotic conditions, and buffer II (150 mM Na$^+$). (**A**, **B**) Representative saturation binding experiments with [^{3}H]**12**. (**C**) Determined correlation between Na$^+$ concentration and K_d value; r^2 = 0.98. Data from at least two independent experiments performed in triplicate.

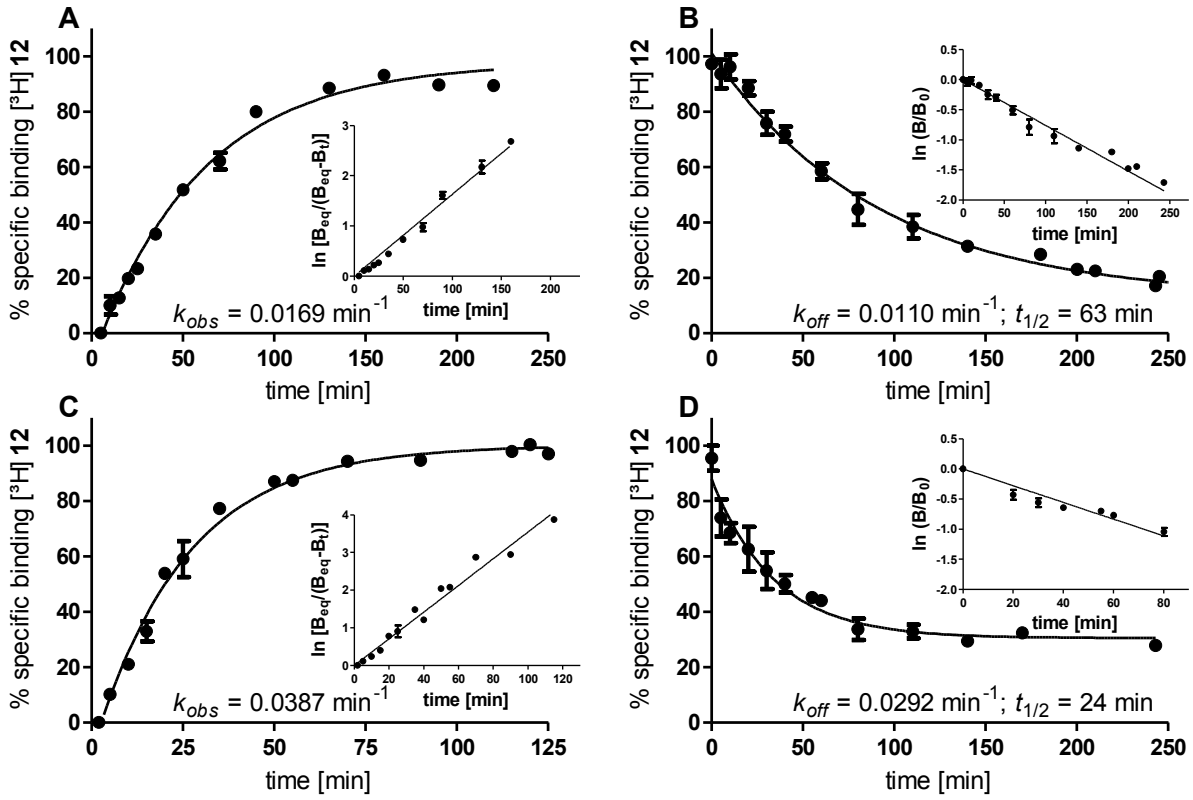

Figure 5.5. Y_4R binding characteristics of the radioligand [³H]**12**. Data determined at CHO-hY_4-G_{qi5}-mtAEQ cells at 22 °C in buffer I (HEPES, sodium-free) (**A**, **B**) and buffer II (HEPES, 150 mM Na^+) (**C**, **D**). (**A**, **C**) Y_4R association kinetics of [³H]**12** (buffer I: c = 1 nM; buffer II: c = 5 nM). Inset: Linearization $\ln[B_{eq}/(B_{eq}-B_t)]$ versus time. (**B**, **D**) Y_4R dissociation kinetics of [³H]**12** (buffer I: c = 1 nM; buffer II: c = 5 nM, pre-incubation time: 2 h) determined in the presence of a 100-fold excess of **11**. Fitting of the data according to a monophasic exponential decay. Inset: Linearization $\ln[B/B_0]$ versus time. Data represent mean values ± SEM from two independent experiments performed in triplicate.

Flow cytometric saturation binding studies with the fluorescent ligand **13** at hY_4R-expressing CHO cells revealed comparable K_d values in buffer I (K_d = 9.2 nM), buffer I containing 0.3 M glycine (K_d = 9.4 nM) and buffer II (K_d = 16.5 nM) (Figure 5.6A and Figure 5.6D; Supporting Information, Figure S13). At concentrations around the K_d value, nonspecific binding amounted to 3% of the total binding in buffer I and 5% in buffer II. Association to the receptor was complete after 25 min (buffer I: k_{obs} = 0.08312 min^{-1}, Figure 5.6B; buffer II: 0.1209 min^{-1}, Figure 5.6E). Dissociation from the receptor was monophasic (Figure 5.6C) with a k_{off} of 0.1664 min^{-1} in buffer I. After 15 minutes, the residual specific binding of the compound amounted to approximately 30%. In the isotonic buffers, buffer I containing glycine and buffer II, the fluorescent ligand showed low nonspecific binding (8% of total binding). However, after incubation of the cells for 60 min, **13** was not displaceable by an excess of **7** (Figure 5.6F, Supporting Information Figure S13). Therefore, the cellular localization of the fluorescent ligand was studied by confocal microscopy.

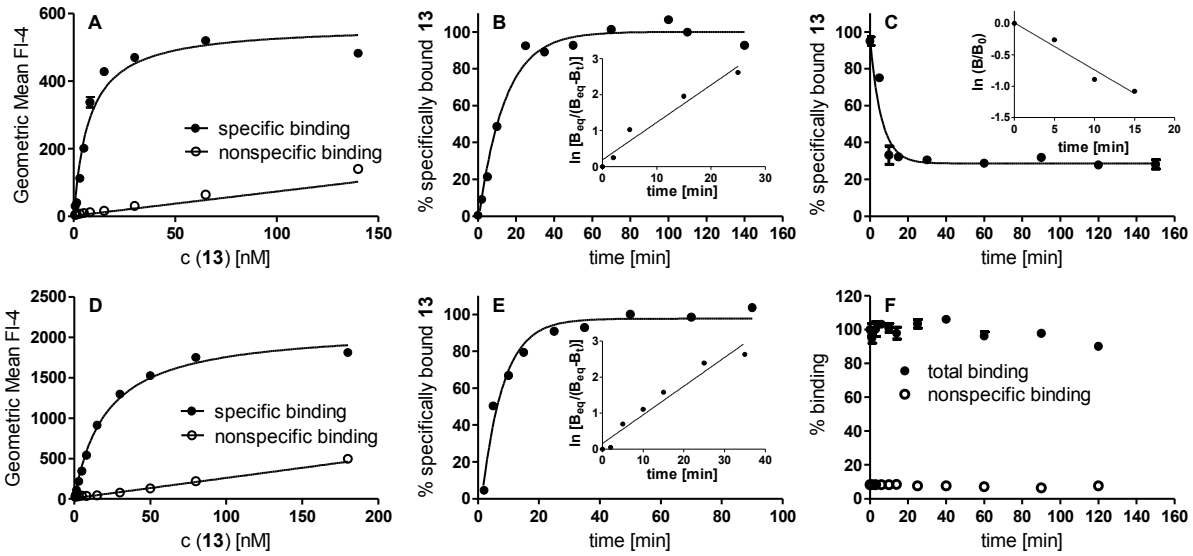

Figure 5.6. Y_4R binding characteristics of the fluorescent ligand **13**. Data determined by flow cytometry at CHO-hY_4-G_{qi5}-mtAEQ cells at 22 °C in buffer I (HEPES, sodium-free) (**A**, **B**, **C**) and buffer II (HEPES, 150 mM sodium) (**D**, **E**, **F**). (**A**, **D**) Representative saturation binding experiments with **13**. (**B**, **E**) Representative Y_4R association kinetics of **13** (c = 10 nM). Inset: Linearization $\ln[B_{eq}/(B_{eq}-B_t)]$ versus time. (**C**, **F**) Representative Y_4R dissociation kinetics of **13** (c = 10 nM; pre-incubation time: 60 min) determined in the presence of an 80-fold excess of **7**. Fitting of the data according to a monophasic exponential decay. Inset: linearization $\ln[B/B_0]$ versus time. Buffer II: dissociation of **13** was not observed.

Table 5.2. Binding data of [^{3}H]**8**, [^{3}H]**12** and **13** in buffers I and II.

	Saturation binding	Binding kinetics		
Compound	K_d [nM][a]	k_{obs} [min^{-1}][b]	k_{off} [min^{-1}][c]	$K_{d(kin)}$ [nM][d]
[^{3}H]**8**	6.0 ± 1.3[f]	0.0239[f]	0.0172[f]	25.5[f]
[^{3}H]**12**	1.1 ± 0.1[e]	0.0169[e]	0.0110[e]	1.86[e]
	20.9 ± 2.0[f]	0.0387[f]	0.0292[f]	15.37[f]
13	9.2 ± 2.5[e]	0.0831[e]	0.1664[e]	
	16.5 ± 2.3[f]	0.1209[f]	-	-

[a] Equilibrium dissociation constant determined on CHO-hY_4-G_{qi5}-mtAEQ cells; mean ± SEM from at least two independent experiments performed with [^{3}H]**8**, [^{3}H]**12** (in triplicate) and **13** (in duplicate), respectively. [b] Apparent association constant, mean from two independent experiments performed with [^{3}H]**8**, [^{3}H]**12** (in triplicate) and **13** (in duplicate) respectively. [c] Dissociation constant, mean from two independent experiments performed with [^{3}H]**8**, [^{3}H]**12** (in triplicate) and **13** (in duplicate), respectively. Monophasic exponential fit. [c] Kinetically derived dissociation constant $K_{d(kin)}$, calculated from the association rate constant k_{on} and k_{off} ([^{3}H]**8**: $k_{on} = (k_{obs}-k_{off})/[L]$ = 0.00068 nM^{-1}*min^{-1} ; [^{3}H]**12**: $k_{on}=(k_{obs}-k_{off})/[L]$= 0.0059 nM^{-1} · min^{-1}(buffer I); k_{on}=0.0019 nM^{-1} · min^{-1} (buffer II); $K_{d(kin)} = k_{off}/k_{on}$). [e] Data determined in buffer I. [f] Data determined in buffer II.

5.3.4 Confocal microscopy of CHO hY$_4$R cells incubated with the fluorescent ligand **13**

In accordance with the results from flow cytometric binding experiments, the nonspecific binding determined in the presence of a 100-fold excess of non-fluorescent hPP was low, irrespective of the composition of the buffer (Figure 5.7). In the absence of the competitor hPP, the fluorescent ligand **13** showed no time-dependent intracellular accumulation when the cells were incubated in hypotonic buffer I. It should be noted that the cells swell considerably under these conditions (cf. Supporting Information, Fig. S14). By contrast, the ligand was significantly enriched intracellularly with time in isotonic buffers, that is, buffer I containing glycine or buffer II, respectively. Low cellular accumulation in the presence of hPP indicates receptor-mediated internalization of the fluorescent ligand. This explains why compound **13** remained cell-associated when flow cytometric dissociation experiments were performed after pre-incubation of the cells with the fluorescent ligand for 60 min in isotonic buffers (Figure 5.6F, Supporting Information Figure S13B). Regardless of that, competition binding experiments with **13** can be performed as shown below. Obviously, the extent of internalization is positively correlated with the number of Y$_4$Rs occupied by the fluorescent ligand.

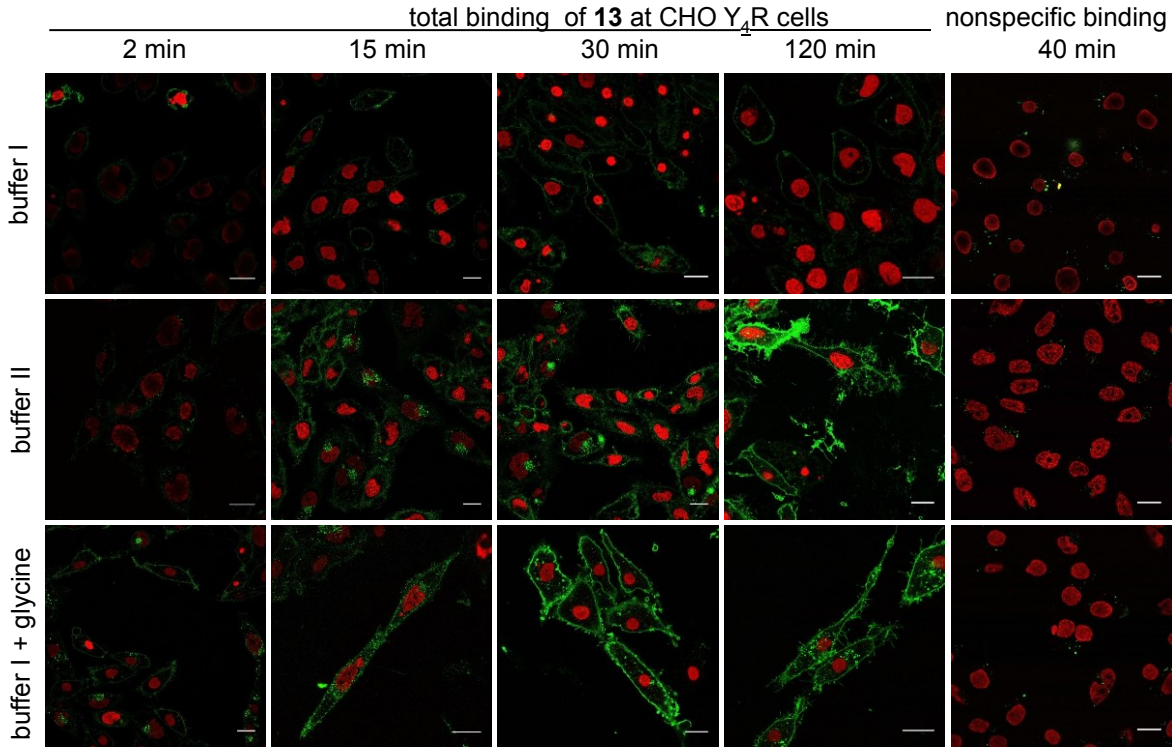

Figure 5.7. Time–dependent binding of the fluorescent ligand **13** at CHO hY$_4$R cells in different buffers (buffer I (hypotonic); buffer I containing 0.3 M glycine and buffer II (isotonic)). Cells were incubated with the fluorescent ligand (10 nM) at room temperature. Nonspecific binding was determined in the presence of 1 µM hPP. All images were acquired with a Leica SP 8 microscope. Settings: 63x/1.40 objective, Hoechst 33342 as nuclear counterstain (red), **13** (green), 75 µm pinhole; scale bar: 20 µm.

The different sensitivity of the binding of the radioligand and the fluorescent ligand with respect to the composition of the buffer was surprising as both ligands are derivatives of the same peptide. In principle, mechanical stretch, here the swelling of the cells (cf. Supporting Information, Figure S14), can induce a switch of the GPCR conformation from the inactive to the active state (Zou et al., 2004). However, the sodium concentration rather than the osmolarity effected the binding affinity of the radioligand [^{3}H]**12**. This is in agreement, e. g., with studies on the influence of alkali cations on Y_4R binding of [^{125}I]hPP (Parker et al., 2004) and on vasopressin V_1b receptor binding of [^{3}H]AVP (Koshimizu et al., 2016). By contrast, the osmolarity of the buffer was crucial in case of the fluorescent ligand **13**, as isotonic conditions regardless of the nature of the osmotically active ingredients, especially, Na^+ and glycine, decreased the affinity and increased the receptor-mediated internalization of the fluorescent ligand. This can not be explained yet, but there is clear evidence that binding affinity and the extent of internalization strongly depend on the type of the label attached to the hY_4R agonist. Depending on hypotonic or isotonic conditions, distinct distributions of the cell populations became obvious in the scattergram (cf. Supporting Information Figure S15).

5.3.5 Y_4R competition binding

The radioligand [^{3}H]**8** was used for the determination of binding data of hPP, **7** and **8** on the Y_4R in buffer II (Supporting Information Figure S16). The K_i values of hPP (K_i = 0.86 ± 0.02 nM), **7** (K_i = 4.2 ± 0.1 nM), and **8** (K_i = 9.1 ± 0.9 nM) were in good agreement with data determined with the radioligand [^{3}H]**12** in buffer II (cf. Table 1.3). In case of the ‘cold’ analog of the radioligand, propionyl-[Lys^4]hPP, the K_i value was in good agreement with the K_d value (9.1 nM vs. 6.0 nM).

The binding data of the peptides **7** - **13** and the reference compounds hPP, **4** and **6**, were determined at the Y_4R, using the radioligand [^{3}H]**12** and the fluorescent ligand **13** in buffer I and buffer II (cf. Figure 5.8, Table 5.3). In radioligand and fluorescent binding studies K_i values of hPP and UR-MK188 (**6**) were in good agreement with published data (K_i(hPP): 0.50 nM (Keller et al., 2016), 0.53 nM (Berlicki et al., 2013); K_i(**6**): 130 nM (Keller et al., 2013)). In case of the ‘cold’ analog of the radioligand **12** (buffer I: 1.5 nM; buffer II: 14.3 nM) and the fluorescent peptide **13** (buffer I: 4.2 nM; buffer II: 9.1 nM), the K_i values were in good agreement with the K_d values (cf. Table 5.2). Generally, the K_i values of the peptides at the Y_4R determined in buffer I were in excellent agreement with the EC_{50} values determined in the functional assay (Table 5.1). Interestingly, in buffer II higher K_i values were determined for all peptides. As previously reported, the affinities of hPP(Parker et al., 2002) and of the antagonist **6** (Kuhn et al., 2016) remained unaffected by an exchange of the binding buffer.

A clear difference in affinity became obvious in case of **9** and **10** when using buffer I or buffer II (Table 5.3). The impact of the composition of the buffer was most pronounced for **4** (buffer I: K_i = 2.2 nM; buffer II: K_i = 242 nM).

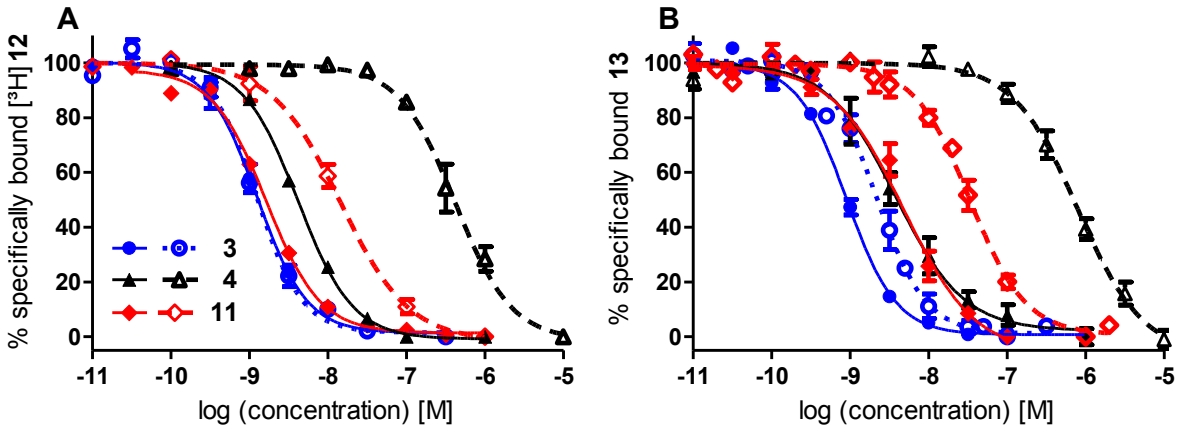

Figure 5.8. Displacement curves from competition binding experiments performed with [^{3}H]**12** and the fluorescent ligand **13**. Data determined at CHO-hY$_4$R-G$_{qi5}$-mtAEQ cells in buffer I (solid lines) and buffer II (dashed lines). (**A**) Displacement of [^{3}H]**12** (buffer I: K_d = 1.1 nM, c = 1.0 nM; buffer II: K_d = 20.9 nM, c = 5.0 nM). (**B**) Displacement of **13** (buffer I: K_d = 10.8 nM, c = 10 nM; buffer II: K_d = 16.5 nM, c = 10 nM). Data represent mean values ± SEM of at least three independent experiments performed in triplicate (**A**) or duplicate (**B**).

Table 5.3.Y$_4$R binding data determined with **13** and [^{3}H]**12** in buffer I and buffer II.

	13 K_i [nM][a]		[^{3}H]**12** K_i [nM][b]		Ratio of K_i (buffer II: buffer I)	
Compd.	buffer I	buffer II	buffer I	buffer II	**13**	[^{3}H]**12**
hPP	0.45 ± 0.04	1.4 ± 0.20	0.6 ± 0.1	0.8 ± 0.1	3	1
4	1.91 ± 0.42	518 ± 127	2.2 ± 0.1	242 ± 58	271	111
6	187 ± 32	216 ± 28	296 ± 5.2	239 ± 36	1	1
7	1.93 ± 0.2	21.5 ± 2.3	1.3 ± 0.2	7.6 ± 1.4	11	6
8	-	-	2.2 ± 0.2	9.1 ± 0.6	-	4
9	15.9 ± 3.1	232 ± 24	1.8 ± 0.3	92 ± 5	15	52
10	4.1 ± 0.5	33.3 ± 9.6	0.7 ± 0.1	19.0 ± 2.3	8	27
11	2.3 ± 0.7	22.7 ± 3.5	0.8 ± 0.0	7.9 ± 1.0	10	10
12	7.1 ± 0.9	33.9 ± 4.5	1.5 ± 0.2	14.3 ± 3.3	5	9
13	-	-	4.2 ± 0.2	9.1 ± 0.9	-	2

[a] Flow cytometric binding assay with **13** (c = 10 nM). [b] Radioligand competition binding assay with [^{3}H]**12** (buffer I: c = 1 nM; buffer II: c = 5 nM). Data represent mean values ± SEM of at least three independent experiments performed in triplicate (a) or duplicate (b) on CHO cells stably expressing the Y$_4$R.

5.3.6 NPY receptor subtype selectivity

The K_i values of the peptides were also investigated in competition binding experiments on live cells expressing human Y_1, Y_2 and Y_5 receptors to determine the NPY receptor subtype selectivity using [^{3}H]propionyl-pNPY as radioligand (cf. Supporting Information). The nonspecific binding of the latter at the respective NPY receptor expressing cells was low.

The fluorescent ligand **13** and the 'cold' analog of the new Y_4R radioligand exhibited lower Y_1R and Y_2R affinities (>3000 nM) than the precursor **11** (three-digit nM range) (Table 5.4). However, all investigated peptides turned out to be high-affinity Y_5R ligands with K_i values in the range of 10-40 nM. Interestingly, oxidation of the two thioether groups in **7** resulted in lower affinity at the Y_5R (167 nM), whereas oxidation of methionine (cf. compounds **9**, **10**) had no impact on the Y_4R affinity. K_i values of **7** and the oxidized analogs determined in radioligand binding experiments were in the same range.

Table 5.4. NPY receptor binding data.

	Y_1R	Y_2R	Y_4R K_i [nM]		Y_5R
Compd.	K_i [nM][a]	K_i [nM][b]	[^{3}H]**12**[c]	**13**[d]	K_i [nM][e]
hPP	>3000	>5000	0.6 ± 0.1	0.45 ± 0.04	19.8 ± 1.5
7	249 ± 29	>6000	1.3 ± 0.2	1.93 ± 0.2	9.1 ± 1.4
8	>1000	>1000	2.2 ± 0.2	-	18.6 ± 1.5
9	603 ± 86	>10,000	1.8 ± 0.3	15.9 ± 3.1	167 ± 7
10	807 ± 17	>8000	0.7 ± 0.1	4.1 ± 0.5	25.2 ± 2.8
11	280 ± 11	962 ± 77	0.8 ± 0.0	2.3 ± 0.7	12.7 ± 0.1
12	>4500	>7000	1.5 ± 0.2	7.1 ± 0.9	26.7 ± 5.0
13	>5000	>3600	4.2 ± 0.2	-	39.7 ± 10

[a] Radioligand competition binding assay with [^{3}H]propionyl-pNPY (K_d = 7 nM, c = 5 nM) using MCF-7-hY_1 cells in buffer II (Keller et al., 2011a). [b] Radioligand competition binding assay with [^{3}H]propionyl-pNPY (K_d = 1.4 nM, c = 1 nM) using CHO-hY_2-G_{qi5}-mtAEQ cells in buffer I (Ziemek et al., 2006). [c] Radioligand competition binding assay with [^{3}H]**12** (K_d = 1.1 nM, c = 1 nM) using CHO-hY_4R_{Gqi5}-mtAEQ cells in buffer I. [d] Flow cytometric binding assay with **13** (K_d = 10.8 nM, c = 10 nM) using CHO-hY_4R_{Gqi5}-mtAEQ cells in buffer I. [e] Radioligand competition binding assay with [^{3}H]propionyl-pNPY (K_d = 4.83 nM, c = 4 nM) using HEC-1B-hY_5R cells in buffer II (Moser, 2000).

5.3.7 Effect of Na^+ and osmolarity on the binding of [^{3}H]propionyl-pNPY to the Y_1, Y_2 and Y_5R and binding of [^{3}H]**8**, [^{3}H]**12** and **13** to the Y_5R

Due to the observed impact of Na^+ on Y_4R binding, saturation binding experiments were also performed at the Y_1R, Y_2R and Y_5R (Tables 5.5 and 5.6; cf. Supporting Information Figures S17-S19, S21) using [^{3}H]propionyl-pNPY as radioligand. The K_d values determined at MCF-7

cells expressing the Y_1R were in the same range (K_d = 5.3 nM and 6.6 nM, respectively) in both, buffer I supplemented with glycine (c = 0.3 M) and buffer II. At CHO cells stably expressing the Y_2R, a K_d value (1.4 nM) could only be determined in buffer I, whereas in buffer II, buffer I supplemented with 0.3 M glycine or 0.3 M sucrose (cf. Supp. Information Table S2), saturation was not achieved at concentrations of [^{3}H]propionyl-pNPY up to 60 and 200 nM, respectively. The B_{max} values (sites/cell) at the MCF-7-hY_1 and CHO hY_2 cells were comparable to those reported previously (Keller et al., 2011a; Pluym et al., 2013). Due to the high Y_5R affinity of the 'cold' analog **12**, saturation binding experiments were also performed at HEC-1B-hY_5 cells (Moser, 2000) using [^{3}H]**12** as radioligand (Table 5.6; Supporting Information Figure S21). An effect of Na^+ on Y_5R binding was detected neither for [^{3}H]propionyl-pNPY nor for [^{3}H]**12** (K_d values: [^{3}H]propionyl-pNPY: 24.5 nM (buffer I containing 0.3 M glycine) and 11.0 nM (buffer II); [^{3}H]**12**: 11.3 nM (buffer I containing 0.3 M glycine) and 16.4 nM (buffer II)), although the nonspecific binding was higher in the glycine containing buffer. Saturation binding experiments of [^{3}H]**8** (K_d = 6.9 ± 0.9 nM) and **13** (K_d = 26.5 ± 4.8 nM) afforded K_d values (Supporting Information Figures S20, S22) comparable to K_i values (cf. Table 5.4). In addition, displacement of the radioligands [^{3}H]propionyl-pNPY and [^{3}H]**12** by selected compounds in both buffers revealed no impact of Na^+ on ligand affinity. The determined K_i values of the antagonist CGP 71683A (naphthalene-1-sulfonic acid {*trans*-4-[(4-aminoquinazolin-2-ylamino)methyl]cyclohexyl-methyl}amide) (Criscione et al., 1998) and selected peptides were consistent regardless of the used radioligand (Table 5.7).

Table 5.5. K_d values of [^{3}H]propionyl-pNPY at the Y_1 and Y_2 receptors.

	hY_1R		hY_2R	
	K_d [nM][a]	sites/cell[b]	K_d [nM][c]	sites/cell[b]
buffer I[d]	5.3 ± 1.9	89600	1.4 ± 0.1	236,900[e]
buffer I containing 0.3 M glycine	n.d.[f]	n.d.[f]	-[g]	-[g]
buffer I containing 0.3 M sucrose	n.d.[f]	n.d.[f]	-[g]	-[g]
buffer II	6.6 ± 0.3	47900[h]	-[g]	-[g]

[a] Equilibrium dissociation constant determined on MCF-7-hY_1 cells; mean ± SEM from at least two independent experiments performed in triplicate. [b] Estimated B_{max} (sites/cell) calculated from the determined B_{max} in saturation binding experiments and the specific radioactivity of [^{3}H]propionyl-pNPY. [c] Equilibrium dissociation constant determined on CHO-hY_2 cells; mean ± SEM from at least two independent experiments performed in triplicate. [d] Buffer I containing 0.3 M glycine for experiments on MCF-7-hY_1 cells. [e] Reported: 175,000 sites/cell (Pluym et al., 2013). [f] Not determined; saturation binding assay was not performed at the Y_1R using the respective buffers. [g] Could not be determined; no saturation achieved. [h] Reported: 100,000-150,000 sites/cell (Keller et al., 2011a).

Table 5.6. K_d values of [^{3}H]**12** and [^{3}H]propionyl-pNPY at the Y_5 receptor in different buffers.

	[^{3}H]**12**		[^{3}H]propionyl-pNPY	
	K_d [nM][a]	sites/cell[b]	K_d [nM][a]	sites/cell[b]
buffer I + glycine	16.4 ± 2.3	941,000	24.5 ± 4.9	888,000
buffer II	11.4 ± 0.2	1,056,000	11.0 ± 2.1	861,000[c]

[a] Equilibrium dissociation constant determined on HEC-1B-hY_5 cells in buffer I containing 0.3 M glycine and buffer II, respectively; mean ± SEM from at least two independent experiments performed in triplicate. [b] Estimated B_{max} (sites/cell) calculated from the determined B_{max} in saturation binding experiments and the specific radioactivity of [^{3}H]**12** and [^{3}H]propionyl-pNPY, respectively. [c] Reported: 1,000,000 sites/cell (Moser, 2000).

Table 5.7. Y_5R binding data determined by competition of the radioligands [^{3}H]propionyl-pNPY ([^{3}H]prop.-**2**) and [^{3}H]**12** in buffer I containing glycine and buffer II**.**

	K_i [nM] in buffer I		K_i [nM] in buffer II		Ratio of K_i values, buffer II : buffer I	
Compd.	[^{3}H]**12**[a]	[^{3}H]prop.-**2**[b]	[^{3}H]**12**[a]	[^{3}H]prop.-**2**[b]	[^{3}H]**12**	[^{3}H]prop.-**2**
CGP71683A	1.6 ± 0.2	3.8 ± 0.4	1.9 ± 0.4	1.4 ± 0.3	1.2	0.4
pNPY	15.3 ± 1.1	10.7 ± 1.2	11.0 ± 1.5	6.7 ± 1.1	0.7	0.6
7	5.2 ± 1.0	5.8 ± 0.2	7.2 ± 0.8	9.1 ± 1.4	1.4	1.6
11	8.4 ± 1.2	11.1 ± 3.1	12.0 ± 1.2	14.1 ± 1.4	1.4	1.3

[a] Radioligand competition binding assay with [^{3}H]**12** (buffer I containing 0.3 M glycine: K_d = 16.4 nM, c = 10 nM; buffer II: K_d = 11.4 nM, c = 10 nM). [b] Radioligand competition binding assay with [^{3}H]propionyl-pNPY (buffer I containing 0.3 M glycine: K_d = 24.5 nM, c = 4 nM; buffer II: K_d = 11.0 nM, c = 4 nM); mean ± SEM from three independent experiments (performed in triplicate) using HEC-1B-hY_5R cells.

5.4 Conclusions

Replacement of the methionine residues in **7** by norleucine to prevent oxidation of sulfur in the reference compound gave the chemically more stable peptide **11**, which was converted to radiolabeled and fluorescent molecular tools for the Y_4 receptor, e. g. for the determination of competition binding data of Y_4R ligands. Surprisingly, equilibrium binding and kinetics of the radioligand [^{3}H]**12** and the fluorescent ligand **13** were effected by the buffer composition in a different way: [^{3}H]**12** binding was dependent on the sodium concentration, whereas binding and receptor-mediated internalization of **13** were strongly effected by the osmolarity of the buffer. Fluorescent ligands are often considered superior to radioligands as molecular

tools. However, the present study demonstrates that, despite an identical peptide scaffold, fundamental differences between both types of probes may exist and should be carefully taken into account in the interpretation of experimental results.

5.5 Supporting Information

5.5.1 Synthesis of the ligands [^{3}H]propionyl-pNPY, **8** and [^{3}H]**8**

[^{3}H]propionyl-pNPY. A solution of succinimidyl [^{3}H]propionate (500 µL = 2.5 mCi; 32 nmol; specific activity: 80 Ci/mmol (2.96 TBq/mmol), purchased from American Radiolabeled Chemicals, St. Louis, MO via Hartman Analytics, Braunschweig, Germany) in hexane/EtOAc (9:1) was transferred from the delivered ampoule into a 1.5 mL reaction vessel with screw cap, and the solvent was removed in a vacuum concentrator (30 °C, 30 min). A solution of pNPY (0.5 mg, 109 nmol, in (v/v) 12.5% water, 84.75% DMF, 2.75% DIPEA) (80 µL) was added, and the vessel was vigorously shaken at rt for 2 h. The mixture was acidified by addition of 2% aqueous TFA (70 µL) followed by addition of MeCN/H_2O (10:90) (180 µL). [^{3}H]propionyl-pNPY was purified using a HPLC system from Waters. A Luna C18(2) column (3 µm, 150 × 4.6 mm, Phenomenex, Aschaffenburg, Germany) was used as stationary phase at a flow rate of 0.8 mL/min. Acetonitrile supplemented with 0.04% TFA (A) and 0.05% aq TFA (B) were used as mobile phase. The following linear gradient was applied: A/B: 0–22 min: 10:90 – 36:64, 22–27 min: 36:64, 27–28 min: 36:64–95:5, 28–35 min: 95:5. For the purification of the radiolabeled peptide three HPLC runs were performed. The radioligand was collected in 2-mL reaction vessels with screw caps, and the volumes of the combined eluates were reduced by evaporation to approximately 900 µL. Ethanol (100 µL) was added to obtain a solution of the radioligand in 10% ethanol for storage. By four-point calibration with propionyl-pNPY (0.1, 0.2, 0.5 and 0.8 µM; injection volume: 100 µL, UV-detection: 220 nm) a concentration of the radioligand of 13.65 µM was determined. For this purpose, two samples were prepared by diluting 2 µL of the radioligand solution with 128 µL MeCN/0.05% aq TFA (10:90). Volumes of 100 µL of each sample were injected. The following linear gradient was applied: A/B: 0–20 min: 15:85 – 50:50, 20–22 min: 50:50 – 95:5, 22–28 min: 95:5. To measure the radioactivity, from each of the two samples 3 µL were counted in 3 mL of liquid scintillator (Rotiszint eco plus, Carl Roth, Karlsruhe, Germany) with a Beckmann LS 6500 liquid scintillation counter (Beckman Coulter, Krefeld, Germany) in pentuplicate. To determine the radiochemical purity and to prove the identity of the radioligand, a solution of the radiolabeled peptide (100 µL, final concentration: 0.25 µM), spiked with ‘cold’ propionyl-pNPY (final concentration: 9.1 µM) was analyzed by HPLC with combined UV/radiochemical detection. The radiochemical purity was > 99%. Calculated specific activity: 46.32 Ci/mmol (1.714 TBq/mmol). Chemical yield: hexa(hydrotrifluoroacetate) of [^{3}H]propionyl-pNPY: 58.9 µg, 13.65 nmol, 42.7%. Radiochemical yield: 0.627 mCi (23.21 MBq), 25.1%. The stock solution of [^{3}H]propionyl-pNPY (c = 13.65 µM) was stored at 4 °C.

Propionyl-[Lys^4]hPP (8). Compound **7** (3.92 mg, 0.94 µmol) was dissolved in Millipore water (1500 µL), 0.1 M borate buffer (38.1 mg/mL di-sodium tetraborate decahydrate; pH 9.5; 930 µL) and a solution of succinimidyl propionate in DCM (0.26 mg/mL) were added (300 µL). To prevent two-fold acylation, the reaction was monitored by HPLC. The product was purified by

preparative HPLC (column: Kinetex-XB C18, 5 µm, 250 mm × 21 mm, Phenomenex, Aschaffenburg, Germany; gradient: MeCN/10% MeCN, 0.1% aq TFA: 0–30 min: 15:85 – 60:40, 30–38 min: 95:5; t_R = 19.4 min). Lyophilisation of the eluate afforded propionyl-[Lys^4]hPP as a white fluffy solid (0.72 mg, 0.17 µmol). HRMS (*m/z*): $[M+5H]^{5+}$ calcd. for $C_{189}H_{296}N_{54}O_{53}S_2$, 847.8386; found, 847.8397. RP-HPLC (220 nm): 98% (column: Synergi Hydro-RP C18, 4 µm, 250 × 4.6 mm, Phenomenex; gradient: MeCN 0.04% TFA/0.05% TFA: 0–30 min: A/B 30:70–42:58, 30–31 min: 42:58–95:5, 31–40 min: 95:5. t_R = 16.2 min, k = 3.9) $C_{189}H_{296}N_{54}O_{53}S_2 \cdot C_{10}H_5F_{15}O_{10}$ (4239.19 + 570.10).

[^{3}H]propionyl-[Lys^4]hPP ([^{3}H]8). A solution of succinimidyl [^{3}H]propionate (340 µL = 1.7 mCi; 21.2 nmol; specific activity: 80 Ci/mmol (2.96 TBq/mmol) in hexane/EtOAc (9:1) was transferred from the delivered ampoule into a 1.5 mL reaction vessel with screw cap, and the solvent was removed in a vacuum concentrator (30 °C, 30 min). A solution of the precursor peptide [Lys^4]hPP (**7**) (0.35 mg, 81 nmol in 0.1 M sodium borate buffer pH 9.5) (135 µL) was added, the vessel was vigorously shaken at rt for 2.5 h, and diluted by the addition of MeCN/0.05% aq TFA 30:70 (v/v) (215 µL). [^{3}H]**8** was purified using a HPLC system from Waters. A Synergi Hydro-RP C18, 4 µm, 250 × 4.6 mm (Phenomenex) served as stationary phase at a flow rate of 0.8 mL/min. Acetonitrile supplemented with 0.04% TFA (A) and 0.05% aq TFA (B) were used as mobile phase (linear gradient: 0–30 min: A/B 30:70–42:58, 30–31 min: 42:58–95:5, 31–40 min: 95:5). For the purification of the radiolabeled peptide five HPLC runs were performed. The radioligand was collected in 2-mL reaction vessels with screw caps, and the solvent of the combined eluates was removed in a vacuum concentrator. The product was dissolved in a mixture of EtOH/10 mM HCl 2:98 (v/v) (400 µL). To determine the radiochemical purity and to prove the identity of the radioligand, a solution of the radiolabeled peptide (0.07 µM), spiked with 'cold' **8** (final concentration: 18 µM), was analyzed by HPLC with combined UV/radiochemical detection (linear gradient: 0–30 min: A/B 30:70–45:55, 30–31 min: 42:58–95:5, 31–40 min: 95:5; injection volume: 100 µL). The radiochemical purity was 90%. For the quantification of the radioligand, an aliquot (2 µL) of the stock solution of [^{3}H]**8** in EtOH/10 mM HCl 2:98 was added to 118 µL of MeCN/0.05% aq TFA 30:70 (v/v), and 110 µL of this solution were injected (performed in duplicate). By four-point calibration with **8** (0.2, 0.5, 1.0, 3.0 µM; injection volume: 110 µL, UV-detection: 220 nm) a concentration of the radioligand of 24.5 µM was determined. The activity of [^{3}H]**8** was determined as follows: two samples were prepared by diluting 1 µL of stock solution by adding 199 µL of acetonitrile/water 30:70. From each sample, 50 µL were counted in 3 mL of scintillator (Rotiszint eco plus) with a Beckman LS 6500 liquid scintillation counter in triplicate. Calculated specific activity: 34.91 Ci/mmol (1.291 TBq/mmol). Chemical yield: penta(hydrotrifluoroacetate) of [^{3}H]**8**: 41.5 µg, 9.80 nmol, 46.2%. Radiochemical yield: 0.342 mCi (12.65 MBq), 20.1% in 400 µL. The stock solution of [^{3}H]**8** (c = 24.5 µM) was stored at 4 °C.

HPLC analyses (radiodetection) performed after storage for two week revealed slight decomposition of [^{3}H]**8**. Therefore, ascorbic acid (final concentration: 0.24 mM) was added. However, after storage at 4 °C for 2 years analysis of the radioligand (radiolabeled peptide (0.44 µM), spiked with 'cold' **8** (final concentration: 18 µM); linear gradient: 0–30 min: A/B 30:70–42:58, 30–31 min: 42:58–95:5, 31–40 min: 95:5; injection volume: 100 µL) repeated revealed a decomposition of the radioligand by 95%.

5.5.2 Synthesis of [Lys^4,Nle^{17,30}]hPP (**11**)

SPPS was performed automatically on a Syro-I peptide synthesizer (Biotage, Uppsala, Sweden) by using the Fmoc/tBu strategy. The peptide-chain assembly was performed on a 0.018 mmol scale on the Fmoc-Rink amide MBHA resin. The amino-acid (AA) double couplings (2 x 40 min) were carried out by using Fmoc-AA-OH/HOBt (5 eq. each), HBTU (4.9 eq.), and DIPEA (10 eq.) in DMF/NMP (7:3 v/v). Fmoc cleavage was carried out with a 3 min treatment with 30% piperidine in DMF, followed by a 14 min treatment with 15% piperidine in DMF. After the peptide-chain assembly was completed, the resin was washed with DMF, DCM and Et_2O (three times each) and vacuum dried overnight. The fully deprotected peptide was cleaved from the resin by using TFA/H_2O/TIA/TIS/EDT (90:3:2:2:3 v/v). After 3 h, the peptide was precipitated with cold Et_2O and isolated by centrifugation at 8 °C for 5 min. The crude peptide was further washed three times with cold Et_2O to remove the residual scavengers and, finally, vacuum dried overnight. The product was purified by preparative HPLC (220 nm; column: YMC-Actus-Triart C8 250 x 20 mm ID, S 5 µm,12 nm; gradient: MeCN/0.1% aq TFA: 0–30 min: 10:90 – 50:50, 31–36 min: 90:10; flow rate: 20 mL/min; t_R = 24.8 min). HRMS (*m/z*): $[M+6H]^{6+}$ calcd. for $C_{188}H_{296}N_{54}O_{52}$, 691.3769; found, 691.3795. $C_{188}H_{296}N_{54}O_{52} \cdot C_{12}H_6F_{18}O_{12}$ (4144.69 + 684.12).

5.5.3 Purity, identity and long-term stability of [^{3}H]**8** determined by HPLC

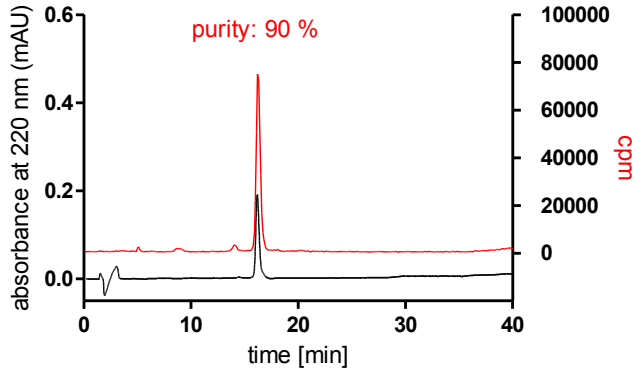

Figure S1. HPLC analysis for purity and identity control of the radiolabeled peptide [^{3}H]propionyl-[Lys^4]hPP ([^{3}H]**8**) (0.17 µM) (red), spiked with 'cold' **8** (18 µM). t_R = 16.2 min; injection volume: 100 µL.

Radiochemical purity: 90 %. The minor differences in t_R result from serial detection of the UV and radiometric signals.

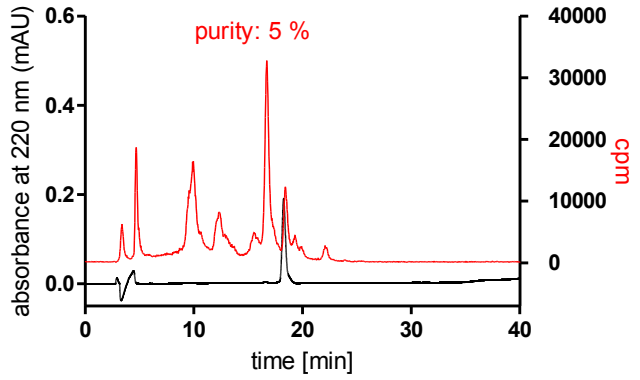

Figure S2. HPLC analysis of [^{3}H]**8** (0.44 µM) (red), spiked with 'cold' **8** (18 µM), analyzed after 2 years of storage at 4 °C in EtOH/10 mM HCl 2/98 (v/v), supplemented with ascorbic acid (0.24 mM). t_R = 18.4 min; injection volume: 100 µL. A different gradient was applied compared to HPLC analysis in Figure S1.

Radiochemical purity after 2 years: 5 %. The minor differences in t_R result from serial detection of the UV and radiometric signals.

5.5.4 Chemical stability of the peptides hPP and **7**-**11**

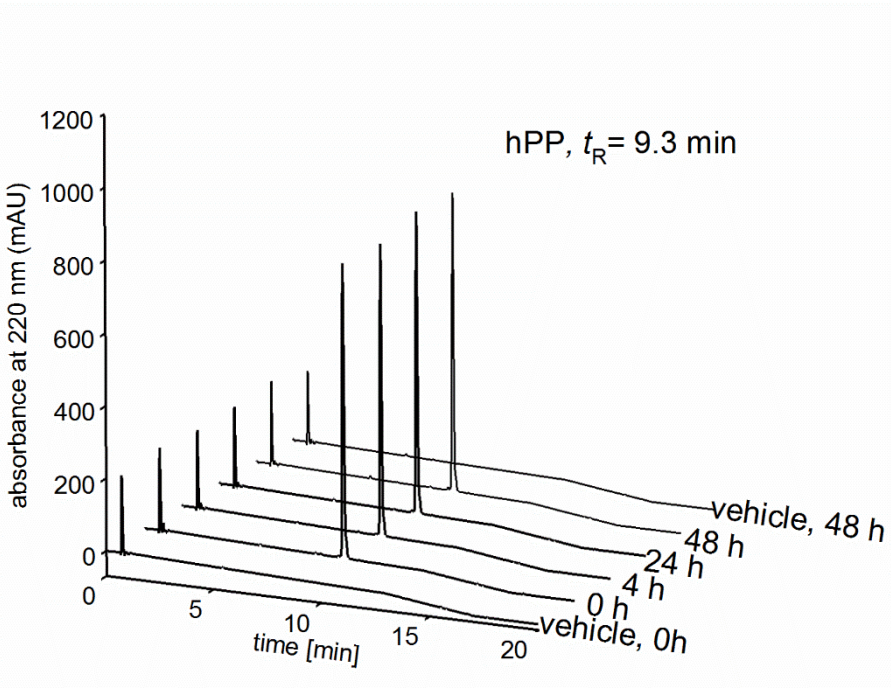

Figure S3. Reversed-phase HPLC analysis of hPP after incubation in phosphate buffered saline (PBS, pH 7.4) at 21 °C for 48 h (detection at 220 nm). The peptide was stable under these conditions.

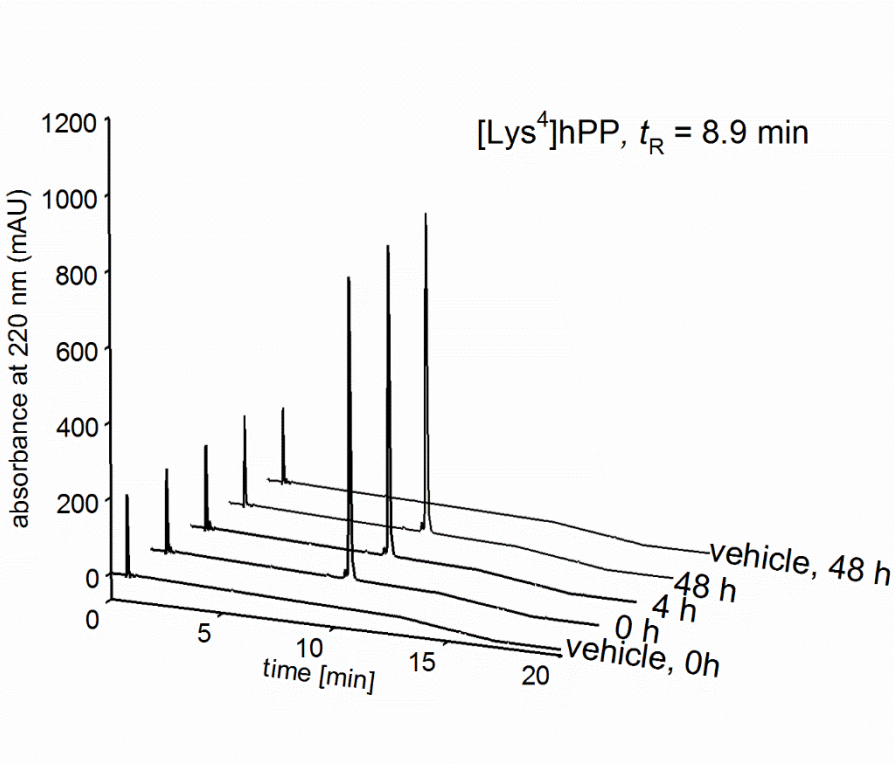

Figure S4. Reversed-phase HPLC analysis of **7** after incubation in PBS (pH 7.4) at 21 °C for 48 h (detection at 220 nm). The peptide was stable under these conditions.

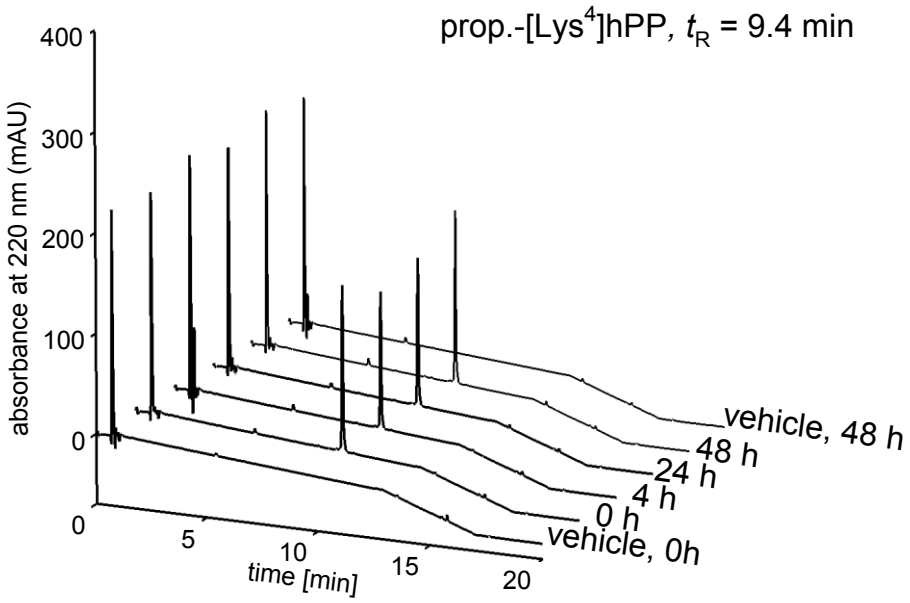

Figure S5. Reversed-phase HPLC analysis of **8** after incubation in PBS (pH 7.4) at 21 °C for 48 h (detection at 220 nm). The peptide was stable under these conditions.

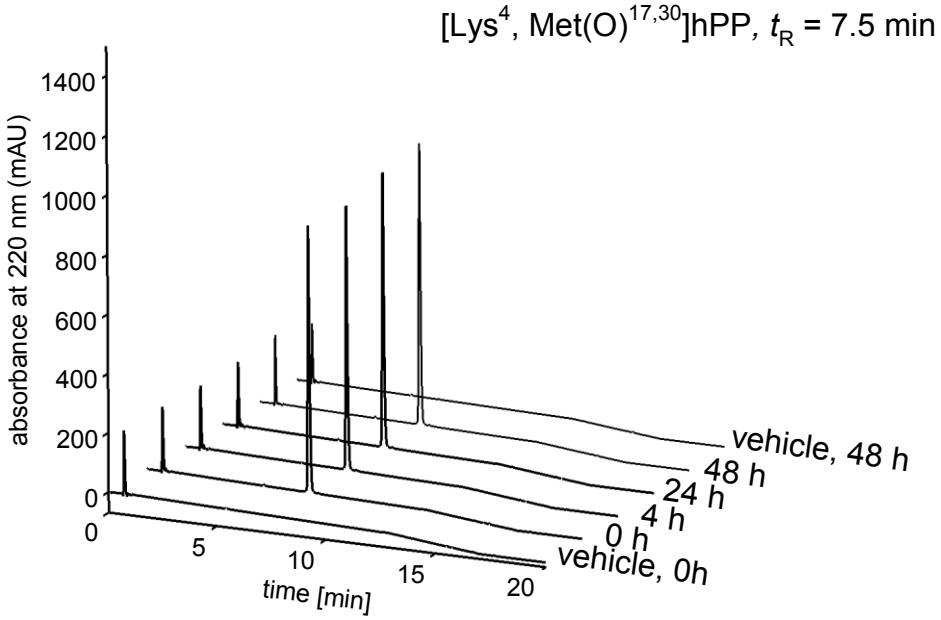

Figure S6. Reversed-phase HPLC analysis of **9** after incubation in PBS (pH 7.4) at 21 °C for 48 h (detection at 220 nm). The peptide was stable under these conditions.

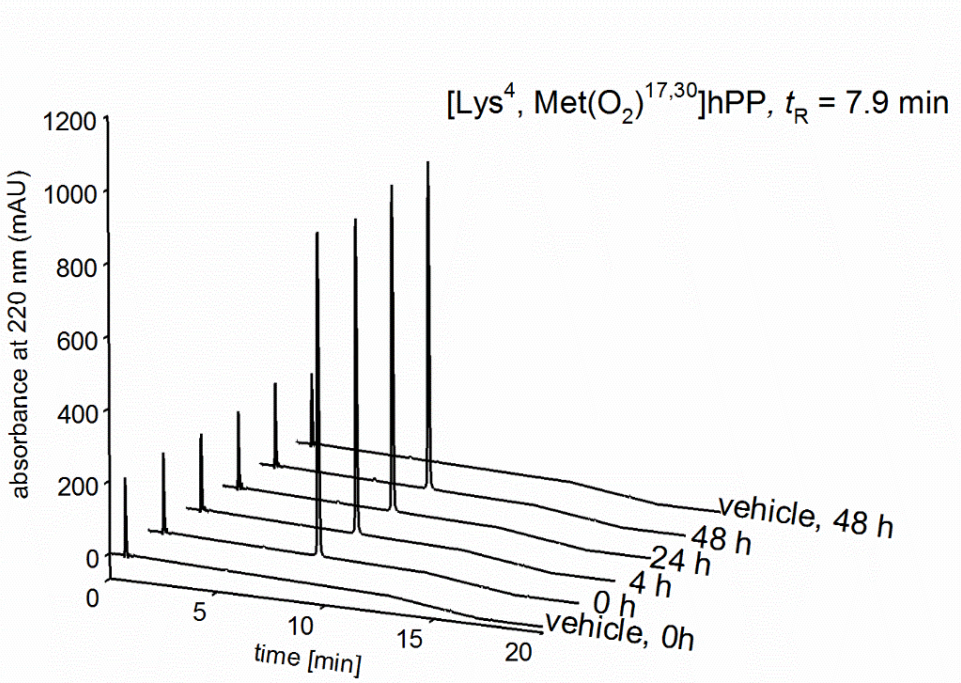

Figure S7. Reversed-phase HPLC analysis of **10** after incubation in PBS (pH 7.4) at 21 °C for 48 h (detection at 220 nm). The peptide was stable under these conditions.

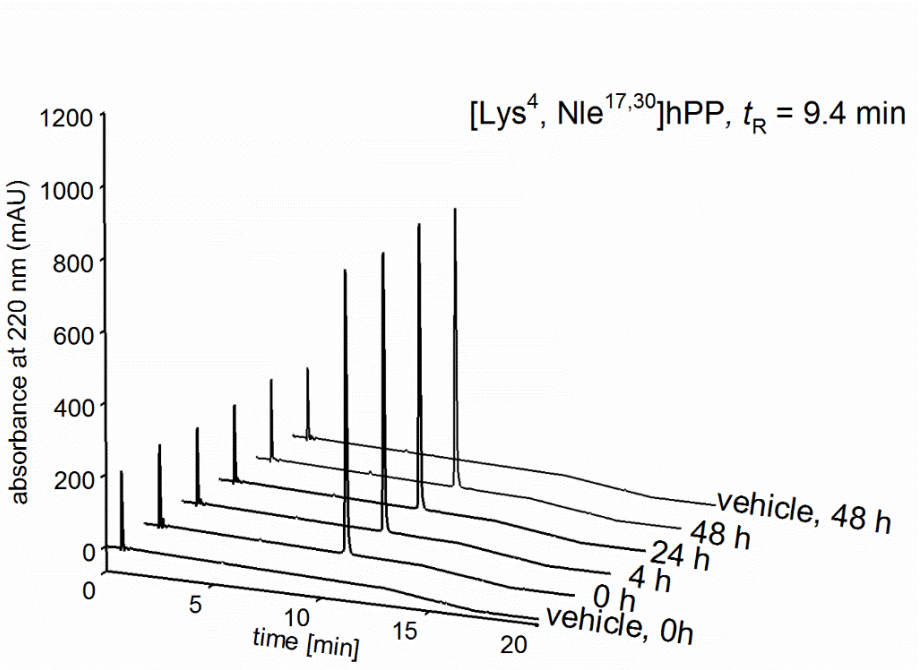

Figure S8. Reversed-phase HPLC analysis of 11 after incubation in PBS (pH 7.4) at 21 °C for 48 h (detection at 220 nm). The peptide was stable under these conditions.

5.5.5 Fluorescence spectra and quantum yields of peptide **13**

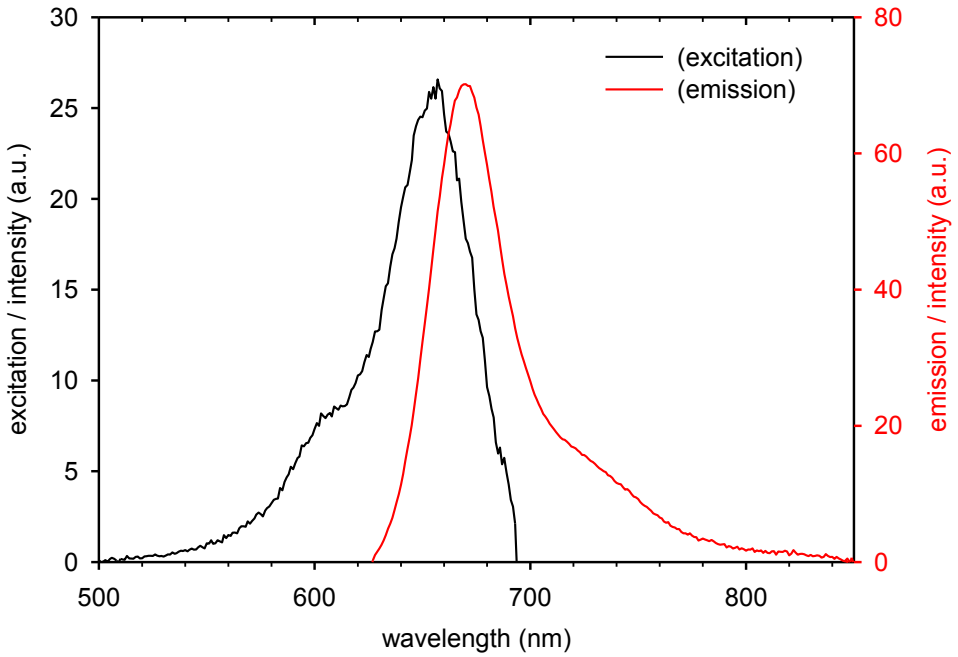

Figure S9. Excitation and corrected emission spectrum of **13** in PBS pH 7.4 supplemented with 1% BSA (c = 3.2 µM). Spectrum was recorded with a Cary Eclipse spectrofluorimeter at 22 °C with the slit adjustments (ex./em. slit) 5/10 nm for excitation and 10/5 nm for emission.

Table S1. Excitation and emission maxima and fluorescence quantum yields Φ (22 °C, cresyl violet perchlorate as reference), of the cyanine labeled peptide **13**, determined in PBS and PBS supplemented with 1% BSA.

PBS, pH 7.4		PBS, pH 7.4 containing 1% BSA	
$\lambda_{ex}/\lambda_{em}$	Φ (%)	$\lambda_{ex}/\lambda_{em}$	Φ (%)
646/664	21	655/667	56

5.5.6 Osmolality of the buffers used in NPY receptor binding studies

Table S2. Osmolality values determined for different buffers using a semi-micro osmometer (K-7400, Knauer, Berlin, Germany).

Buffer	buffer I	buffer II	buffer I	buffer I	buffer I	buffer I
Containing	no sodium	NaCl 150 mM	NaCl 50 mM	NaCl 50 mM glycine 0.19 M	NaCl 100 mM	glycine 0.3 M
mosmol/kg	51	353	142	360	283	370

5.5.7 Saturation binding with [^{3}H]**8** at the hY$_4$R

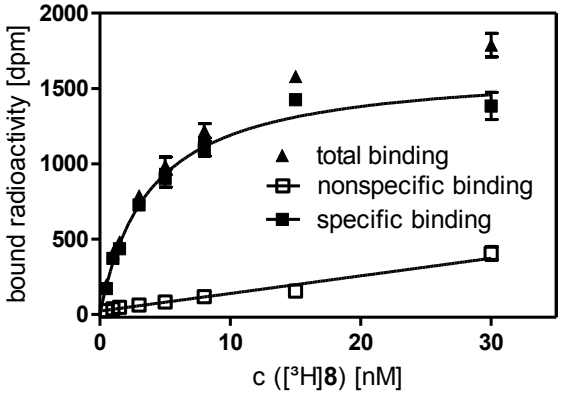

Figure S10. Representative Y$_4$R saturation binding of the radioligand [^{3}H]**8** determined at CHO-hY$_4$-G$_{qi5}$-mtAEQ cells at 22 °C in buffer II. Nonspecific binding was determined in the presence of a 200-fold excess of **7**. Three independent experiments were performed in triplicate; K_d = 6.0 ± 1.3 nM.

5.5.8 Kinetic experiments with [^{3}H]**8** at the hY$_4$R

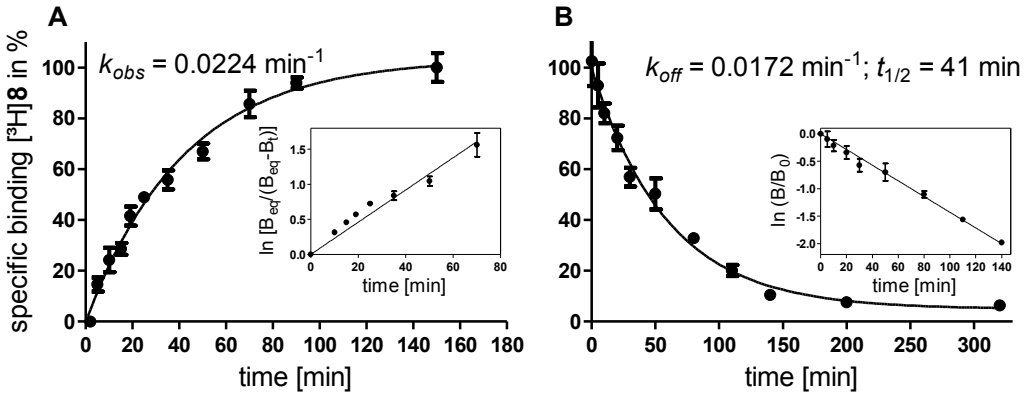

Figure S11. Kinetic experiments of the radioligand [^{3}H]**8** determined at CHO-hY$_4$-G$_{qi5}$-mtAEQ cells at 22 °C in buffer II. (**A**) Representative Y$_4$R association kinetics of [^{3}H]**8**; (c = 10 nM). Inset: Linearization ln[B_{eq}/(B_{eq}-B_t)] versus time. (**B**) Representative Y$_4$R dissociation kinetics of [^{3}H]**8** (c = 10 nM, pre-incubation time: 90 min) determined in the presence of a 100-fold excess of **7**. Fitting of the data according to a monophasic exponential decay. Inset: Linearization ln[B/B_0] versus time. Two independent experiments were performed in triplicate.

5.5.9 Saturation binding with [³H]**12** at the hY$_4$R

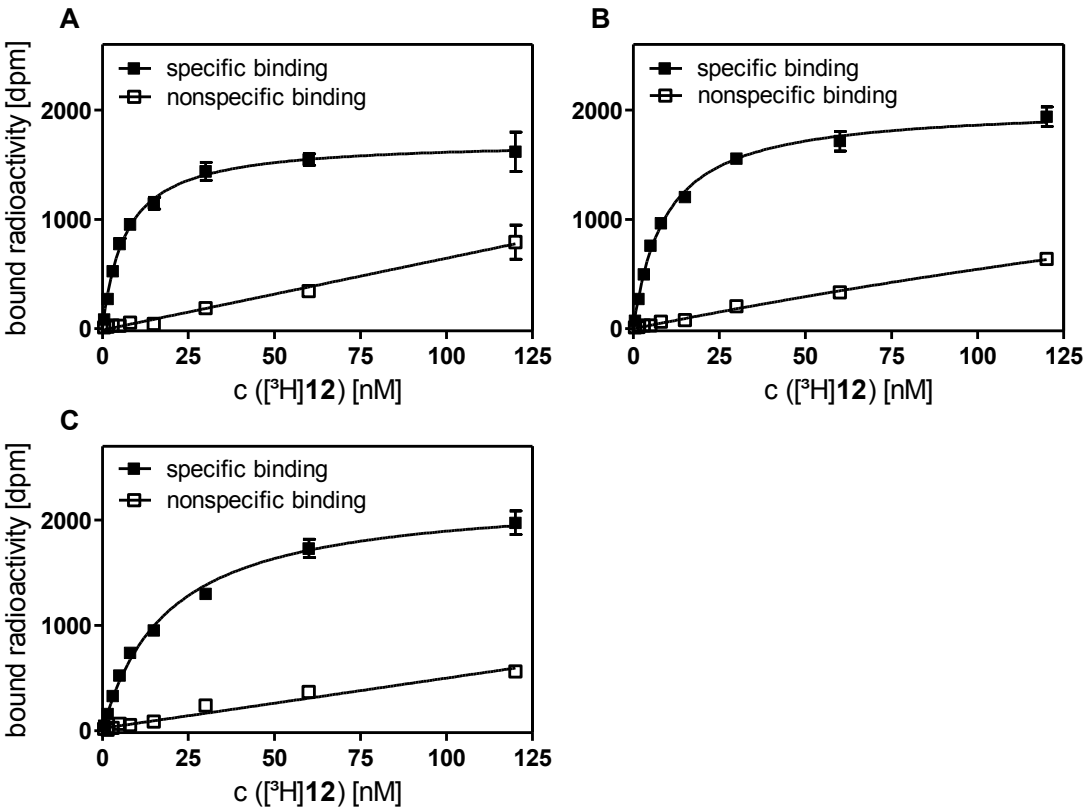

Figure S12. (**A**) Representative saturation binding experiment with [^{3}H]**12** at CHO-hY$_4$R-G$_{qi5}$-mtAEQ cells in buffer I supplemented with NaCl (final concentration 50 mM) ([^{3}H]**12**: K_d = 7.2 ± 0.5 nM). (**B**) Representative saturation binding experiment with [^{3}H]**12** at CHO-hY$_4$R-G$_{qi5}$-mtAEQ cells in buffer I supplemented with NaCl (final concentration 50 mM) adjusted to isotonic conditions with glycine (final concentration 0.19 M) ([^{3}H]**12**: K_d = 8.4 ± 0.9 nM). (**C**) Representative saturation binding experiment with [^{3}H]**12** at CHO-hY$_4$R-G$_{qi5}$-mtAEQ cells in buffer I supplemented with NaCl (final concentration 100 mM) ([^{3}H]**12**: K_d= 18.0 ± 0.5 nM). Nonspecific binding was determined in the presence of a 100-fold excess of **11**. At least two independent experiments were performed in triplicate.

5.5.10 Binding characteristics of the fluorescent ligand **13** in buffer I containing glycine at the hY_4R

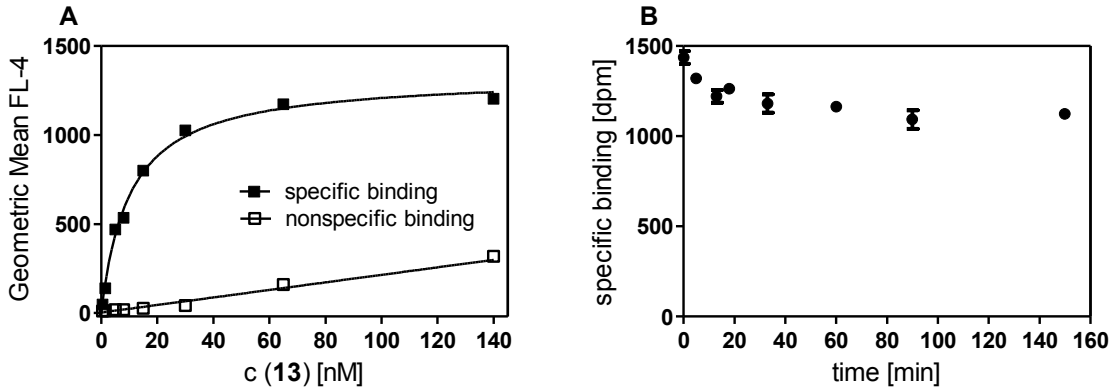

Figure S13. Y_4R binding characteristics of the fluorescent ligand **13** determined by flow cytometry at CHO-hY_4-G_{qi5}-mtAEQ cells in buffer I supplemented with glycine (final concentration 0.3 M). (**A**) Representative saturation binding experiments with **13**. Nonspecific binding was determined in the presence of a 100-fold excess of hPP. (**B**) Representative Y_4R dissociation kinetics of **13** (c = 10 nM; pre-incubation time: 60 min) determined in the presence of a 80-fold excess of [Lys^4]hPP (**7**). Nonspecific binding was determined in the presence of a 100-fold excess of **7**. Dissociation of **13** was not observed. Two independent experiments were performed in duplicate.

5.5.11 Morphology and volumes of CHO-hY$_4$R cells under hypotonic and isotonic conditions

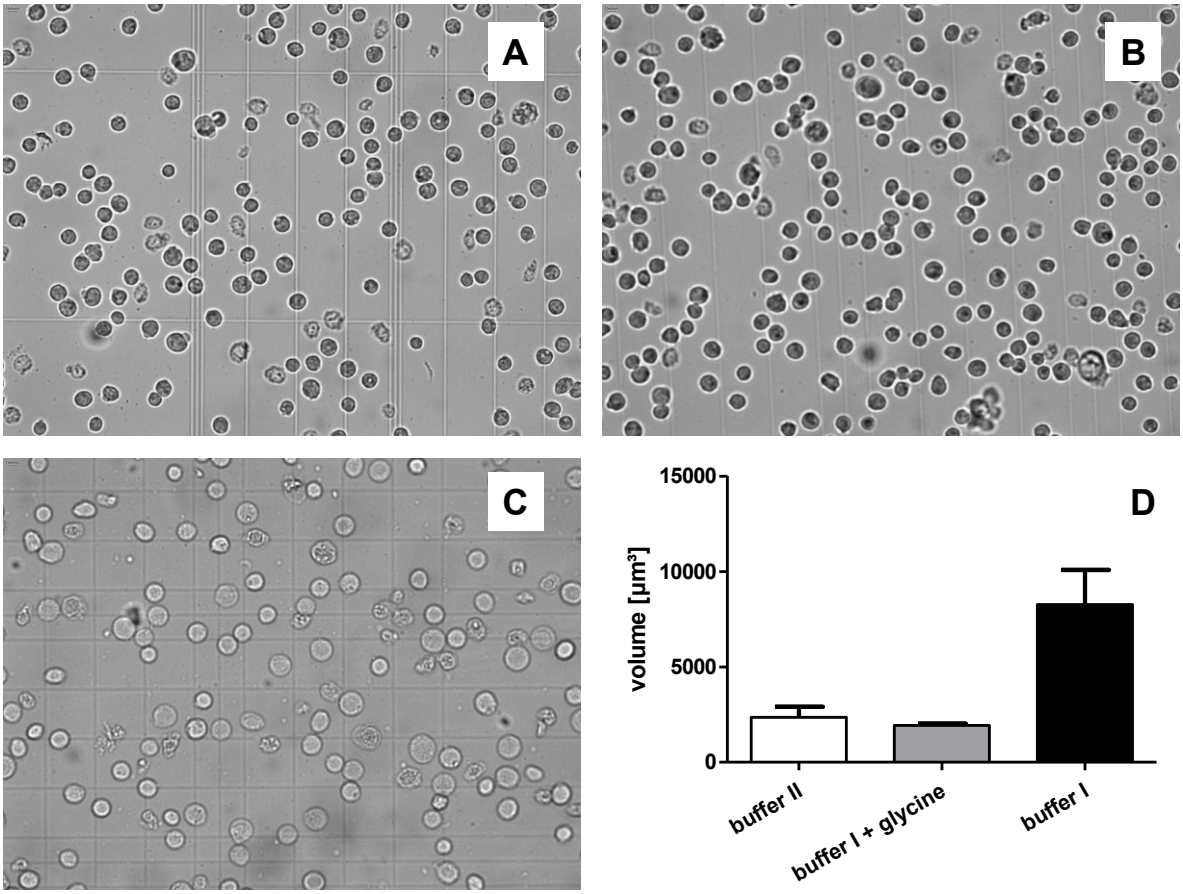

Figure S14. Morphology of CHO-hY$_4$-G$_{qi5}$-mtAEQ cells in isotonic buffer II (**A**), buffer I containing glycine (0.3 M) to obtain isotonicity (**B**), and hypotonic buffer I (**C**). (**D**) Comparison of the cell volumes in different buffers, calculated for spheres (n = 25; mean values ± SEM).

CHO-hY$_4$-Gqi5-mtAEQ cells from a 75-cm^2 culture flask were treated with 3 mL trypsin/EDTA. Aliquots of 1 mL were added to 9 mL of the respective buffer (buffer I, buffer I containing 0.3 M glycine and buffer II) before centrifugation (400 *g*, 5 min). Afterwards, the supernatants were discarded, and the cells were resuspended in the respective buffer (200 µL). Cells were examined in a hemocytometer (Neubauer improved, BLAUBRAND, Brand, Wertheim, Germany) using a Leitz DMRB microscope (Leica Microsystems, Wetzlar, Germany) with a PL Fluorstar objective (morphology: 10x/0.30; diameter: 40x/0.7, pH2) with a DCM-510 ocular microscope camera (OCS.tec, Erding, Germany). Diameters of 25 cells were measured in each buffer by using the ScopePhoto V3.0.12.498 software (Hangzhou Scopetek Opto-electric, Hangzhou, China). The volumes of the cells were calculated assuming spheres ($4/3 \times \pi \times r^3$). Images of the cells were taken in the respective buffer (10x objective).

5.5.12 Scattergrams of CHO-hY$_4$R cells in the presence of **13** in different buffers

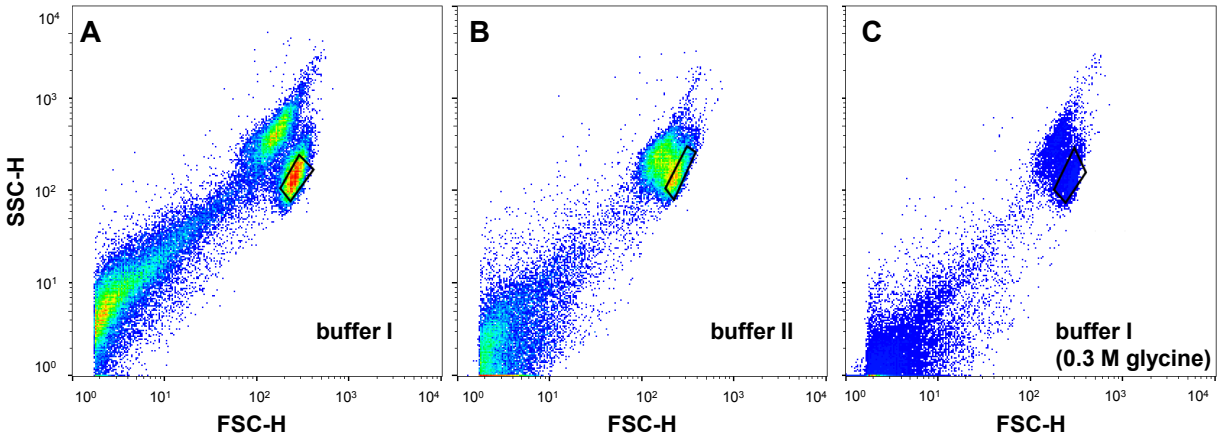

Figure S15. Scattergrams of CHO-hY$_4$R$_{Gqi5}$-mtAEQ cells in the presence of the labeled peptide **13** (140 nM) in hypotonic buffer I (**A**), isotonic buffer II (**B**) and isotonic buffer I containing 0.3 M glycine (**C**). The subpopulation framed in black was chosen for binding studies.

5.5.13 Competition binding with [³H]**8** at the hY$_4$R

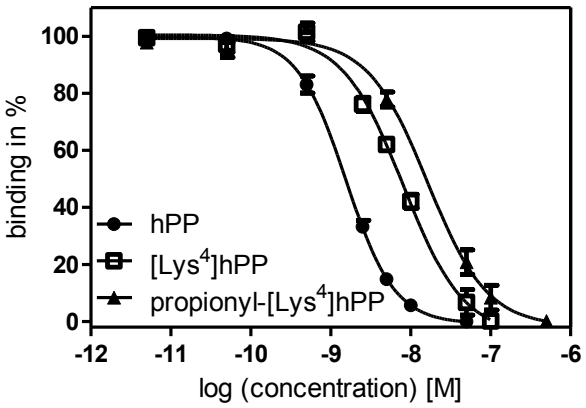

Figure S16. Displacement curves from competition binding experiments performed with [³H]propionyl-[Lys⁴]hPP (K_d = 6.0 nM, c = 5 nM) using CHO-hY$_4$R$_{Gqi5}$-mtAEQ cells in buffer II. Data represent mean values ± SEM from at least two independent experiments performed in triplicate.

5.5.14 Saturation binding with [³H]propionyl-pNPY at the hY$_1$R, hY$_2$R, and hY$_5$R

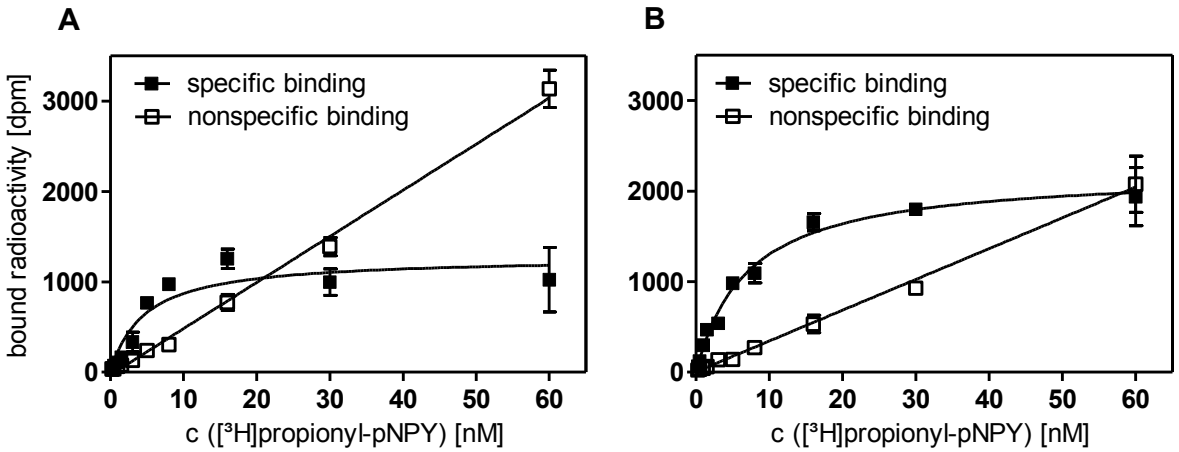

Figure S17. (**A**) Representative saturation binding experiment with [³H]propionyl-pNPY at MCF-7-hY$_1$ cells in buffer I containing 0.3 M glycine (K_d = 5.1 ± 1.9 nM). (**B**) Representative saturation binding experiment with [³H]propionyl-pNPY at MCF-7-hY$_1$ cells in buffer II (K_d = 6.6 ± 0.3 nM). At least two independent experiments were performed in triplicate.

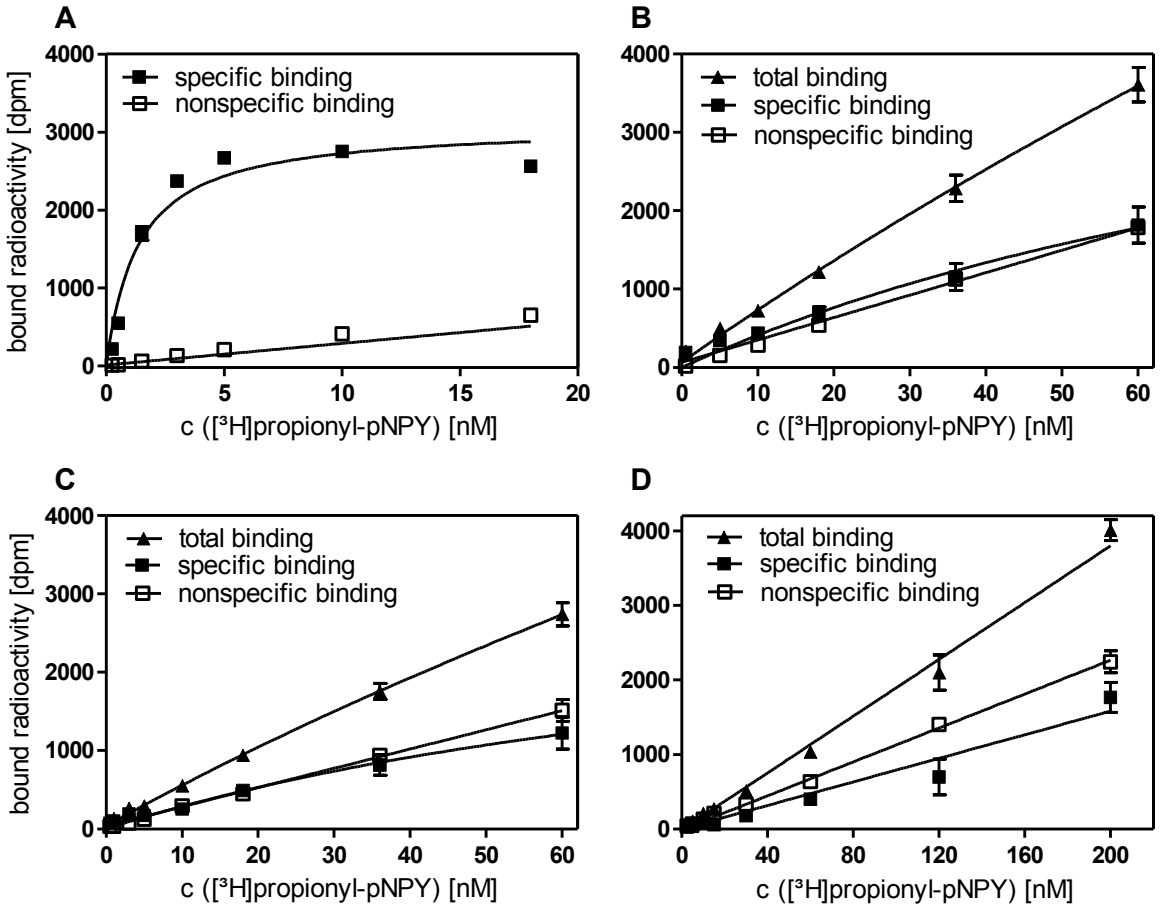

Figure S18. (**A**) Representative saturation binding experiment with [^{3}H]propionyl-pNPY at CHO-hY_2R-G_{qi5}-mtAEQ cells in buffer I (K_d= 1.4 ± 0.1 nM) (n=4). (**B**) Representative binding experiment with [^{3}H]propionyl-pNPY at CHO-hY_2R-G_{qi5}-mtAEQ cells in buffer I containing 0.3 M glycine (n=2). (**C**) Representative binding experiment with [^{3}H]propionyl-pNPY at CHO-hY_2R-G_{qi5}-mtAEQ cells in buffer I containing 0.3 M sucrose (n=2). (**D**) Representative binding experiment with [^{3}H]propionyl-pNPY at CHO-hY_2R-G_{qi5}-mtAEQ cells in buffer II (n=3). Experiments were performed in triplicate.

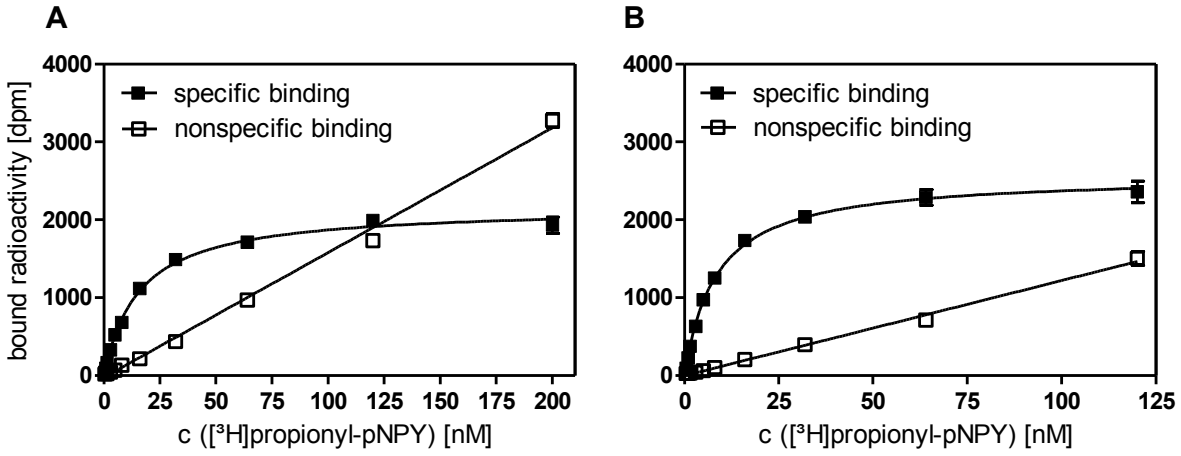

Figure S19. (**A**) Representative saturation binding experiment with [^{3}H]propionyl-pNPY at HEC-1B-hY_5 cells in buffer I supplemented with glycine (final concentration 0.3 M) (K_d = 24.5 ± 4.9 nM). (**B**) Representative saturation binding experiment with [^{3}H]propionyl-pNPY at HEC-1B-hY_5 cells in buffer II (K_d = 11.0 ± 2.1 nM). Nonspecific binding was determined in the presence of a 100-fold excess of pNPY. At least two independent experiments were performed in triplicate.

5.5.15 Saturation binding with [^{3}H]**8** at the hY$_5$R

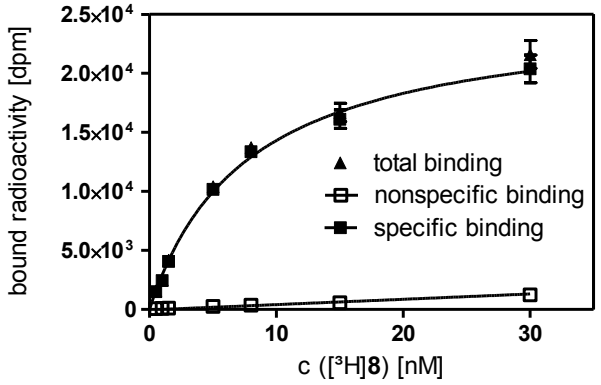

Figure S20. Representative saturation binding experiment of the radioligand [^{3}H]**8** determined at HEC-1B-hY$_5$R cells at 22 °C in buffer II. Nonspecific binding was determined in the presence of a 200-fold excess of CGP 71683A. Three independent experiments were performed in triplicate; K_d = 6.9 ± 0.9 nM.

5.5.16 Saturation binding with [^{3}H]**12** at the hY$_5$R

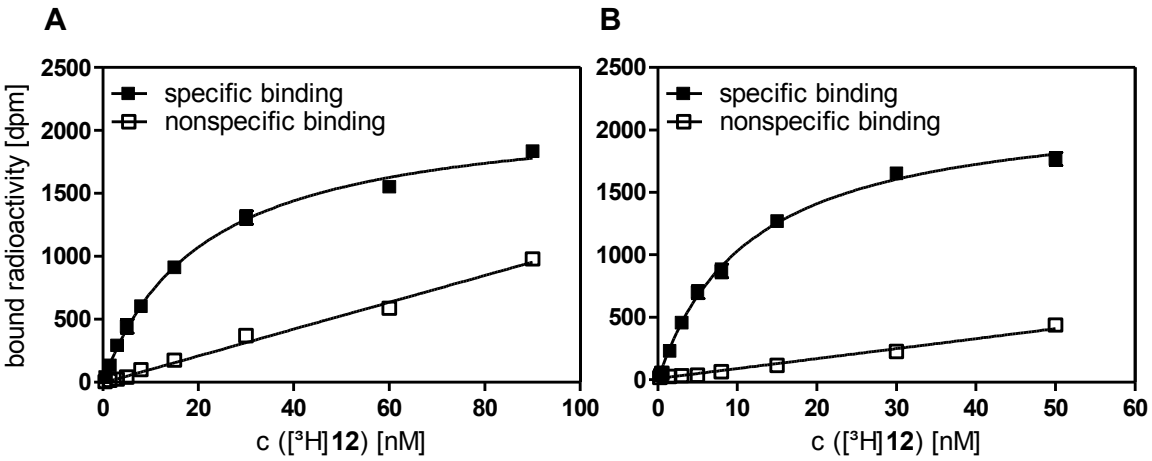

Figure S21. (**A**) Representative saturation binding experiment with [^{3}H]**12** at HEC-1B-hY$_5$ cells in buffer I supplemented with glycine (final concentration 0.3 M) (K_d = 16.4 ± 2.3 nM). (**B**) Representative saturation binding experiment with [^{3}H]**12** at HEC-1B-hY$_5$ cells in buffer II (K_d = 11.4 ± 0.2 nM). Three independent experiments were performed in triplicate.

5.5.17 Saturation binding with **13** at the hY$_5$R

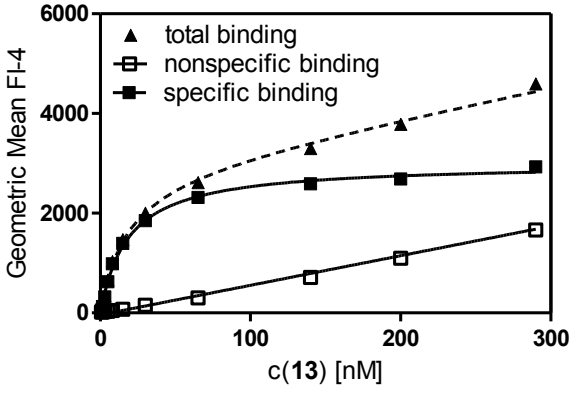

Figure S22. Representative saturation binding experiment of **13** on HEC-1B-hY$_5$R cells in buffer II. K_d = 26.5 ± 4.8 nM; nonspecific binding was determined in the presence of an 80-fold excess of CGP 71683A; three independent experiments were performed in duplicate; assay was performed as previously described for saturation binding experiments with **13** on CHO hY$_4$R cells.

5.6 References

Balasubramaniam, A.; Mullins, D. E.; Lin, S.; Zhai, W.; Tao, Z.; Dhawan, V. C.; Guzzi, M.; Knittel, J. J.; Slack, K.; Herzog, H.; Parker, E. M. (2006). Neuropeptide Y (NPY) Y4 Receptor Selective Agonists Based on NPY(32−36): Development of an Anorectic Y4 Receptor Selective Agonist with Picomolar Affinity. *J. Med. Chem.* 49(8): 2661-2665.

Berglund, M. M.; Lundell, I.; Eriksson, H.; Söll, R.; Beck-Sickinger, A. G.; Larhammar, D. (2001). Studies of the human, rat, and guinea pig Y4 receptors using neuropeptide Y analogues and two distinct radioligands. *Peptides* 22(3): 351-356.

Berglund, M. M.; Schober, D. A.; Esterman, M. A.; Gehlert, D. R. (2003a). Neuropeptide Y Y4 receptor homodimers dissociate upon agonist stimulation. *J. Pharmacol. Exp. Ther.* 307(3): 1120-1126.

Berglund, M. M.; Schober, D. A.; Statnick, M. A.; McDonald, P. H.; Gehlert, D. R. (2003b). The use of bioluminescence resonance energy transfer 2 to study neuropeptide Y receptor agonist-induced beta-arrestin 2 interaction. *J. Pharmacol. Exp. Ther.* 306(1): 147-156.

Berlicki, Ł.; Kaske, M.; Gutiérrez-Abad, R.; Bernhardt, G.; Illa, O.; Ortuño, R. M.; Cabrele, C.; Buschauer, A.; Reiser, O. (2013). Replacement of Thr32 and Gln34 in the C-Terminal Neuropeptide Y Fragment 25–36 by cis-Cyclobutane and cis-Cyclopentane β-Amino Acids Shifts Selectivity toward the Y4 Receptor. *J. Med. Chem.* 56(21): 8422-8431.

Cheng, Y.; Prusoff, W. H. (1973). Relationship between the inhibition constant (K1) and the concentration of inhibitor which causes 50 per cent inhibition (I50) of an enzymatic reaction. *Biochem. Pharmacol.* 22(23): 3099-3108.

Clark, J. T.; Sahu, A.; Kalra, P. S.; Balasubramaniam, A.; Kalra, S. P. (1987). Neuropeptide Y (NPY)-induced feeding behavior in female rats: comparison with human NPY ([Met17]NPY), NPY analog ([norLeu4]NPY) and peptide YY. *Regul. Pept.* 17(1): 31-39.

Criscione, L.; Rigollier, P.; Batzl-Hartmann, C.; Rueger, H.; Stricker-Krongrad, A.; Wyss, P.; Brunner, L.; Whitebread, S.; Yamaguchi, Y.; Gerald, C.; Heurich, R. O.; Walker, M. W.; Chiesi, M.; Schilling, W.; Hofbauer, K. G.; Levens, N. (1998). Food intake in free-feeding and energy-deprived lean rats is mediated by the neuropeptide Y5 receptor. *J. Clin. Invest.* 102(12): 2136-2145.

Dautzenberg, F. M.; Higelin, J.; Pflieger, P.; Neidhart, W.; Guba, W. (2005). Establishment of robust functional assays for the characterization of neuropeptide Y (NPY) receptors: identification of 3-(5-benzoyl-thiazol-2-ylamino)-benzonitrile as selective NPY type 5 receptor antagonist. *Neuropharmacology* 48(7): 1043-1055.

Dumont, Y.; Quirion, R. (2000). [(125)I]-GR231118: a high affinity radioligand to investigate neuropeptide Y Y(1) and Y(4) receptors. *Br. J. Pharmacol.* 129(1): 37-46.

Eriksson, H.; Berglund, M. M.; Holmberg, S. K.; Kahl, U.; Gehlert, D. R.; Larhammar, D. (1998). The cloned guinea pig pancreatic polypeptide receptor Y4 resembles more the human Y4 than does the rat Y4. *Regul. Pept.* 75-76: 29-37.

Gehlert, D. R.; Schober, D. A.; Gackenheimer, S. L.; Beavers, L.; Gadski, R.; Lundell, I.; Larhammar, D. (1997). [125I]Leu31, Pro34-PYY is a High Affinity Radioligand for Rat PP1/Y4 and Y1 Receptors: Evidence for Heterogeneity in Pancreatic Polypeptide Receptors. *Peptides* 18(3): 397-401.

Kamiji, M. M.; Inui, A. (2007). NPY Y2 and Y4 Receptors Selective Ligands: Promising Anti-Obesity Drugs? *Curr. Top. Med. Chem.* 7(17): 1734-1742.

Keller, M.; Bernhardt, G.; Buschauer, A. (2011a). [3H]UR-MK136: A Highly Potent and Selective Radioligand for Neuropeptide Y Y1 Receptors. *ChemMedChem* 6(9): 1566-1571.

Keller, M.; Erdmann, D.; Pop, N.; Pluym, N.; Teng, S.; Bernhardt, G.; Buschauer, A. (2011b). Red-fluorescent argininamide-type NPY Y1 receptor antagonists as pharmacological tools. *Bioorg. Med. Chem.* 19(9): 2859-2878.

Keller, M.; Kaske, M.; Holzammer, T.; Bernhardt, G.; Buschauer, A. (2013). Dimeric argininamide-type neuropeptide Y receptor antagonists: Chiral discrimination between Y1 and Y4 receptors. *Bioorg. Med. Chem.* 21(21): 6303-6322.

Keller, M.; Kuhn, K. K.; Einsiedel, J.; Hubner, H.; Biselli, S.; Mollereau, C.; Wifling, D.; Svobodova, J.; Bernhardt, G.; Cabrele, C.; Vanderheyden, P. M.; Gmeiner, P.; Buschauer, A. (2016). Mimicking of Arginine by Functionalized N(omega)-Carbamoylated Arginine As a New Broadly Applicable Approach to Labeled Bioactive Peptides: High Affinity Angiotensin, Neuropeptide Y, Neuropeptide FF, and Neurotensin Receptor Ligands As Examples. *J. Med. Chem.* 59(5): 1925-1945.

Keller, M.; Weiss, S.; Hutzler, C.; Kuhn, K. K.; Mollereau, C.; Dukorn, S.; Schindler, L.; Bernhardt, G.; König, B.; Buschauer, A. (2015). Nω-Carbamoylation of the Argininamide Moiety: An Avenue to Insurmountable NPY Y1 Receptor Antagonists and a Radiolabeled Selective High-Affinity Molecular Tool ([3H]UR-MK299) with Extended Residence Time. *J. Med. Chem.* 58(22): 8834-8849.

Koshimizu, T. A.; Kashiwazaki, A.; Taniguchi, J. (2016). Combined sodium ion sensitivity in agonist binding and internalization of vasopressin V1b receptors. *Sci. Rep.* 6: 25327.

Kuhn, K. K.; Ertl, T.; Dukorn, S.; Keller, M.; Bernhardt, G.; Reiser, O.; Buschauer, A. (2016). High Affinity Agonists of the Neuropeptide Y (NPY) Y4 Receptor Derived from the C-Terminal Pentapeptide of Human Pancreatic Polypeptide (hPP): Synthesis, Stereochemical Discrimination, and Radiolabeling. *J. Med. Chem.* 59(13): 6045-6058.

Li, J. B.; Asakawa, A.; Terashi, M.; Cheng, K.; Chaolu, H.; Zoshiki, T.; Ushikai, M.; Sheriff, S.; Balasubramaniam, A.; Inui, A. (2010). Regulatory effects of Y4 receptor agonist (BVD-74D) on food intake. *Peptides* 31(9): 1706-1710.

Li, L.; Mayer, M.; Schneider, E.; Schreiber, E.; Bernhardt, G.; Peng, S.; Buschauer, A. (2003). Preparation of fluorescent nonpeptidic neuropeptide Y receptor ligands: analogues of the quinazoline-type anti-obesity Y5 antagonist CGP 71683A. *Arch. Pharm. (Weinheim, Ger.)* 336(12): 585-590.

Lieb, S.; Littmann, T.; Plank, N.; Felixberger, J.; Tanaka, M.; Schafer, T.; Krief, S.; Elz, S.; Friedland, K.; Bernhardt, G.; Wegener, J.; Ozawa, T.; Buschauer, A. (2016). Label-free versus conventional cellular assays: Functional investigations on the human histamine H1 receptor. *Pharmacol. Res.* 114: 13-26.

Liu, M.; Mountford, S. J.; Richardson, R. R.; Groenen, M.; Holliday, N. D.; Thompson, P. E. (2016a). Optically Pure, Structural, and Fluorescent Analogues of a Dimeric Y4 Receptor Agonist Derived by an Olefin Metathesis Approach. *J. Med. Chem.* 59(13): 6059-6069.

Liu, M.; Richardson, R. R.; Mountford, S. J.; Zhang, L.; Tempone, M. H.; Herzog, H.; Holliday, N. D.; Thompson, P. E. (2016b). Identification of a Cyanine-Dye Labeled Peptidic Ligand for Y1R and Y4R, Based upon the Neuropeptide Y C-Terminal Analogue, BVD-15. *Bioconjug. Chem.* 27(9): 2166-2175.

Liu, W.; Chun, E.; Thompson, A. A.; Chubukov, P.; Xu, F.; Katritch, V.; Han, G. W.; Roth, C. B.; Heitman, L. H.; Ijzerman, A. P.; Cherezov, V.; Stevens, R. C. (2012). Structural Basis for Allosteric Regulation of GPCRs by Sodium Ions. *Science* 337: 232.

Martel, J. C.; Fournier, A.; St-Pierre, S.; Dumont, Y.; Forest, M.; Quirion, R. (1990). Comparative structural requirements of brain neuropeptide Y binding sites and vas deferens neuropeptide Y receptors. *Mol. Pharmacol.* 38(4): 494-502.

Moser, C., Bernhardt, Günther, Michel, J., Schwarz, H. und Buschauer, Armin (2000). Cloning and functional expression of the hNPY Y_5 receptor in human endometrial cancer (HEC-1B) cells. *Can J. Physiol. Pharmacol.* 78: S. 134-142. .

Parker, E. M.; Babij, C. K.; Balasubramaniam, A.; Burrier, R. E.; Guzzi, M.; Hamud, F.; Gitali, M.; Rudinski, M. S.; Tao, Z.; Tice, M.; Xia, L.; Mullins, D. E.; Salisbury, B. G. (1998). GR231118 (1229U91) and other analogues of the C-terminus of neuropeptide Y are potent neuropeptide Y Y1 receptor antagonists and neuropeptide Y Y4 receptor agonists. *Eur. J. Pharmacol.* 349(1): 97-105.

Parker, M. S.; Lundell, I.; Parker, S. L. (2002). Pancreatic polypeptide receptors: affinity, sodium sensitivity and stability of agonist binding. *Peptides* 23(2): 291-303.

Parker, M. S.; Parker, S. L.; Kane, J. K. (2004). Internalization of neuropeptide Y Y1 and Y5 and of pancreatic polypeptide Y4 receptors is inhibited by lithium in preference to sodium and potassium ions. *Regul. Pept.* 118(1–2): 67-74.

Parker, M. S.; Sah, R.; Sheriff, S.; Balasubramaniam, A.; Parker, S. L. (2005). Internalization of cloned pancreatic polypeptide receptors is accelerated by all types of Y4 agonists. *Regul. Pept.* 132(1–3): 91-101.

Pluym, N.; Baumeister, P.; Keller, M.; Bernhardt, G.; Buschauer, A. (2013). [3H]UR-PLN196: A Selective Nonpeptide Radioligand and Insurmountable Antagonist for the Neuropeptide Y Y2 Receptor. *ChemMedChem* 8(4): 587-593.

Rudolf, K.; Eberlein, W.; Engel, W.; Wieland, H. A.; Willim, K. D.; Entzeroth, M.; Wienen, W.; Beck-Sickinger, A. G.; Doods, H. N. (1994). The first highly potent and selective non-peptide neuropeptide Y Y1 receptor antagonist: BIBP3226. *Eur. J. Pharmacol.* 271(2–3): R11-R13.

Schneider, E.; Mayer, M.; Ziemek, R.; Li, L.; Hutzler, C.; Bernhardt, G.; Buschauer, A. (2006). A simple and powerful flow cytometric method for the simultaneous determination of multiple parameters at G protein-coupled receptor subtypes. *Chembiochem* 7(9): 1400-1409.

Walker, M. W.; Smith, K. E.; Bard, J.; Vaysse, P. J. J.; Gerald, C.; Daouti, S.; Weinshank, R. L.; Branchek, T. A. (1997). A Structure-Activity Analysis of the Cloned Rat and Human Y4 Receptors for Pancreatic Polypeptide1. *Peptides* 18(4): 609-612.

Wang, X.; Zielinski, M. C.; Misawa, R.; Wen, P.; Wang, T. Y.; Wang, C. Z.; Witkowski, P.; Hara, M. (2013). Quantitative analysis of pancreatic polypeptide cell distribution in the human pancreas. *PLoS One* 8(1): e55501.

Yan, H.; Yang, J.; Marasco, J.; Yamaguchi, K.; Brenner, S.; Collins, F.; Karbon, W. (1996). Cloning and functional expression of cDNAs encoding human and rat pancreatic polypeptide receptors. *Proc. Natl. Acad. Sci. U. S. A.* 93(10): 4661-4665.

Yulyaningsih, E.; Zhang, L.; Herzog, H.; Sainsbury, A. (2011). NPY receptors as potential targets for anti-obesity drug development. *Br. J. Pharmacol.* 163(6): 1170-1202.

Zhang, L.; Bijker, M. S.; Herzog, H. (2011). The neuropeptide Y system: pathophysiological and therapeutic implications in obesity and cancer. *Pharmacol. Ther.* 131(1): 91-113.

Ziemek, R.; Brennauer, A.; Schneider, E.; Cabrele, C.; Beck-Sickinger, A. G.; Bernhardt, G.; Buschauer, A. (2006). Fluorescence- and luminescence-based methods for the determination of affinity and activity of neuropeptide Y2 receptor ligands. *Eur. J. Pharmacol.* 551(1-3): 10-18.

Ziemek, R.; Schneider, E.; Kraus, A.; Cabrele, C.; Beck-Sickinger, A. G.; Bernhardt, G.; Buschauer, A. (2007). Determination of Affinity and Activity of Ligands at the Human Neuropeptide Y Y4 Receptor by Flow Cytometry and Aequorin Luminescence. *J. Recept. Signal Transduct. Res.* 27(4): 217-233.

Zou, Y.; Akazawa, H.; Qin, Y.; Sano, M.; Takano, H.; Minamino, T.; Makita, N.; Iwanaga, K.; Zhu, W.; Kudoh, S.; Toko, H.; Tamura, K.; Kihara, M.; Nagai, T.; Fukamizu, A.; Umemura, S.; Iiri, T.; Fujita, T.; Komuro, I. (2004). Mechanical stress activates angiotensin II type 1 receptor without the involvement of angiotensin II. *Nat. Cell Biol.* 6(6): 499-506.

Chapter 6

Summary

The neuropeptide Y (NPY) family comprises the 36-amino acid peptides neuropeptide Y (NPY), peptide YY (PYY), and pancreatic polypeptide (PP). In humans, the biological effects of these peptides are mediated by four functionally expressed receptor subtypes, designated Y_1, Y_2, Y_4 and Y_5 receptors (Y_1R, Y_2R, Y_4R, Y_5R). Among the NPY receptors the Y_4R is unique, as it prefers PP over NPY and PYY as the endogenous ligand. PP is predominantly expressed in an endocrine cell type (PP cells) of the pancreas, and is, for example, considered to be involved in satiety signaling, the regulation of food intake and energy metabolism. With this in view, Y_4R agonists are discussed as potential anti-obesity drugs. For the characterization of Y_2 and Y_4R ligands, pharmacological tools are indispensable. Therefore, the first part of this work was aiming at establishing a [^{35}S]GTPγS binding assay and a luciferase gene reporter assay for the hY_2R and hY_4R, since these assays complement each other by providing different readouts. The second part of this thesis aimed at the development of full length radio- and fluorescence-labeled hPP analogs, which are more stable compared to the endogenous ligand and [Lys^4]hPP.

In the [^{35}S]GTPγS binding assay at the hY_2R, pharmacological data of selected agonists and antagonists were in good agreement with functional studies in the steady-state GTPase assay and the calcium mobilization assay at the hY_2R. Most strikingly, the [^{35}S]GTPγS assay at the hY_4R revealed potencies of hPP and GW1229, which were lower by a factor 19 and 180, respectively, compared to reported data for the steady-state GTPase assay. Further investigations at the Y_4R revealed that the signal-to-noise ratio was not improved by the variation of the Mg^{2+} ion concentration. Increasing Na^+ concentrations led to minor changes of the potency of hPP, whereas [Lys^4]hPP and GW1229 were markedly less potent in the presence of sodium. This is in agreement with the data from radioligand binding assays at the hY_4R. Nevertheless, the [^{35}S]GTPγS assay is compromised by a low signal-to-noise ratio impairing the robustness of the data.

By using a CRE-controlled luciferase reporter gene assay, agonistic and antagonistic activities of several ligands could be determined in HEK293T cells, stably expressing the human Y_2 and Y_4 receptor, respectively. The conditions were optimized regarding concentration of the vehicle (DMSO or DMF), the forskolin concentration, the period of incubation and the addition of bacitracin as a protease inhibitor. Although a tremendous reduction of the bioluminescene signal by DMSO and DMF became obvious, at concentrations <0.2%, required to keep forskolin (2 µM) and test compounds in solution (over 4.5 h), the effect of the solvent was negligible. Under optimized conditions the determined potencies of selected ligands at the respective receptor were generally higher compared to reported results from other functional assays.

For the development of radio- and fluorescence-labeled hPP analogs, we selected [Lys^4,Nle^{17,30}]hPP as a template, as the methionine residues in position 17 and 30 in [Lys^4]hPP are prone to oxidation. [^{3}H]propionyl-[Lys^4,Nle^{17,30}]hPP and the cyanine-labeled fluorescent peptide S0223[Lys^4,Nle^{17,30}]hPP were synthesized and characterized in saturation and kinetic Y_4R binding experiments, in functional studies and with respect to NPY receptor subtype selectivity. Interestingly, radioligand affinity (K_d in Na^+-free buffer: 1.1 nM) clearly decreased with increasing sodium ion concentration, whereas dissociation and Y_4R-mediated internalization of the fluorescent ligand (K_d in Na^+-free buffer: 10.8 nM) were strongly effected by the osmolarity of the buffer as demonstrated by confocal microscopy. The labeled compounds were also used to determine the affinities of unlabeled compounds in competition binding assays. Displacement of the labeled ligands revealed a tendency to higher apparent affinities for a set of reference peptides in hypotonic (Na^+-free) compared to isotonic buffers. The differences were negligible in case of hPP but up to 270-fold in case of GW1229 (GR231118). However, it could be demonstrated that, despite an identical peptide scaffold, fundamental differences between both types of probes might exist and should be carefully taken into account in the interpretation of experimental results.

Chapter 7

Appendix

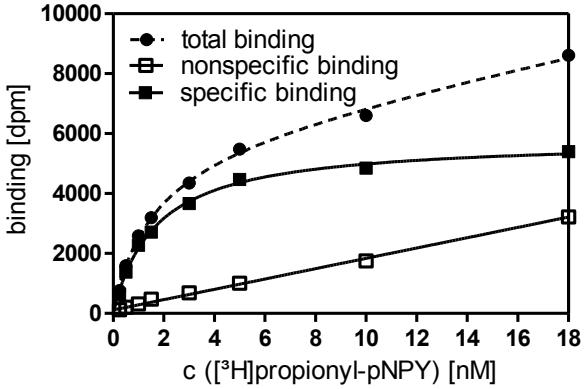

Figure 7.1. Representative saturation binding experiment of [^{3}H]propionyl-pNPY on SK-N-MC cells expressing the Y_1R. K_d = 1.9 ± 0.3 nM (Keller et al., 2015); nonspecific binding was determined in the presence of BIBP3226; two independent experiments were performed in triplicate in 48-well format.

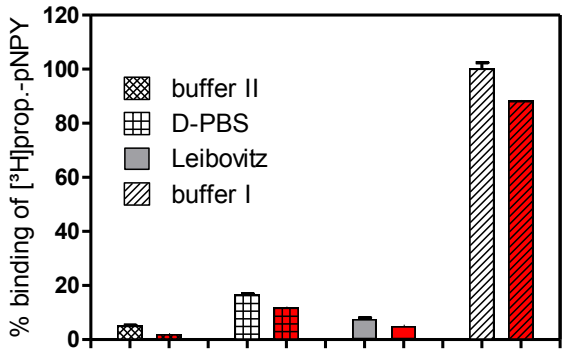

Figure 7.2. Binding experiments with [^{3}H]propionyl-pNPY (5 nM) at CHO cells expressing the Y_2R in different buffer systems. Differences in total (transparent columns) and specific binding (red columns) of the radioligand could be observed at the Y_2R dependent on the used buffer. Total binding in buffer I was set to 100%. Nonspecific binding was determined in the presence of 1 µM pNPY. Composition of buffer I and buffer II see section 5.2.6; D-PBS (1.8 mM $CaCl_2$, 2.68 mM KCl, 1.47 mM KH_2PO_4, 3.98 mM $MgSO_4 \cdot 7H_2O$, 136.9 mM NaCl, 8.06 mM $Na_2HPO_4 \cdot 7H_2O$), Gibco Leibovitz's L-15 medium (containing 140 mM NaCl, 1.3 mM $CaCl_2$, 1 mM $MgCl_2$, amino acids, vitamins, pH 7.4). Experiment was performed in triplicate in Primaria 24-well plates; plates were processed as previously described for [^{3}H]propionyl-[Lys^4]hPP (see section 5.2.7).

Table 7.1. Determination of K_i values on NPY receptor subtypes.

	K_i [nM]			
Compound	Y_1R[a]	Y_2R[b]	Y_4R[c]	Y_5R[d]
BIBP3226	4.8 ± 0.2	n.d.	n.d.	n.d.
BIBO3304	1.1 ± 0.1	n.d.	n.d.	n.d.
pNPY	4.4 ± 1.3	1.7 ± 0.13	n.d.	6.7 ± 1.1
propionyl-pNPY	11.7 ± 0.9	2.1 ± 0.2	26.5 ± 4.1	10.3 ± 0.5
pNPY 2-36	n.d.	5.8 ± 1.1	n.d.	n.d.

[a] Radioligand competition binding assay with [^{3}H]propionyl-pNPY (K_d = 7 nM, c = 5 nM) using MCF-7-hY_1 cells (Keller et al., 2011) in buffer II. [b] Radioligand competition binding assay with [^{3}H]propionyl-pNPY (K_d = 1.4 nM, c = 1 nM) using CHO-hY_2-G_{qi5}-mtAEQ cells (Ziemek et al., 2006) in buffer I. [c] Radioligand competition binding assay with [^{3}H]propionyl-[Lys^4,Nle^{17,30}]hPP (K_d = 1.1 nM, c = 1 nM) using CHO-hY_4R_{Gqi5}-mtAEQ cells (Ziemek et al., 2007) in buffer I. [d] Radioligand competition binding assay with [^{3}H]propionyl-pNPY (K_d = 4.83 nM, c = 4 nM) using HEC-1B-hY_5R cells in buffer II (Moser, 2000). Data represent mean values ± SEM from at least two independent experiments performed in triplicate.

References

Keller, M.; Bernhardt, G.; Buschauer, A. (2011). [3H]UR-MK136: A Highly Potent and Selective Radioligand for Neuropeptide Y Y1 Receptors. *ChemMedChem* 6(9): 1566-1571.

Keller, M.; Weiss, S.; Hutzler, C.; Kuhn, K. K.; Mollereau, C.; Dukorn, S.; Schindler, L.; Bernhardt, G.; König, B.; Buschauer, A. (2015). Nω-Carbamoylation of the Argininamide Moiety: An Avenue to Insurmountable NPY Y1 Receptor Antagonists and a Radiolabeled Selective High-Affinity Molecular Tool ([3H]UR-MK299) with Extended Residence Time. *J. Med. Chem.* 58(22): 8834-8849.

Moser, C., Bernhardt, Günther, Michel, J., Schwarz, H. und Buschauer, Armin (2000). Cloning and functional expression of the hNPY Y_5 receptor in human endometrial cancer (HEC-1B) cells. *Can J. Physiol. Pharmacol.* 78: S. 134-142. .

Ziemek, R.; Brennauer, A.; Schneider, E.; Cabrele, C.; Beck-Sickinger, A. G.; Bernhardt, G.; Buschauer, A. (2006). Fluorescence- and luminescence-based methods for the determination of affinity and activity of neuropeptide Y2 receptor ligands. *Eur. J. Pharmacol.* 551(1-3): 10-18.

Ziemek, R.; Schneider, E.; Kraus, A.; Cabrele, C.; Beck-Sickinger, A. G.; Bernhardt, G.; Buschauer, A. (2007). Determination of Affinity and Activity of Ligands at the Human Neuropeptide Y Y4 Receptor by Flow Cytometry and Aequorin Luminescence. *J. Recept. Signal Transduct. Res.* 27(4): 217-233.

Eidesstattliche Erklärung

Ich erkläre hiermit an Eides statt, dass ich die vorliegende Arbeit ohne unzulässige Hilfe Dritter und ohne Benutzung anderer als der angegebenen Hilfsmittel angefertigt habe; die aus anderen Quellen direkt übernommenen Daten und Konzepte sind unter Angabe des Literaturzitats gekennzeichnet.

Weitere Personen waren an der inhaltlich-materiellen Herstellung der vorliegenden Arbeit nicht beteiligt. Insbesondere habe ich hierfür nicht die entgeltliche Hilfe eines Promotionsberaters oder anderer Personen in Anspruch genommen. Niemand hat von mir, weder unmittelbar noch mittelbar, geldwerte Leistungen für Arbeiten erhalten, die im Zusammenhang mit dem Inhalt der vorgelegten Dissertation stehen.

Die Arbeit wurde bisher weder im In- noch im Ausland in gleicher oder ähnlicher Form einer anderen Prüfungsbehörde vorgelegt.

Regensburg, den _____ _____

Name